Alkane dehydrocyclization mechanism

Burtron H. Davis *

Center for Applied Energy Research, University of Kentucky, 2540 Research Park Drive, Lexington, KY 40511, USA

Abstract

A review of results impacting the dehydrocyclization mechanisms for monofunctional catalysts proposed to date has been made. The data indicate that, while alkane conversions at low temperatures (about 300°C or less) may involve reversible adsorption, irreversible adsorption of the alkane is the rate determining step at higher temperatures representative of naphtha reforming. The extent of irreversible adsorption depends upon hydrogen partial pressure, with alkane adsorption being irreversible near atmospheric pressure and gradually changing to reversible adsorption at naphtha reforming pressure. At all pressures, primary aromatic products are formed by a mechanism involving direct six-carbon ring formation. At low pressures, the cyclopentane cyclization product yields carbon on catalyst and cracked products. At higher pressures, the cyclopentane structures undergo nonselective hydrogenolysis to produce isomers of the alkane feed by a monofunctional metal catalyzed pathway. A common cyclization pathway is proposed for the formation of C_5- and C_6-ring structures. With bifunctional catalysts, the acid catalyzed cyclization is more rapid than the monofunctional metal cyclization. ©1999 Elsevier Science B.V. All rights reserved.

Keywords: Mechanism; Alkane dehydrocyclization; Alkane; Hydrogenolysis; Naphtha reforming; Isotopic tracer studies

1. Introduction

Dehydrocyclization of alkanes to produce aromatics was discovered independently by a number of groups [1–7]. It was recognized as an important discovery since the aromatics that were produced had a high octane number whereas the alkanes they were produced from had a low octane number. Thus, the announcement by UOP workers was delayed because of the importance attached to it by the US government due to fears arising from the political crisis that eventually led to World War II [4]. The discovery of naphtha reforming with the bifunctional chlorided Pt-Al$_2$O$_3$ catalyst increased the interest in dehydrocyclization [8]. Even today, the search continues for more selective dehydrocyclization catalysts as indicated by the recent introduction of the Pt-KL zeolite catalyst [9,10]. Looking to the future, coal and natural gas will probably provide an increasing fraction of the liquid hydrocarbon fuels. The Fischer–Tropsch synthesis, where coal is first reacted with water to form the CO + H$_2$ synthesis gas, is one of several routes which offer promise for converting coal to liquids. Since the liquids from the Fischer–Tropsch Synthesis contain a large fraction of alkanes, dehydrocyclization could assume an even more important role in the reforming process.
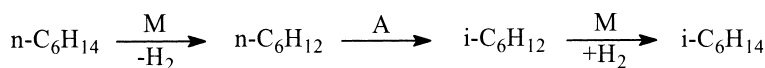
Examples of the reaction classes occurring in the reforming process which impact the octane number and yield of the gasoline are:
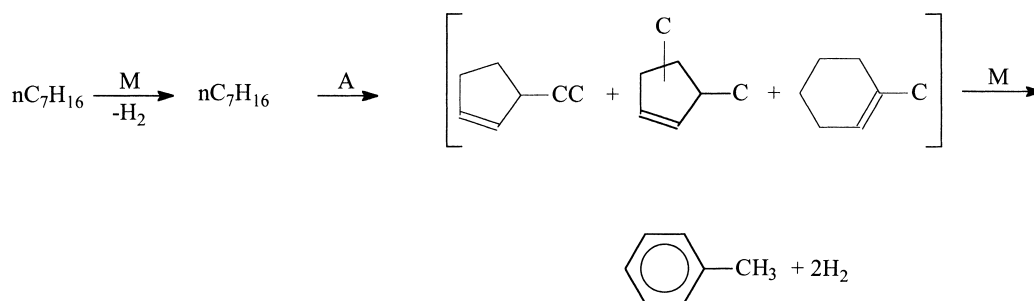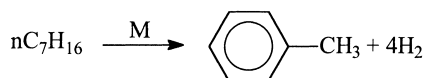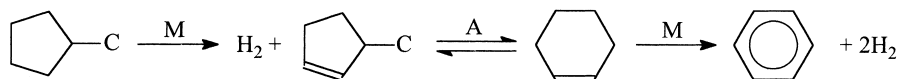
1. Dehydrogenation
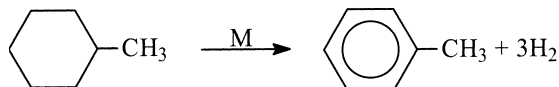
* Tel.: +1-606-257-0251; fax: +1-606-257-0302.
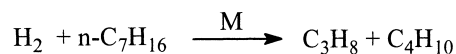
E-mail address: davis@caer.uky.edu (B.H. Davis)
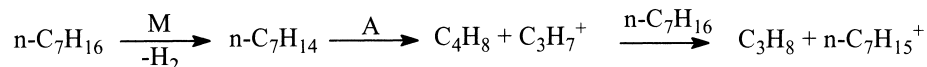
2. Isomerization

$$\text{n-}C_6H_{14} \xrightarrow[-H_2]{M} \text{n-}C_6H_{12} \xrightarrow{A} \text{i-}C_6H_{12} \xrightarrow[+H_2]{M} \text{i-}C_6H_{14}$$

3. Aromatization

$$\text{(cyclopentane-C)} \xrightarrow{M} H_2 + \text{(cyclopentene-C)} \underset{A}{\rightleftarrows} \text{(cyclohexene)} \xrightarrow{M} \text{(benzene)} + 2H_2$$

$$nC_7H_{16} \xrightarrow{M} \text{(toluene)}-CH_3 + 4H_2$$

$$nC_7H_{16} \xrightarrow[-H_2]{M} nC_7H_{16} \xrightarrow{A} \left[\text{(cyclopentene-CC)} + \text{(cyclopentene-C with C)} + \text{(cyclohexene-C)} \right] \xrightarrow{M}$$

$$\text{(toluene)}-CH_3 + 2H_2$$

4. Cracking (hydrocracking)

$$\text{n-}C_7H_{16} \xrightarrow[-H_2]{M} \text{n-}C_7H_{14} \xrightarrow{A} C_4H_8 + C_3H_7^+ \xrightarrow{\text{n-}C_7H_{16}} C_3H_8 + \text{n-}C_7H_{15}^+$$

$$H_2 + \text{n-}C_7H_{16} \xrightarrow{M} C_3H_8 + C_4H_{10}$$

('A' refers to an acid site and 'M' to a metal site).

The first three reactions lead to higher octane number products but reaction (4) may be undesirable since it decreases the yield of gasoline. It should also be realized that these reaction schemes may not be unique in a reaction network where a large number of reactants may lead to over 100 reaction products. For example, there may be an acid catalyzed cyclization which competes with reaction (3) [11]. In fact, under reforming conditions, the bifunctional acid catalyzed cyclization pathway be dominant [12–14]; however, the above reactions are probably the dominant ones for the process monofunctional pathway [15–17].

Invariably, during hydrocarbon conversion, carbonaceous deposits are formed on the metallic function and the acidic support. The nature of these carbon deposits has not been defined in much detail. Several,

predominantly Somorjai and coworkers [18], have advanced the view that much of the surface of platinum single crystal catalyst is covered by carbonaceous deposits that play a major role in protecting some small fraction of active centers of the catalyst.

Carbon atoms have been generated by the 'carbon arc' method [19] and these were deposited in, for example, benzene held at −196°C [20]. Upon warming to room temperature the carbon atoms react with benzene to form a variety of compounds. With saturated hydrocarbons, the atomic carbon reacts by insertion in a C–H bond to produce a product containing one more carbon than the reactant. When benzene is the reactant, toluene and other aromatic products can be formed. Thus, a free carbon atom would be unstable on a platinum surface even at room temperature, let alone at 480°C where dehydrocyclization reactions are
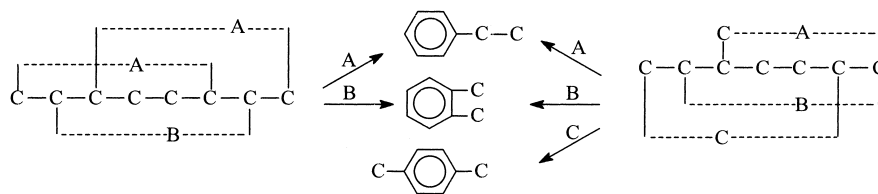
Scheme 1.

effected. While dehydrocyclization may produce minor amounts of aromatics with one, or even two, more carbon atoms than the original feed, they must arise using other pathways or reactive intermediate surface species than atomic carbon (e.g., [21]). We should conclude that the carbonaceous deposits on the platinum function must be multiply bonded to platinum and/or to hydrogen.

## 2. Aromatic distribution and early mechanisms

Two general approaches are available for investigating heterogeneous catalysis: (a) study one reactant over a wide variety of catalysts and (b) study many reactants over a single catalyst. An elegant example of the single reactant approach was conducted by Kokes and coworkers (e.g., [22]) who showed that a metal oxide catalyst, ZnO, resembled in many respects Group VIII metal catalysts in the hydrogenation of alkenes. For the single reactant approach to mechanistic studies, it is generally desirable to have a chemical selectivity in addition to the kinetic data. As outlined in Scheme 1, *n*-octane and 3-methylheptane provide a chemical selectivity (in Scheme 1 we anticipate our

Table 1
Aromatic distribution reported by early workers using chromia catalysts

Reactant	C_8 aromatics (mol%)			
	EB	OX	MX	PX
n-octane	33	33	27	4
3-methylheptane	15	25	–	60
2-methylheptane	–	–	100	–
3-ethylhexane	100	–	–	–
2,3-dimethylhexane	25	75	–	–

Approach (b) has been used extensively with a variety of reactants in studies directed toward elucidating the cyclization steps. The aromatic distribution obtained by early workers from the conversion of some representative alkanes over chromia are presented in Table 1. The accuracy of these distributions have been confirmed many times using more accurate GC analytical techniques. In spite of an abundance of aromatic isomers that could not result from a direct C_6-ring formation, the early thinking materialized as the Twigg mechanism [23] which incorporated the 'half-hydrogenated' state that was being applied in the 1930s to explain alkene hydrogenation and isotope exchange reactions (e.g., [24]).
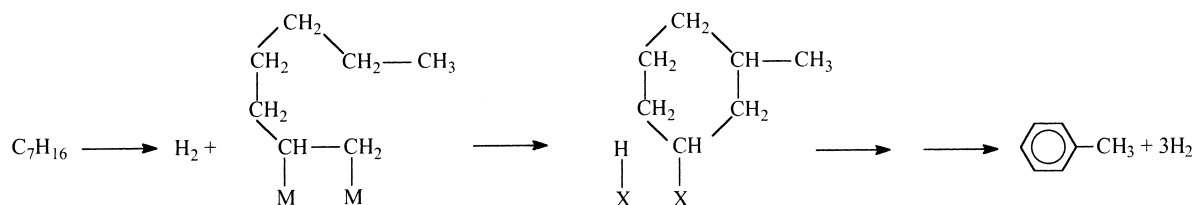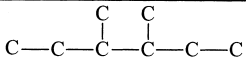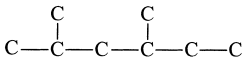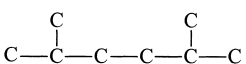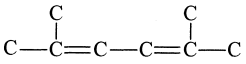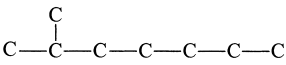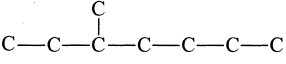

conclusions by showing the selectivity resulting from a direct six-carbon ring formation).

The chemical selectivity of these, and other reactants, are used to compare several catalyst systems and to infer reaction pathways.

2.1. Twigg mechanism

Numerous schemes, including bicyclic intermediates, were advanced to account for the aromatics not allowed by direct C_6 ring closure. These

Reactant	Aromatic, Mole %			
	EB[a]	OX[a]	MX[a]	PX[a]
C—C—C(C)—C(C)—C—C	14	**70**	12	4
C—C(C)—C—C(C)—C—C	3	3	**90**	3
C—C(C)—C—C—C(C)—C	--	--	5	**94**
C—C(C)=C—C=C(C)—C	--	--	2	**98**
C—C(C)—C—C—C—C—C	**21**	**28**	4	**47**
C—C—C(C)—C—C—C—C	4	2	**88**	6

a. EB, ethylbenzene; OX, o-xylene; MX, m-xylene; PX, p-xylene

☐ Expected for 1-6 ring formation.

Scheme 2.

early studies are covered in excellent review articles [15–17,25].

The Twigg mechanism implied that cyclization leads to an adsorbed cyclohexane; that is, dehydrogenation to form the aromatic occurred after ring formation.

The aromatics from the conversion of several C_8-alkanes with one catalyst (Pt-nonacidic alumina) provide an example of approach (b), and are illustrated in Scheme 2.

Many of the early mechanistic studies were based on kinetic measurements. Alkenes were deduced to be an intermediate since their rate of formation did not extrapolate to zero at short reaction times whereas the rate of aromatics formation did approach zero [26]. However, for heterogeneous catalysis, kinetic studies can, at best, be suggestive. Thus, one must resort to other techniques to unravel details of the reaction mechanism. One powerful technique involves the use of isotopic tracers.

There are three general approaches for the utilization of isotopes in dehydrocyclization studies. In the first approach, a specific position of the reactant is labeled with either a stable or radioactive isotope. The positions of the product that are labeled with the isotope are determined and a mechanism consistent with the label distribution is deduced. This approach has been called the 'labeled molecule' approach [27]. In another approach, a possible intermediate compound is labeled with an isotope and is then converted in competition with another reactant, the kinetic isotope approach. Another technique is to make an abrupt switch from a labeled reactant to an unlabeled reactant, or vice versa, and then to follow the isotopic composition of the products for increasing time following the switch, the transient method [28]. To date, the transient approach has not been applied to dehydrocyclization but both the labeled molecule and the kinetic isotope method have been widely utilized. This paper will critically review the results obtained using these approaches and place them within a mechanistic framework.

Experimental expediency has caused most mechanistic studies to be carried out at atmospheric pressure.

However, the commercial reforming process uses a total pressure of 60–500 psi (0.41–3.4 MPa) to retard a rapid decline in catalyst activity. At another extreme, many spectroscopic techniques that are now used to characterize catalysts must operate at high vacuum conditions (ca. 10^{-8} to 10^{-10} atm). For example, Somorjai and coworkers (e.g., [29]) have carried out the dehydrocyclization of *n*-heptane in parallel with LEED studies at these low pressures. Consequently, an assessment of the influence of pressure on the mechanism is needed.

3. Dehydrocyclization catalysts

Both metal and metal oxides have been widely used as catalysts to convert alkanes into aromatics.

3.1. Metal oxide catalysts

Chromia, the catalyst that provided the initial impetus for dehydrocyclization studies, suffered from two shortcomings: (1) at atmospheric pressure rapid 'coke' formation prevented sufficient catalyst life for commercial use and (2) the catalyst was not sufficiently active at the higher hydrogen pressures where the rate of 'coking' should be retarded. These catalysts have been extensively reviewed [15–17,25] and will only be covered in this report in the section on radiotracers. Supported molybdena catalysts also received attention but when their commercial use resulted in an explosion/fire at Amoco's plant [30] the interest in them waned.

3.2. Pt catalysts

In the 1950s, the use of the Pt-Al$_2$O$_3$ catalyst for naphtha reforming became a commercial success [8]. More recently, the Pt-Al$_2$O$_3$ catalyst has been displaced in the commercial process by supported bimetallic or even multimetallic catalysts; the first of these was the Pt/Re combination developed by Chevron workers [31].

Nearly all of the naphtha reforming catalysts have the catalytically active material dispersed on a support. Initially, little attention was paid to the support other than as a means of providing a high surface area. With

the development of the Pt-Al$_2$O$_3$ catalyst, the support became as important as the metal since the isomerization activity was partially, or completely, provided by the support. The early work of Pines and coworkers [32] have called attention to the effect of the support even for the chromia-alumina catalyst.

The influence of the support on the aromatic selectivity is clearly demonstrated by the results presented in Fig. 1. With the Pt-acidic alumina catalyst the aromatic distribution is at, or closely approaches, the equilibrium value; however, when the alumina support is made nonacidic by incorporation of alkali metal ions, the two isomers allowed by direct C$_6$-ring closure accounted for 95% or more of the aromatic products. It is widely accepted that Pt on acidic alumina provides a bifunctional reaction pathway in which the metal serves as a site for cyclization and for alkene formation; the acidity serves to convert the *n*-alkene to *iso*-alkenes and cyclic naphthenes by a typical acid catalyzed carbenium ion reaction. This means that the reforming process must be concerned with a delicate balance of metal and acid catalysis in order to maximize the yield of high octane product [33]. The acidity function of bifunctional catalysts, as shown by the data in Fig. 1, prevents the use of chemical selectivity to study reactions over the metal function. In the present report, we will emphasize studies where the acid function has been drastically reduced by 'base neutralization'.

To prepare nonacidic catalysts that have reproducible properties is not a simple process. Except for using a KOH containing solution for the final wash to prepare Pt-1, the same recipe was used to prepare two supported catalysts, Pt-1 and Pt-2 [34]. 1,1-Dimethylcyclohexane can undergo conversion by isomerization to form xylenes or by demethylation to form toluene. For a similar total conversion level, the difference between Pt-1 and Pt-2 is obvious (Fig. 2); for clarity, only toluene and *o*- and *m*-xylene are shown. On the other hand, Pt-1 and Pt-2 gave a similar aromatic distributions for the dehydrocyclization of *n*-octane. This indicates that the selectivity is not absolutely determined by the catalyst but may also depend on the reactant.

Results for the dehydrocyclization of *n*-octane show that as the metal loading on nonacidic alumina increased from 0.05 to 0.6 wt.% Pt, the ethylbenzene: *o*-xylene (OX : EB) ratio changed from a 1.4 : 1
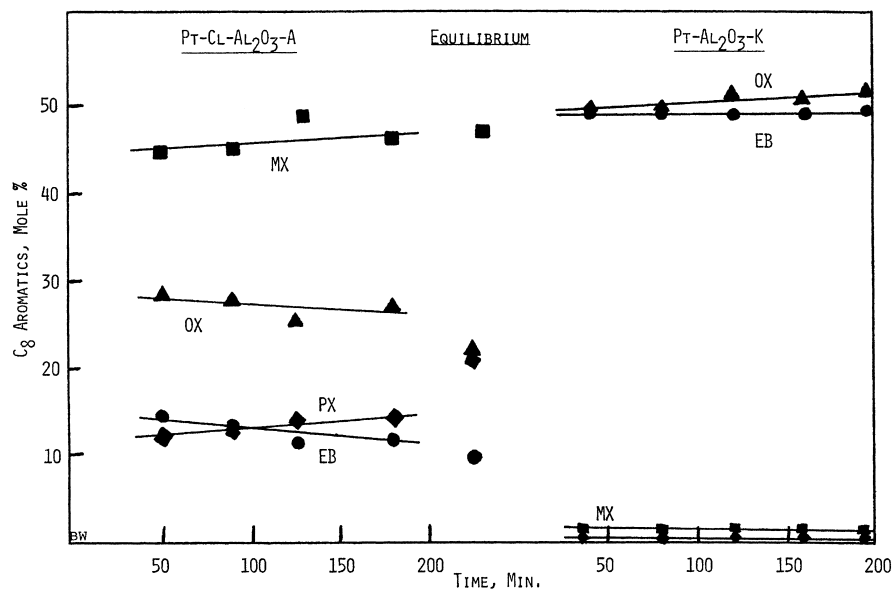
Fig. 1. Comparison of the aromatics from the conversion of *n*-octane at 482°C and atmospheric pressure over Pt on acidic (left) and nonacidic (right) alumina support . (Equilibrium C_8-aromatic composition indicated in center of figure.) (EB, ethylbenzene; OX, *o*-xylene; MX, *m*-xylene; PX, *p*-xylene).
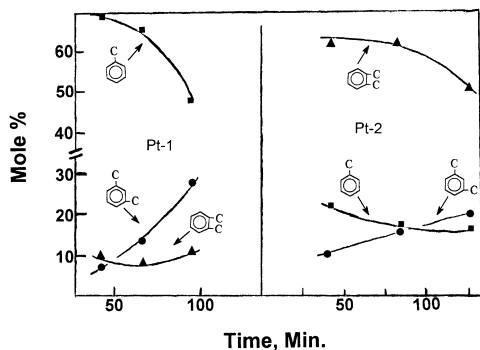

Fig. 2. Conversion of 1,1-dimethylcyclohexane over two different Pt-Al_2O_3-K catalysts (see text for catalyst description).

Table 2
The selectivity (OX : EB) for the conversion of *n*-octane over Pt-Al_2O_3-K catalysts containing various Pt loading[a]

Pt loading (wt.%)	*o*-xylene/ethylbenzene		
	1[b]	2[b]	3[b]
0.05	1.4	–	–
0.14	1.3	1.3	1.2
0.22	1.4	1.2	1.3
0.35	1.6	1.0	1.0
0.6	1.0	1.0	1.0

[a] 482°C, LHSV = 0.3, no added hydrogen, 1 atm.
[b] Sample numbers.

selectivity to favor OX at low loadings to an equal selectivity for each isomer at the two highest loadings (Table 2) [35]. Likewise, if we neglect the small amount of *m*-xylene in calculating the aromatic distribution from 3-methylheptane dehydrocyclization with Pt-C catalysts, it is apparent that the selectivity changed from favoring *p*-xylene at the low Pt loading to the formation of nearly equal amounts of each isomer at 1.2% Pt loading (Fig. 3). Loadings higher than 1.2% Pt on carbon could not be used

in these selectivity studies due to the high activity of the catalyst for hydrogenolysis of aromatic products. These results show that the selectivity changed with increasing metal loading from favoring one isomer to a nearly equal selectivity for all isomers allowed by direct C_6-ring closure. In addition, the hydrogenolysis-demethylation activity increased from a negligible level at the lowest loading to such a high level as to preclude selectivity studies at about 2 wt.% Pt or higher.

Many of the Pt catalysts are prepared by impregnation with chloroplatinic acid so there is a concern

Table 3
C_8-aromatic distribution for the dehydrocyclization of 3-methylheptane at 482°C (from [39])

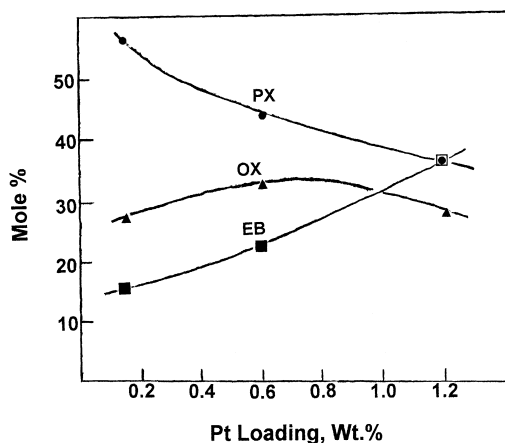| Catalyst	Sample	Time on stream (min)	C_8-aromatic products (mol%)			
			Exhylbenzene	Xylene isomers		
				p-	*m-*	*o-*
Pt-Al$_2$O$_3$-K, 0.6%	1	33	22	47	4.3	27
	3	102	19	52	<1.0	29
Pt-Cl-Al$_2$O$_3$-K, 0.6%	1	39	15	42	19	24
	3	117	16	45	16	23
Pt-Cl-Al$_2$O$_3$-K, 1.7%	1	40	17	38	22	22
	3	130	18	35	25	22
Pt-SiO$_2$, 0.6%	1	36	19	48	4.2	28
	2	83	16	51	5.0	28

Fig. 3. C_8-aromatic distribution over Pt-C catalysts with increasing Pt content (neglecting the *m*-xylene; EB, ethylbenzene; OX, *o*-xylene; PX, *p*-xylene).

Table 4
C_8-aromatic isomer distribution calculated by disregarding *m*-xylene[a]

Catalyst	Ethylbenzene	*o*-xylene	*p*-xylene
Pt-Al$_2$O$_3$-K	23	28	49
Pt-Cl-Al$_2$O$_3$-K, 1.7%	22	29	49
Pt-Cl-Al$_2$O$_3$-K, 0.6%	18	30	52
Pt-SiO$_2$	20	31	50
Cr$_2$O$_3$-Al$_2$O$_3$-A (482°C)	17	36	47
Cr$_2$O$_3$-Al$_2$O$_3$-A (500°C)	18	35	47
Cr$_2$O$_3$-Al$_2$O$_3$-B (482°C)	19	31	50
Cr$_2$O$_3$-Al$_2$O$_3$-B (500°C)	18	31	51

[a] For first sample for each run.

whether the retained chloride influences the cyclization pathway. McHenry and coworkers [36] found that the dehydrocyclization activity of Pt-Cl-Al$_2$O$_3$ catalysts was directly related to the amount of platinum that was soluble in hydrofluoric acid. They felt that the soluble platinum was a chloroplatinum complex; however, later work showed that Pt was soluble only after exposure of the catalyst to air [37,38]. In view of the later work, it does not seem likely that a dehydrocyclization–soluble Pt relationship was demonstrated in [36].

The conversion of 3-methylheptane at atmospheric pressure demonstrates that the chlorine containing catalyst, even on nonacidic alumina, yields an isomer distribution that differs from one without chlorine (Table 3) [39]. The amount of isomerization of *m*-xylene, as well as for each of the other three aromatic products, when passed over the catalyst, with or without added hydrogen, is negligible in comparison to the amount of alkane dehydrocyclization under the same reaction conditions. Thus, secondary isomerization of the initially formed aromatics is not the source of *m*-xylene.

m-Xylene is not allowed by direct C_6-cyclization of 3-methylheptane but is the only C_8-product from the cyclization of both 2- and 4-methylheptane. The aromatic distribution shown in Table 4 was calculated by assuming that *m*-xylene is a result of isomerization of the reactant and should be neglected in the aromatic distribution; neglecting the *m*-xylene led to identical aromatic compositions for a variety of metal and metal oxide catalysts. This suggests that cyclization follows a similar pathway over both types of catalysts; the chlorine merely provides an isomerization pathway. Since 0.8 wt.% Cl, added to the

Pt-Al$_2$O$_3$-K catalyst as NH$_4$Cl, did not significantly change the isomer distribution, the chlorine added as chloroplatinic acid is probably a specific type. Also chromia, when the assumption is made concerning the formation of *m*-xylene from 3-methylheptane, yielded a C$_8$-aromatic distribution that is essentially the same as all of the Pt catalysts (Table 4). Thus, it is concluded that the metal oxide and metal catalysts produce a similar aromatic product distribution.

3.3. Promoted Pt catalysts

Sulfur is a severe poison for Pt-Al$_2$O$_3$ catalysts. H$_2$S poisons our Pt-Al$_2$O$_3$ catalyst even when it was present in the ppm level. However, when 15 wt.% thiophene was added to the *n*-octane charge, the atmospheric pressure dehydrocyclization activity actually increased as long as there was incomplete conversion of the thiophene. Thus, we have the surprising situation where H$_2$S, present from the partial conversion of thiophene, does not act to poison the catalyst in the presence of thiophene [40]. Furthermore, as shown in Table 5, thiophene changed the Pt-Al$_2$O$_3$ selectivity from equal amounts of *o*-xylene and ethylbenzene to one where the *o*-xylene : ethylbenzene ratio deviates significantly from 1 : 1 and may even approach the 2 : 1 ratio expected for ring closure based on the number of pathways leading to each isomer. It also appeared that a large quantity of alkene or alkyne (when the pure alkene without added hydrogen is the reactant) effected a similar alteration of the aromatic distribution.

Table 5
Product distribution from dehydrocyclization of *n*-octane over Pt-Al$_2$O$_3$ (nonacidic) and promoted Pt-Al$_2$O$_3$ after approximately 3 h on stream

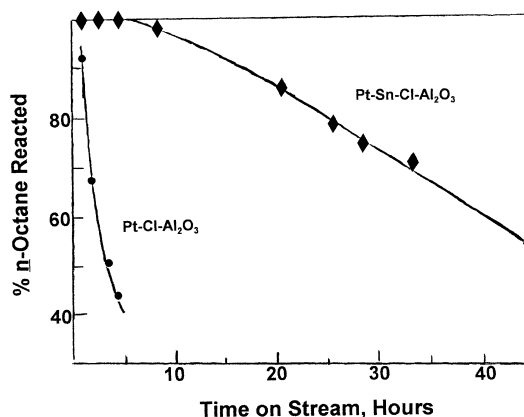| Catalyst	C$_8$-Aromatic (mol%)			
	Ethylbenzene	*p*-xylene	*m*-xylene	*o*-xylene
0.6% Pt	48.3	1.0	1.9	48.8
Pt-Sn	32.2	2.9	6.3	59.0
Pt-thiophene	43.0	Trace	Trace	57.0
0.2% Pt		43.0		57.0
Olefin	43.0	0.4	0.6	56.0
Alkyne	42.0	1.0	1.5	54.0
Pt-Re[a]	40.2	1.2	1.5	57.2

[a] *sec*-butyl amine added to the charge.

Fig. 4. Conversion of *n*-octane over Pt- and Pt-Sn-Al$_2$O$_3$ with the same reaction conditions.

Workers at Chevron found that a Pt-Al$_2$O$_3$ catalyst modified by rhenium had a higher activity and retained the activity better than Pt-Al$_2$O$_3$ [41]. Initially, it was believed that the Pt-Re formed an alloy which was more resistant to sintering and this accounted, at least partially, for the superiority of the Pt-Re catalyst. Prior to the discovery announcement by Chevron, we were trying to modify Pt-Al$_2$O$_3$ catalysts with metallic and non-metallic promoters. We were guided, or perhaps misguided, by results from homogeneous catalysis to try the Pt-Sn combination. As can be deduced from Fig. 4, the Pt-Sn catalyst was more active as well as much more resistant to aging than Pt alone. Other studies showed that there was a maximum conversion for a Pt : Sn ratio of about 1 : 4 for a 0.6% Pt loading. As can be seen in Table 5, the Pt-Sn catalyst had a *o*-xylene/ethylbenzene selectivity of nearly 2 : 1.

It was not effective to use the sodium or potassium containing nonacidic alumina for the Pt-Re catalyst since the alkali metal was a severe poison for the metal function. However, adding *sec*-butyl amine to the feed to the Pt-Re on acidic alumina catalyst poisoned the support acidity and nearly eliminated the conversion to aromatics that were not allowed by a direct C$_6$-ring closure. As seen in Table 5, the 1.4 : 1 *o*-xylene : ethylbenzene ratio with Pt-Re is similar to other promoted Pt catalysts.

Overall, both gaseous and metallic promoters may be used to increase the catalytic activity and to alter the aromatic selectivity. The selectivity data for the conversion of *n*-octane, at later time on stream,
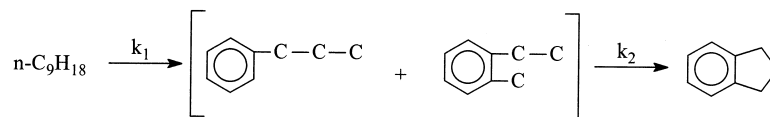
Scheme 3.

Table 6
Conversion of *n*-nonane in the presence and absence of thiophene[a] (from [40])

Catalyst	Time on stream (min)	Conversion to aromatics (mol%)	Thiophene in product (mol%)	C$_9$-aromatics (mol%)						
				PrBz	Toluene				Indan	Indene
					o-ethyl	*m*-ethyl	*p*-ethyl			
Pt-Al$_2$O$_3$-K (no thiophene)	37	40		25.6	47.7	6.1	0.6		15.2	5.5
	74	31		25.2	49.8	6.5	1.2		12.5	4.8
	111	24		24.8	51.0	6.7	1.9		11.4	4.3
	149	21		23.5	50.2	7.9	0.2		11.7	4.6
	186	18		23.6	52.8	7.3	1.6		10.6	4.1
Pt-Al$_2$O$_3$-K (with thiophene)	39	45	7.2[b]	30.3	65.5	Trace	Trace		4.2	–
	79	31	8.2[b]	30.8	69.2	Trace	Trace		Trace	Trace
	123	28	8.6[b]	–	–	–	–		–	–
	161	22	8.6[b]	30.1	68.5	Trace	Trace		Trace	–

[a] 482°C, 3.5 cm^3 of H$_2$/min; LHSV = 0.3.
[b] 15.1% thiophene in the *n*-nonane charge.

Table 7
Selectivity for bicyclic aromatic formation over Pt and moderated Pt catalysts for the first sample collected at about 50 min[a] (from [40])

Reactant	Pt metal moderator	Total aromatic (glc area %)	Bicyclic aromatic (glc area %)	Bicyclic/total cyclic
n-nonane	None	42	21.0	0.5
	Thiophene	45	2.0	0.04
	Tin	66	1.2	0.02
n-decane	None	23	15.0	0.4
	Thiophene	45	4.3	0.1
	Tin	72	4.8	0.07

[a] 482°C, atmospheric pressure; LHSV = 0.3.

are summarized in Table 5 and clearly demonstrate that a variety of promoters alter the aromatic selectivity of *o*-xylene : ethylbenzene = 1 : 1 for Pt-Al$_2$O$_3$ to approach *o*-xylene : ethylbenzene = 2 : 1 for all of the promoted catalysts.

For *n*-nonane and higher carbon number alkanes, a second cyclization to form a bicyclic indan or naphthalene structure is possible; e.g. Scheme 3.

As can be seen by the data in Tables 6 and 7, both tin and thiophene behave similarly and drastically decrease the extent of the second cyclization to produce a bicyclic aromatic. The data in Table 7 represent the

first sample collected; the data in Table 6 suggest that the difference would have been greater at later time on stream. If Re has the same influence on the second cyclization activity as Sn and thiophene, the improved catalyst life of the commercial Pt-Re catalyst may be due to a decrease in the rate of bicyclic (and polycyclic coke) ring compounds.

A most striking alteration of catalytic property by promoters was shown in the work by Sinfelt [42]. Using a Ni-Cu alloy catalyst, it was shown that the specific activity for dehydrogenation of cyclohexane remained nearly constant as the Ni : Cu alloy became
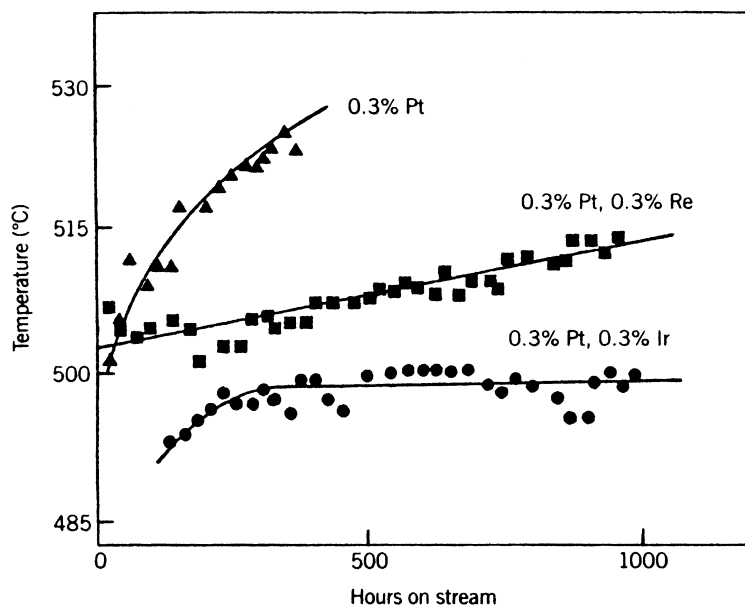
Fig. 5. Data on the reforming 99–171°C boiling range naphtha showing the temperature required to produce 100 octane number product as a function of time on stream for alumina-supported platinum, platinum-rhenium, and platinum-iridium catalysts at 14.6 atm pressure (from [43]).

richer in Cu. However, the activity for the hydrogenolysis of ethane to methane decreased very rapidly as the Cu content of the alloy increased. Sinfelt has shown that similar results can be obtained with bimetallic mixtures whose solubilities do not allow alloy formation. These have been termed 'cluster' catalysts by Sinfelt and are presumably the basis of a commercial reforming catalyst [43].

Sinfelt and coworkers [43] developed a Pt-Ir alumina catalyst that was considered to exist as small bimetallic clusters. The authors presented extensive characterization data to indicate that the clusters are reasonably uniform in composition and have properties expected for uniform alloy catalysts. The incorporation of Ir modifies the catalytic properties of Pt, especially in decreasing the hydrogenolysis activity. Furthermore, these catalysts are claimed to have even greater stability than the Pt-Re catalyst (Fig. 5).

A catalyst that exhibited early promise as a selective dehydrocyclization catalyst was formed by adding tellurium to a nonacidic zeolite [44–47]. Thus, up to 10 wt.% Te could be added into the pore structure of NaX zeolite merely by heating a physical mixture of the zeolite and elemental Te. Unfortunately, in

a hydrogen flow needed to maintain activity during naphtha conversion, almost all of the Te was lost in a matter of hours or days of operation. This type of catalyst only has academic interest.

The initial report [48] of the selectivity of Pt-KL zeolite catalyst for converting n-hexane to benzene was extended and eventually developed to a commercial catalyst by Chevron workers [9,10]. An early view of the reason for the selectivity of this catalyst was that highly dispersed Pt, atom or small cluster, selectively adsorbed n-hexane by a terminal carbon and that the shape selectivity of the pore structure associated with the Pt allowed only direct 6-carbon ring formation [49]. However, this model could not account for a similar selectivity for a catalyst made by the addition of Pt to a support of Al stabilized MgO [50].

4. Structure of the catalyst

Chromia and molybdena, unsupported or when present on a support, exhibit a very complex structure. The pioneering work of Eischens and Selwood [51] showed very clearly that chromia was spread upon
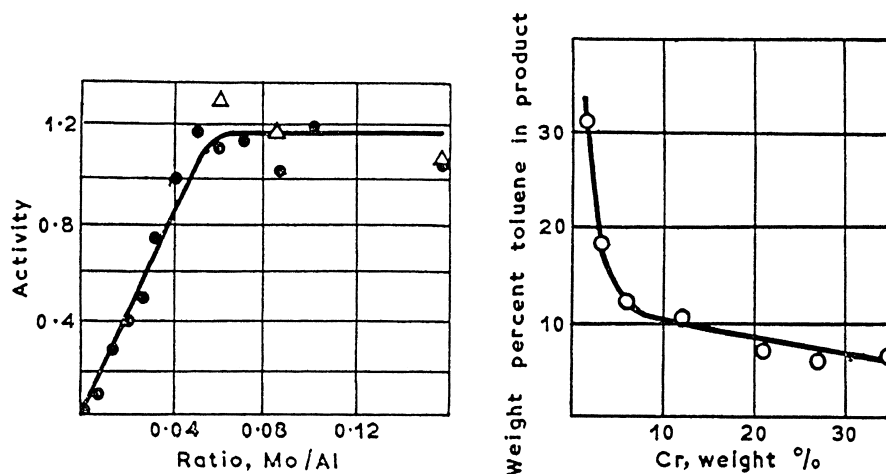
Fig. 6. (left) Effect of molybdena concentration on the activity of activated alumina F, surface area $91\,m^2/g$, for the conversion of heptane to toluene ($\triangle$, 450°C; $\bullet$, 497°C) (from [57]). (right) Catalytic activity for heptane dehycrocyclization as a function of chromium concentration (from [51]).

the surface of the support at low loadings. However, for a catalyst with 10% chromia, three-dimensional chromia particles existed on the support surface. In general, three-dimensional chromia particles are formed more easily on a silica support than on an alumina support, and this difference becomes more pronounced at chromia loadings below about 10 wt.% [52,53]. Chromia-alumina catalysts show evidence for surface acidity, even when some alkali has been incorporated (e.g., [54,55]). Voltz et al. [55] concluded that the differences in acidity between the oxidized and reduced states were one-half of the corresponding differences between the amounts of Cr^{6+} present on the surface. They also indicate that potassium hydroxide decreases the acidity of both the oxidized and reduced catalysts; the potassium increases the surface oxidation of the catalyst over one that does not contain potassium.

Molybdena–alumina catalysts have similar activities for *n*-heptane dehydrocyclization at 1 and 20 atm [56]. Chromia is more active than molybdena at 1 atm but is essentially inactive at 20 atm pressure. The dehydrocyclization activity increases linearly with Mo loading to about 14 wt.% molybdena, and then becomes constant with further increases in Mo loading (Fig. 6); this indicates that molybdena is present on the surface up to a monolayer loading before three dimension molybdena particles begin to form. Holl

et al. [58] indicate that for molybdena-alumina catalysts that are reduced in hydrogen to temperatures of 750°C, the skeletal isomerization of hydrocarbons is essentially by an acidic mechanism. However, when the reduction is at 950°C, the skeletal isomerization behaves like the catalyst was unsupported Mo metal. On the metal, isomerization occurs via a metalloacycle intermediate giving exclusively bond shift migration.

In summary, the surface of chromia and molybdena, unsupported and supported, is complex with a range of metal valence states. Under conditions normally encountered in use as a dehydrocyclization catalyst, both chromia and molybdena show an acidic character. Any mechanistic study with these catalysts must make sure that this acidity has not partially or completely determined the aromatic product or the isotopic label distribution.

Metallic catalysts are in general less complex than metal oxide catalysts; however, metal alloys may meet or exceed the complexity of the metal oxides. The characterization of metal naphtha reforming catalysts has been reviewed recently and will not be repeated here (e.g., [59–62]).

With few exceptions, platinum is considered to be in the metallic state in Pt-alumina catalysts. In most of these catalysts, Pt is very well dispersed so that essentially all Pt atoms are present in an exposed position. Thus, the chemisorption of hydrogen occurs according

to a stochiometry of H/Pt = 1. With usage this ratio will decrease and the Pt particles will be found in the 1.0–10 nm range. As indicated above, McHenry et al. [36] believed they had evidence to support the view that Pt was not present in the metallic state but was in an ionic form that could be extracted with dilute HF or acetylacetone. More recently Botman et al. (e.g., [63]) have presented data that they believe support the view that Pt is present in some positive valence state. In spite of these dissenting views, most believe that platinum is present in a metallic state.

The situation is more complicated when two or more metals are present. There was initially much debate over the state of tin in platinum-tin-alumina catalysts. However, it is now generally accepted that Pt-Sn alloys are formed [59,64]. It is now generally accepted that some, if not all, of the Re is in close association with Pt in Pt-Re-alumina catalysts. Furthermore, it is usually necessary to add sulfur during the 'start-up procedure' for Pt-Re catalysts, and the small amounts of sulfur added during this period are generally considered to be bonded to the Re atoms, and not Pt.

The Pt in Pt-KL or BaKL zeolites is usually present in crystals that are not larger than the pore channels. The Pt in these catalysts is especially prone to crystal growth in the presence of even very low (ppb) sulfur concentrations [59–62]. Because of the lack of interconnection of the long channels of the zeolite, the larger platinum particles effectively block entry into the channels and thereby greatly decreases the catalytic activity.

5. Hydrocarbon conversions

5.1. Bifunctional catalysis

An aspect of the conversion of alkanes that has attracted attention is the role of acidity, when present [65]. The introduction of chlorided Pt-alumina catalysts in the late 1940s provided incentive for much interest in the mechanism of alkane conversion and this was the basis for the development of theories to account for bifunctional catalysis. In the case of naphtha reforming, the interconversion of C_5- and C_6-rings permitted the naphthenes to be converted to aromatics with high selectivity and a bifunctional

mechanism was advanced to account for this [66]. Thus, an equilibrating reaction involving C_5- and C_6-ring compounds was established and the dehydrogenation of the C_6-ring compounds continuously caused the equilibrium to shift to produce six-carbon ring aromatic compounds.

Silvestri et al. [67] converted *n*-heptane over catalysts with 100 ppm H_2S added to the hydrocarbon/hydrogen feed stream. This level of H_2S poisoned the Pt function from converting *n*-heptane to aromatics but still allowed for dehydrogenation to the extent that the *n*-heptane/*n*-heptenes equilibrium was maintained. With either a Pt-carbon catalyst or a Pt-free acidic alumina catalyst, essentially no aromatics were produced. However, when a physical mixture of these two catalysts was utilized under the same reaction conditions, a large increase in the formation of ring products was observed. The authors considered this to demonstrate that alkane cyclization reactions can proceed by a dual functional mechanism and that the acid function can effect cyclization.

In the case of the bifunctional catalyst, isomerization reactions eliminate the ability to utilize tracers, either isotopic or alkyl groups, to understand the cyclization process. For example, it has been shown that, with bifunctional catalysts, the conversion of *n*-octane under normal reforming conditions (100–400 psig; 0.68–2.7 MPa) initially leads to the formation of methylheptanes, dimethylhexanes and ethylhexanes [12–14]. Subsequently, the C_8-alkane isomer mixture is converted to aromatics. Furthermore, the conversion of the C_8-alkane isomer mixture to C_8-aromatics occurs more rapidly than *n*-octane is converted to aromatics using a non-acidic, monofunctional Pt-Al_2O_3 catalyst (Fig. 7). These results indicate that the acid function of a bifunctional catalyst must be involved in the cyclization step, presumably involving a carbocation formed from an alkene produced by alkane dehydrogenation with the metallic function. While of interest from the commercial viewpoint, the bifunctional pathway will not be considered in detail in this discussion. Thus, the following sections emphasize those studies that utilize monofunctional dehydrocyclization catalysts. These monofunctional catalysts are of special interest for *n*-hexane dehydrocyclization since the bifunctional pathway does not produce aromatics in a selective manner; the formation of the five-carbon ring by the acid function must involve a
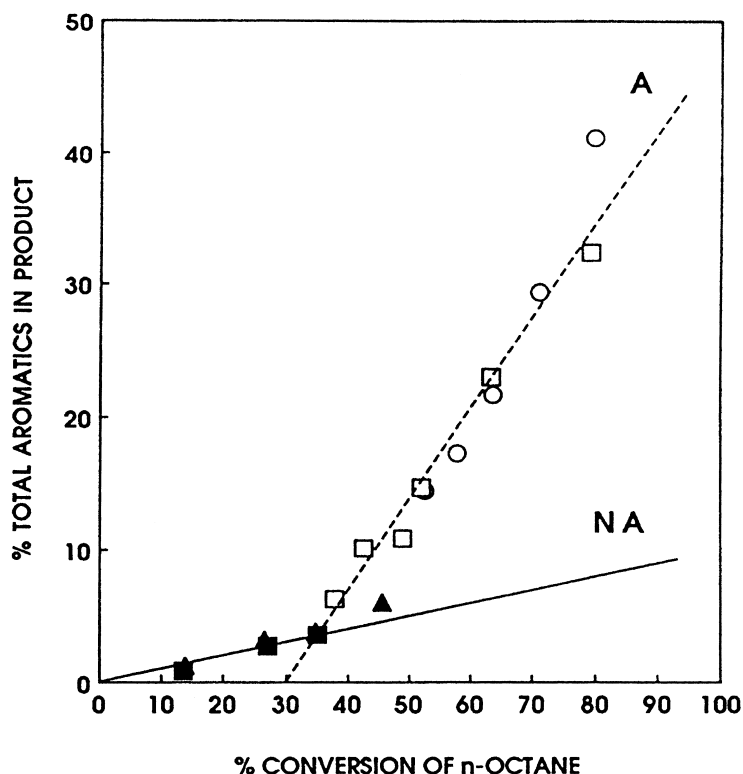
Fig. 7. The total aromatics in the liquid product vs. *n*-octane conversion (including conversion to *iso*-octane isomers) for catalysts based upon acidic (A) and non-acidic (NA) supports. (○) 0.6 wt.% Pt on precipitated alumina, COP; (□) 1.0 wt.% Pt on UCI alumina; (▲) 1.0 wt.% Pt on silica, SIL; (■) 1.0 wt.% Pt on non-acidic alumina, NAA (from [14]).

structure with a high-energy primary carbocation and this inhibits the rate of the bifunctional pathway.

5.2. Hydrogenolysis

5.2.1. Hydrogenolysis of alkane

One of the alkane reactions is hydrogenolysis [68]. It was established that the kinetics of hydrogenolysis of ethane was consistent with the occurrence of dehydrogenation to produce a surface species with carbon having three bonds to the metal surface. This dehydrogenation and multiple bonding to the surface was sufficient to weaken the carbon–carbon bond, to allow it to rupture to produce two C_1 fragments, and the two fragments to be hydrogenated to produce methane (e.g., [68–71]). With higher carbon number alkanes, a selectivity is introduced since there are multiple carbon–carbon bonds. For *n*-hexane three types of carbon–carbon bond positions are available. As shown

Table 8
Relative rates of hydrogenolysis of various C–C bonds in *n*-hexane with Pt catalysts

Catalyst	Relative rates			Reference
	C_1–C_2	C_2–C_3	C_3–C_4	
Pt single crystal (1 0 0)	1.0	2.5	5.5	[72]
Pt single crystal (1 1 1)	2.3	1.0	4.4	[72]
Pt-SiO_2	1.2	1.0	2.9	[68]
Pt-SiO_2-Al_2O3	1.14	1.0	2.9	[69]
Pt film (1 $\mu g/cm^2$)	1.0	1.3	1.8	[70]
Pt-SiO_2 (1.8 nm)	1.0	1.1	3.4	[71]

by data representative of hydrogenolysis of *n*-hexane, it is apparent that at low and intermediate temperatures (100–300°C) similar product distributions are obtained by a number of investigators using a variety of catalysts (Table 8).

Davis et al. [72] report that the positional selectivity for *n*-hexane hydrogenolysis showed a marked dependence on the surface structure of platinum. Surface
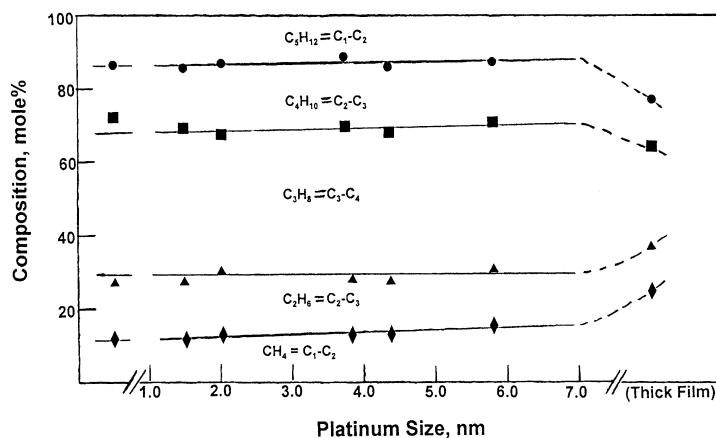
Fig. 8. Dependence of the product distribution from hydrogenolysis of *n*-hexane on Pt particle size (data from [70]).

faces with a high concentration of (1 0 0) microfacets [(1 0 0) and (13 1 1)] exhibit a high specificity for scission of internal C–C bonds. In contrast, those surfaces composed mostly of (1 1 1) microfacets ((1 1 1), (3 3 2) and (10 8 7)) showed a clear preference for central and terminal C–C bond scission. The results reported by Davis et al. [72] differ from those who report a nearly statistical bond hydrogenolysis of *n*-hexane [73,74].

In agreement with the results of Myers and Munns [69], van Schaik [75], Cinneide and Gault [76], Anderson and Shimoyama [70] find a preference for the hydrogenolysis of the central C–C bond. Furthermore, for conversion at 273°C, 100 Torr, H_2/h.c. = 10/1 in a recirculating apparatus, the position of C–C bond attack did not appear to be dependent upon the Pt particle size, except perhaps for very large particles (Fig. 8). For the largest particles, terminal C–C bond hydrogenolysis may be favored but, as shown in Fig. 8, the central C–C bond cleavage is favored for particle sizes in the range normally encountered in naphtha reforming catalysts. The data in Fig. 8 show a relative selectivity of C_1–C_2 : C_2–C_3 : C_3–C_4 = 1 : 1.3 : 1.8.

Leclercq et al. [77] converted 16 different alkanes with a variety of branching with a Pt-alumina catalyst. Ignoring those reactants with a quaternary carbon, the authors favored a 1,1,3-adsorbed species such as postulated by Anderson [78] although all of their results could not be reconciled by a single mechanism. Rather, Leclercq et al. considered their data to support the view of the participation of 1,2-, 1,3-, 1,4-, and 1,5-diadsorbed species. In

close agreement with Davis et al. [72] and Myers and Munns [69], Leclercq et al. found the relative rates of C–C bond hydrogenolysis in *n*-heptane to be C_1–C_2 : C_2–C_3 : C_3–C_4 = 2.0 : 1.0 : 2.3.

As shown by Carter et al. [11], metals like Rh have a reaction rate for *n*-heptane hydrogenolysis that is about 100 times greater than platinum (Fig. 9) [79]. These reactions were conducted at low temperatures (88–300°C) and pressure (1 atm) with H_2/n–C_7H_{16} = 5. Under these conditions, hydrogenolysis competes effectively with isomerization, and both reactions exceed that of dehydrocyclization (Table 9).

Considering all data for *n*-hexane hydrogenolysis presents a picture of constrasts. First, nickel and rhodium show a marked difference from Pt since the two former metals show a dominance of hydrogenolysis of the terminal C–C bond. This is apparently due to Ni and Rh adsorbing the carbon fragment so strongly that, rather than forming methane and *n*-pentane from *n*-hexane, the dominant pathway is for the C_5-fragment to remain absorbed and for the terminal C–C bond cleavage to continue until *n*-hexane has been converted to six methane molecules. In addition, those metals that produce primarily methane are more active for hydrogenolysis than those with statistical or center bond hydrogenolysis.

In summary, Pt, among Group VIIIB metals, is relatively inactive for hydrogenolysis reactions. However, at low temperature and pressure conditions, hydrogenolysis makes a major contribution to the total conversion. At the temperatures and pressures
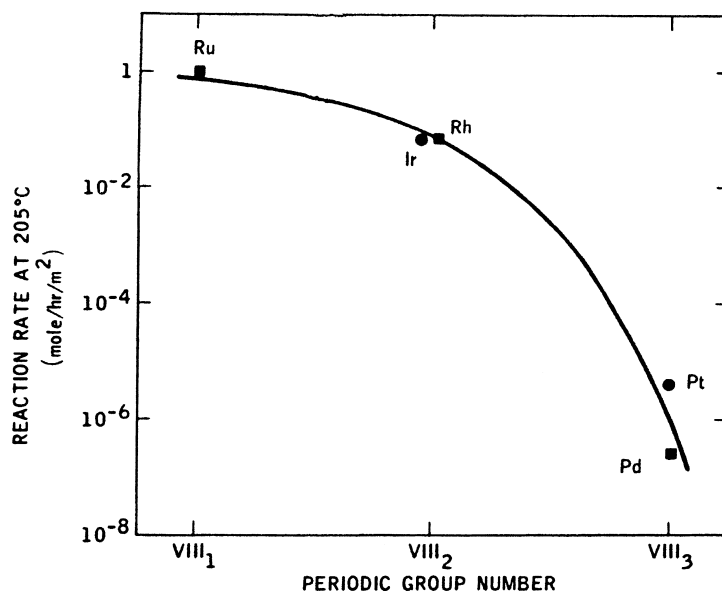
Fig. 9. Catalytic activities of group VIII noble metals for *n*-heptane hydrogenolysis. The activities are compared at a temperature of 205°C at 1 atm pressure and a H_2/nC_7 mole ratio of 5/1 (from [79]).

Table 9
Reactions of *n*-heptane on metals in the presence of hydrogen[a] (from [43])

Metal	Temperature (°C)	Percent total conversion	Percent hydrogenolysis	Percent isomerization	Percent dehydrocyclization
Pd	300	6.4	5.8	0.4	0.2
Rh	113	2.9	2.7	0.2	–
Ru	88	4.0	3.7	0.3	–
Pt	275	2.3	0.6	0.7	1.0
	275	9.4	3.4	3.8	2.2
	275	21.4	8.0	10.0	3.4
Ir	125	1.5	1.3	0.2	–

[a] Conditions: 1 atm, H_2/nC_7 mole ratio = 5.

normally encountered in commercial reforming, hydrogenolysis makes a less significant contribution to the total conversion [80].
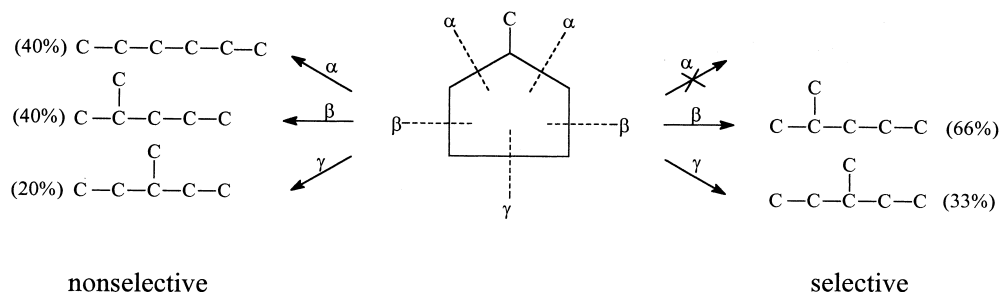
5.2.2. Hydrogenolysis of alkylcyclopentanes

The study of hydrogenolysis of alkylcyclopentanes predates that of dehydrocyclization [81] and these studies were continued by one of the discovers of dehydrocyclization [82,83]. Gault, in his authoritative review, [84] identified two extremes for hydrogenolysis of methylcyclopentane as nonselective (statistical) and selective, as outlined in Scheme 4.

An examination of the data collected in Table 10 show a variety of selectivities. With highly dispersed platinum catalysts, the data agree with the nonselective reaction pathway. Gault [84] concludes, however, that when all data are considered, more than two ring opening pathways are needed to describe the data.

The use of metal films has become a popular approach to evaluate the activity and selectivity of a metal catalyst while eliminating, or at least minimizing, the impact of support effects. By controlling the parameters of preparation, metal films can be deposited so that they produce a narrow range of particle sizes and, at the same time, the average particle size can vary over a wide range. Unfortunately, this approach is limited to temperatures considerably below those where dehydrocyclization occurs at a reasonable rate; at dehydrocyclization temperatures

(40%) C—C—C—C—C—C

C

(40%) C—C—C—C—C

C

(20%) C—C—C—C—C

α
β
γ

α
β
γ

α
β
γ

C—C—C—C—C (66%)

C

C—C—C—C—C (33%)

nonselective   selective

Scheme 4.

Table 10
Products from hydrogenolysis of methylcyclopentane

Catalyst	Reduction temperature (°C)	T (°C)	P_{H_2}	H_2/MCP	Products (mol%)			Reference
					2MP[a]	3MP[a]	H[a]	
PtKL	300	270	0.89	8	32(1.1)[b]	29(1.0)[c]	29	[88]
	300	270	0.98	40	33(1.0)	33(1.0)	33	[88]
PtKL	450	270	0.98	40	39(0.13)	30(1.0)	30	[88]
Pt-SiO$_2$	450	270	0.98	40	51.8(3.1)	16.6(0.54)	30.9	[88]
Pt-Al$_2$O$_3$	450	270	0.96	22	66(2.9)	23(2.5)	9.3	[88]
EUROPAT1(0.17 nm)	227	227	0.99	316	39(2.0)	20(0.49)	41	[89]
	247	247	0.99	316	38(2.1)	18(0.41)	44	[89]
	297	297	0.99	316	38(1.5)	26(0.72)	36	[89]
Pt-SiO$_2$ (2.2 nm)	227	227	0.99	316	46(2.3)	20(0.59)	34	[89]
	247	247	0.99	316	43(2.4)	18(0.49)	39	[89]
	297	297	0.99	316	39(1.5)	26(0.74)	35	[89]
Pt-Al$_2$O$_3$ (2.3 nm)	227	227	0.99	316	50(2.5)	20(0.67)	30	[89]
Pt(0.48)Re(1.8)Al$_2$O$_3$	550	300	0.90	9.5	54(1.5)	37(4.2)	8.8	[90]
Pt-SiO$_2$ (1.8 nm)	300	277	0.95	18	40(2.1)	19(0.50)	38	[71]
PdNaY	350	275	0.94	16	45(1.7)	27(1.6)	17	[91]
Pt-SiO$_2$		210–260	1 atm total	–	56(1.4)	42(25)	1.7	
Pt-Al$_2$O$_3$		210–260			50(1.3)	40(4.0)	10	[92]
PtC		210–260			53(1.3)	42(8.4)	5	[92]
Pt-SiO$_2$	300	250	0.95	20	42.1(2.7)	15.6(0.38)	41.3	[85]
PtNaY	300	250	0.95	20	52.9(2.1)	25.6(1.3)	19.9	[85]
Pt-SiO$_2$		485	6.8	2	36.8(1.5)	24.1(0.62)	39.1	[86]
Pt(0.2%)-Al$_2$O$_3$		250–310	~1	high	41(2.0)	21(0.55)	38	[87]

[a] 2MP = 2-methylheptane; 3MP = 3-methylpentane; H = *n*-hexane.

[b] Numbers in parentheses are 2-MP/3-MP.

[c] Numbers in parentheses are 3-MP/H.

sintering of the film occurs so that only very large metal particles are present. The results from two studies are compared in Fig. 10 [73,93]. While Kramer and Fischbacker [93] obtain less *n*-hexane with the larger Pt particles than Anderson and Shimoyama [73] do, the results for the highly dispersed Pt catalysts are in excellent agreement and are consistent with a nonselective hydrogenolysis reaction pathway.

Gault [94] converted methylcyclopentane with a series of Pt-alumina catalysts wherein the Pt particle size was controlled by varying the Pt content from 0.15 to 20 wt.%. The runs were made in a batch reactor at 315°C and 30 atm (3.03 MPa). The ratios of bond breaking ($R_{\beta/\gamma}$ and $R_{\gamma/\alpha}$ from Scheme 4) are plotted versus increasing platinum content (increasing platinum particle size) in Fig. 11. For the lower loading,
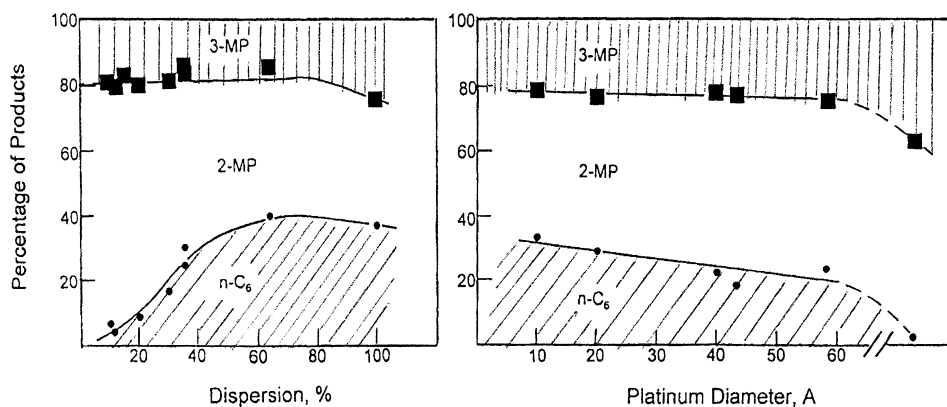
Fig. 10. Selectivity for conversion of methylcyclopentane (left from data in [70]; right from data in [93]).
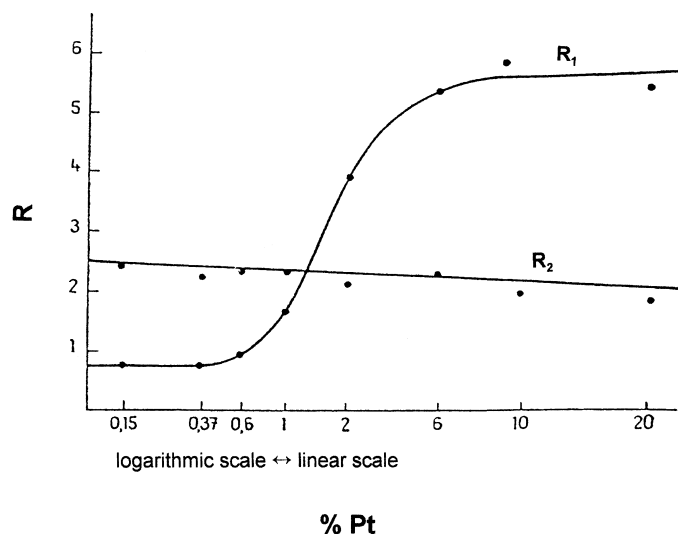

Fig. 11. Dependence of values of R_1 ($R_{\beta/\gamma}$) and R_2 ($R_{\gamma/\alpha}$) on Pt content of catalyst (from [94]).

lower Pt particle size catalyst the ratio $R_{\beta/\gamma}$ is nearly constant at 2.5, slightly higher than the value of 2.0 for pure nonselective bond rupture. The other selectivity strongly depends on Pt particle size.

For the hydrogenolysis of n-alkanes, the rate of C–C bond rupture normally has an inverse dependence on hydrogen pressure. However, the data of Brandenberger et al. [86] show that the rate of ring-opening hydrogenolysis of methylcyclopentane has a positive, rather than negative, dependence on hydrogen partial pressure (Table 11). These results imply that the rate limiting step does not involve dehydrogenation of methylcyclopentane to produce a

Table 11
Platinum-catalyzed ring opening[a] (from [86])

H_2 partial pressure (atm)	6.8	10.2	13.6	17.0
Ring-opening rate (μmol/s g)	9.8	14.0	17.6	19.9
Hexane composition (mol%)				
2-methylpentane	36.8	39.6	41.0	39.6
3-methylpentane	24.1	20.9	22.0	22.3
n-hexane	39.1	39.5	37.0	38.1

[a] 0.71 wt.% Pt/SiO_2, 485°C, 3.4 atm MCP.

carbon that is multiply bonded to a surface Pt atom. Equally important, it is evident that hydrogenolysis is nonselective and that the selectivity for ring-opening

	Calc.	Exp.
3-methylhexane	40	40.8
2,4-dimethylpentane	20	18.5
2-methylhexane	40	40.7
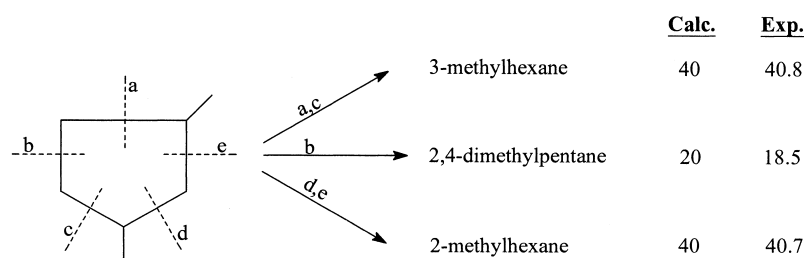
Scheme 5.

Table 12
Products from the conversion of ^{14}C-labeled 1,3-dimethylcyclopentane at 482°C and 18 atm (from [97])

Compounds	Mol%
Methane + ethane	8.5
Propane	3.6
$i + n$-butane	3.9
$i + n$-pentane	1.3
Methylcyclopentane	0.5
2-methylpentane	3.7
3-methylpentane	1.5
n-hexane	2.4
2,4-dimethylpentane	10.3
2-methylhexane	22.8
3-methylhexane	22.7
n-heptane	0.0
Toluene	8.8

does not depend to a measurable extent upon hydrogen partial pressure. In contrast, Levitskii and Minachev [95] reported a selectivity that depends upon hydrogen partial pressure for a Pt-SiO$_2$ catalyst (n-hexane : 2-methylheptane : 3-methylheptane = 1.0 : 4.2 : 1.5 at 10 atm H$_2$ and 1.0 : 1.4 : 0.8 at 50 atm).

Lester [96] obtained data that suggest that hydrocarbons which contained alkyl substitution and with the longest chain having 5-carbons could cyclize on supported Pt-catalysts to form a cyclopentane structure which then underwent intermolecular ring expansion to produce a six-carbon ring intermediate which subsequently dehydrogenated to produce the aromatics. To date, additional reports with the high selectivity for aromatics that was obtained by Lester have not appeared.
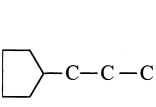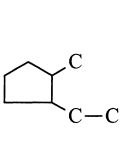
That the 5-carbon ring does not directly expand to a six-carbon ring on a monofunctional Pt catalyst operated at reforming conditions has been conclusively demonstrated by Csicsery and

Burnett [97]. These authors utilized a 2 wt.% Pt-SiO$_2$ catalyst and operated at 482°C and 18 atm (1.8 MPa) with a hydrogen/hydrocarbon ratio of 6. They converted a mixture that contained 2 vol% of ^{14}C-labeled 1,3-dimethylcyclopentane present in a 4 : 1 n-heptane : m-xylene mixture. The ^{14}C content of the products permitted them to identify those that were derived from the conversion of 1,3-dimethylcyclopentane (Table 12). The isopentane products agree with those calculated for a nonselective mechanism (Scheme 5).

Toluene accounts for only about 14% of the toluene plus isoheptane products. Because the 2- and 3-methylhexane hydrogenolysis products can undergo cyclization to produce toluene, the ring expansion pathway must be smaller than represented by 14% toluene. The products from the ring opening reaction are in excellent agreement with those expected for a non-selective hydrogenolysis reaction and with those of Brandenberger et al. [86].

Hardy and Davis [98] converted n-propylcyclopentane and 1-methyl-2-ethylcyclopentane with a Pt-nonacidic alumina catalyst at 482°C and about 14 bar. The products from both C$_8$-isomers fit very well the products predicted for a non-selective hydrogenolysis mechanism (Scheme 6).

Studies were also conducted where each of the two alkyl- or dialkyl-cyclopentane isomers were converted when these compounds were present at about 10–15% in n-heptane. The amount of C$_8$-aromatics and C$_8$-isoalkanes could be determined and the results showed that only 7–8% of the conversion products from the alkylcyclopentanes were C$_8$-aromatics. The data from these runs are compared in Table 13 to the data of Csicsery and Burnet [97] as well as the data obtained by Huang et al. [99] and all show that less than 20% of the alkylcyclopentane underwent

	Predicted	Observed
n-octane	40	33
4-methylheptane	40	42
3-ethylhexane	20	22[a]
other	0	3
n-octane	20	46
3-ethylhexane	20	14[a]
2-methyl-3-ethylpentane	20	10
3,4-dimethylhexane	20	8
4-methylheptane	20	21

a = includes 3-methylheptane if formed.

Scheme 6.

Table 13
Percentage of aromatics produced in the conversion of alkylcyclopentanes

Reactant	Reaction conditions	(Aromatics/(aromatics + hydrogenolysis products)) × 100	Reference
n-heptane labeled (2.5 vol% 1,3 [^{14}C]dimethyl-cyclopentane)	482°C, 18 atm, 6 : 1 H$_2$: hydrocarbon, 2% Pt-SiO$_2$	13.6	[97]
n-heptane (15% n-propylcyclopentane)	482°C, 13 atm, 9 : 1 H$_2$: hydrocarbon, 0.6% Pt on nonacidic alumina	7.1	[98]
n-heptane (8% 1-methyl-2-ethylcyclopentane)	482°C, 13 atm, 9 : 1 H$_2$: hydrocarbon, 0.6% Pt on nonacidic alumina	8.3	[98]
n-octane (2.4% n-[^{14}C]propylcyclo-pentane)	482°C, 13 atm, 7 : 1 H$_2$: hydrocarbon, 2% Pt-KL	10–18	[99]

ring expansion to produce aromatics. Since some of the *iso*-octanes formed by hydrogenolysis can cyclize by direct six-carbon ring formation to produce C$_8$-aromatics, the actual percentage will be less than shown in Table 13. Thus, under reforming conditions the dominant reaction pathway was hydrogenolysis of the cyclopentane ring to produce *iso*-octanes and not ring expansion.

Yamada et al. [90] investigated the impact of the reduction temperature upon a series of Pt-Re-alumina catalysts that were then used for the hydrogenolysis of methylcyclopentane at 300°C and 1 atm total pressure. For the catalyst that was reduced at a low temperature, the three allowed hexane isomers are present in a ratio that is similar to that of a nonselective mechanism. In addition, slightly more than 10% of the products result from hydrogenolysis to produce methane and cyclopentane (Fig. 12). As the reduction temperature increases (and Pt particle size increases), the product distribution changes. Surprisingly, the amount of

n-hexane increases with increasing particle size; this is in contrast with the trend obtained by most workers with increasing Pt particle size. As the amount of Re added to a constant loading of Pt increases, the methylcyclopentane conversion first decreases, then undergoes an increase to about five times that of Pt alone, and appears to reach a constant activity above this level (Fig. 13). The addition of Re to Pt causes the selectivity to change so that the amount of n-hexane decreases with a corresponding increase in both 2- and 3-methylpentane. The cyclopentane content is the same for Pt, Re and the Pt-Re mixtures (Fig. 14)

The selectivity for the hydrogenolysis of methyl-cyclopentane appears more complex for Pt-zeolite catalysts. The pore geometry of the zeolite structure limits the size of the Pt particle to about 1.0 nm; thus, these catalysts should resemble those of highly dispersed Pt catalysts. However, Sachtler and coworkers reported that this was not the case (e.g., [85,100,101]) for Pt-NaY zeolites. From the viewpoint of activity,
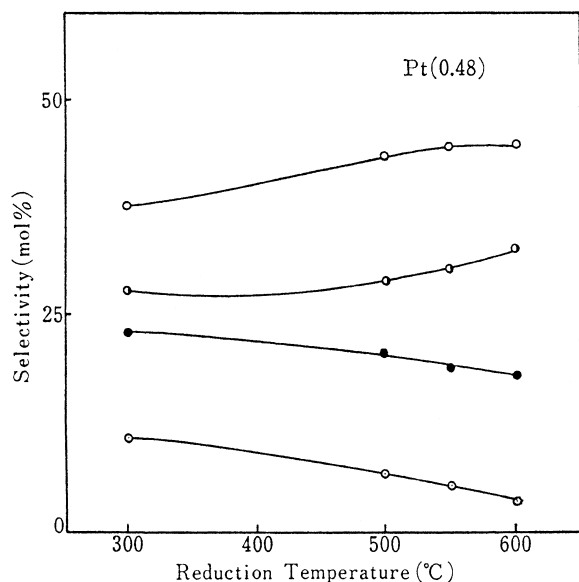
Fig. 12. Effect of reduction temperature on selectivity (W/F: 2.4g h/mol, H_2/methylcyclopentane: 9.5 mol/mol $\bigcirc$: 2-methylpentane, ●: 3-methylpentane, ◑: n-hexane, ⊙: cyclopentane (from [90]).
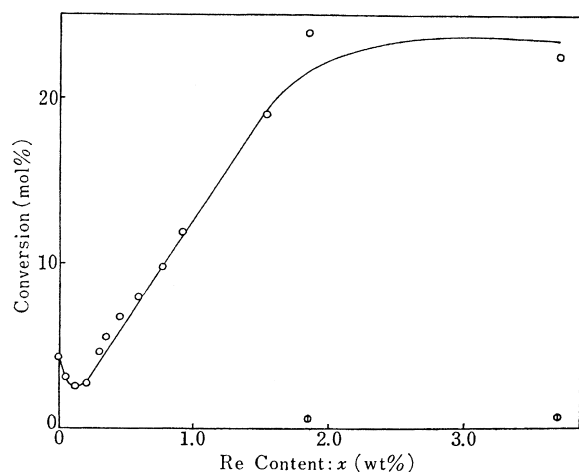

Fig. 13. Effect of Re content on activity (reduction temp.: 550°C, W/F:2.4 g h/mol, H_2/methylcyclopentane: 9.5 mol/mol, $\bigcirc$: Pt (0.48)-Re(x) bimetallic catalyst, ⊕: Re(x) catalyst) (from [90]).

Fig. 14. Effect of Re/(Pt+Re) content on selectivity (Catalyst: Pt (0.48)-Re(x), reduction temp.: 550°C, W/F: 2.4 g h/mol, H_2/methylcyclopentane: 9.5 mol/mol; $\bigcirc$: 2-methylpentane, ●, 3-methylpentane, ◑: n-hexane, ⊙: cyclopentane) (from [90]).

the basicity of the cation appears to play a role. Long range electron transfer from the alkali to the metal has been proposed (e.g., [102]) while others consider the effect to be due to local interactions in the vicinity of the alkali ions [103]. Alvarez and Resasco [104] found that the enhanced activity was more pronounced for higher Pt containing catalysts and concluded that, since the Pt crystals must have the same maximum size in the low and higher Pt containing catalyst, the number of Pt interacting with alkali ions must be larger in the higher Pt loaded catalyst. The Pt loading effect was therefore considered to favor local interactions as the cause for the augmentation of the hydrogenolysis activity.

The difference in Pt supported on silica and KL zeolite is illustrated in Fig. 15. While the Pt-silica catalyst gives approximately a nonselective product distribution, with the Pt-KL zeolite catalyst the amount of 3-methylpentane is increased and the amount of both 2-methylpentane and n-hexane is decreased. These authors compare data for their low and higher Pt-loaded KL zeolite catalysts and for their Pt-CabOSil together with three sets of selectivity data taken from the literature ((a) [88]; (b) [105]; (c) [106]) as a function of dispersion. The data for the Pt-CabOSil are similar to those for the three curves; however, the data for the two zeolite catalysts are very different. The 3-/2-methylpentane ratio is larger for the zeolite catalysts, and for the higher Pt loading, the 3-isomer is formed in larger amounts than the 2-isomer. This is the result that Gault would attribute to selective hydrogenolysis that is associated with
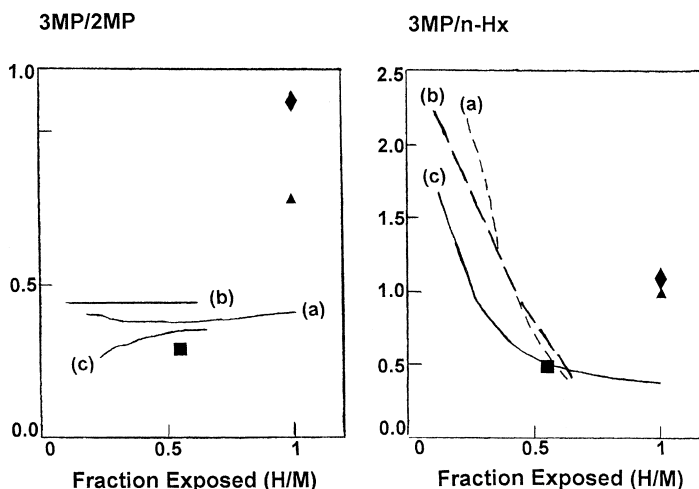
3MP/2MP   3MP/n-Hx

Fig. 15. 3-Methylpentane/2-methylpentane (left) and 3-methylpentane/n-hexane ratio dependence on platinum dispersion (H/M) for the conversion of methylcyclopentane with a Pt-KL zeolite catalysts (a, from [88]; b, from [102]; c, from [103]; ■, Pt-CabOSil; ▲, low Pt-loaded KL zeolite; ◆, high-Pt KL zeolite) from [104]).
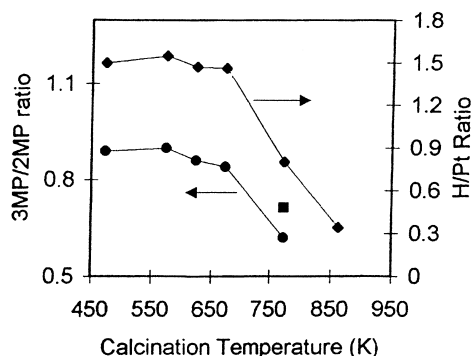

Fig. 16. 3-Methylpentane/2-methylpentane ((●) 3MP/2MP ratio) product ratio (left axis) and H/Pt (◆) chemisorption capacities (right axis) as a function of calcination temperature on the 0.6% Pt/KLTL catalyst. (Reduction temperature of 350°C and methyl-cyclopentane ring opening reaction temperature of 340°C) (from [107]).

large platinum crystals; however, Alverez and Resasco [107] show that this is not the case. They determined the dispersion (H/Pt ratio) and the 3-/2-methylpentane selectivity for increasing calcination temperatures, followed by reduction at 350°C, and found that the ratio remained high and constant up to a calcination temperature greater than 377°C (Fig. 16). Only when the sample was heated above 377°C did the dispersion and the 3-/2-methylpentane ratio decrease, with

the latter approaching that obtained for silica and alumina supported Pt. The situation is similar with the 3-methylpentane/n-hexane ratio where the zeolite samples have selectivities anticipated for much larger Pt particles.

Moretti and Sachtler [100], because methylcyclopentane has a length/width ratio of about 1.7, suggest that methylcyclopentane will align to diffuse so that the length of the molecule is aligned with the pore direction. If the 1.0 nm Pt particle fills the pore cavity, exposing the metal through the cage window, one end of the methylcyclo-pentane will contact the Pt particle. In one orientation, this alignment will cause the C–C bond that leads to 3-methylpentane to be attacked. However, the other alignment will cause the closest approach to favor the C–C bond that produces n-hexane to be attacked, and the data are not consistent with this. Moretti and Sachtler [100] introduce an additional geometrical effect. In one approach the methyl group is pointed to the metal and in the other the tertiary hydrogen will contact the metal; since methylcyclopentane is restricted from turning over in the pore; only the orientation with the tertiary hydrogen approaching the metal will lead to hydrogenolysis to produce n-hexane. Thus, only about half of the methylcyclopentanes that approach the Pt crystal with the methyl end of the molecule will be in the proper orientation to react, and this will cause a decrease in

Table 14
Comparison of products obtained from the conversion of n-octane with Pt-BaKL and Pt-KL catalysts (from [102])

	References [9,10]	Reference [99]
Catalyst	Pt-BaKL-866	Pt-KL
Pressure	6.9 bar	13.8 bar
Temperature	733 K	725 K
LHSV	6	ca. 1
Conversion (%)	30	27
C_8 aromatics		
Ethylbenzene + ortho-xylene	88	93.5
Meta- + paraxylene	12	6.5
Methylheptanes/C_8 aromatic	0.19–0.28[a]	0.52
3-ethylhexane/methylheptanes	0–0.51[a]	0.15
2-methylheptane	(8)[b]	18c(21)[b,c]
3-methylheptane	(34)[b]	26(28)[b]
4-methylheptane	(58)[b]	41(51)[b]
3-ethylhexane		15

[a] Range of values because of overlapping of 3-ethylhexane and 4-methylheptane.

[b] Percentage based upon methylheptanes.

[c] 2-methylheptane peak corrected for coelution of toluene.

the hydrogenolysis rate to produce n-hexane relative to that of 3-methylpentane.

Huang et al. [99] converted n-octane that contained 3 wt.% n-propyl-[1-ring-^{14}C]-cyclopentane with a Pt-KL zeolite catalyst at 482°C and about 14 bar. The preparation, activation and use of these Pt-zeolite catalysts is difficult since many variables must be controlled. Hughes et al. [9,10] reported results for a catalyst that had a long (months) life. The data Huang et al. [99] obtained are compared in Table 14 with those reported by Hughes et al. [9,10]; it is seen that the products at about the same conversion levels are nearly identical, both with respect to the aromatic and the iso-octane isomers. Unlike much of the data obtained for methylcyclopentane hydrogenolysis, Huang et al. found that the hydrogenolysis of n-propylcyclopentane occurred for both the n-propyl side chain and for the cyclopentane ring. Since the ^{14}C-label was in the ring, the identification of isotopically labeled ethyl- and methyl-cyclopentane products clearly show that it originated from the labeled n-propylcyclopentane reactant. The experimental data are in reasonable agreement with the distribution expected for non-selective hydrogenolysis of the eight C–C bonds located both in the n-propyl group and the cyclopentane ring (Table 15).

Table 15
C_8-Alkane distribution calculated for nonselective hydrogenolysis of all C–C bonds in n-propylcyclopentane and the normalized experimental distribution (from [99])

	Experimental[a]	Calculated[b]
a. 3-ethylhexane	51.2[c]	37.5
b. 2-, 3-, and 4-methylheptane	51.2[c]	37.5
c. n-octane	28.3	25.0
d. cyclopentane	10.7	12.5
e. methylcyclopentane	6.12	12.5
f. ethylcyclopentane	3.65	12.5

[a] Average of four runs.

[b] Calculated assuming statistical C–C bond hydrogenolysis.

[c] These products could not be separated using the GC column needed for ^{14}C counting.

Considering all of the data for methylcyclopentane hydrogenolysis, it appears the conversion is essentially nonselective for platinum that is highly dispersed on non-zeolitic supports. For the non-zeolite catalysts that are effective as dehydrocyclization catalysts, it is concluded that any contribution of C_5-ring formation will lead to isomerization through a nonselective mechanism for hydrogenolysis of cyclopentane isomers. It is puzzling that only a few authors report hydrogenolysis of methylcyclopentane to produce methane plus cyclopentane. For Pt-zeolite catalysts hydrogeneolysis of methylcyclopentane is selective but for n-propyl cyclopentane it is nonselective. There is insufficient data to define the overall selectivity character of Pt-zeolite catalysts.

5.2.3. Hydrogenolysis of alkylcyclohexanes

The hydrogenolysis of cyclohexane or alkylcyclohexane does not make a significant contribution during their conversion under normal reforming processes. The results obtained for the conversion of ^{14}C-labeled methylcyclohexane show that more than 95% of the methylcyclohexane was converted to toluene with either Pt-nonacidic alumina or Pt-acidic alumina at 482°C and 400 psig [108]. Demethylation by hydrogenolysis and/or dealkylation/transalkylation was the most prominent side reaction, even with the Pt-acidic alumina catalyst. Cracking to C_6- products made a small contribution to the minor amounts of side reactions.

Dermietzel [109] showed that methyl-labeled toluene, added to a light naphtha, does not undergo

significant conversion (less than 3 wt.%) during reforming at 520°C and pressures in the 0.5–2.0 MPa range.

Iglesia et al. [110] converted *n*-heptane containing a small fraction of ^{13}C-methyl labeled toluene over a Te/NaX zeolite catalyst at 450°C, 4.5 kPa hydrocarbons and 96 kPa hydrogen in a recirculating reactor. The added toluene, when 26% of the *n*-heptane had been converted, still contained 99.5% of the ^{13}C in the methyl position and 0.5% in the *ortho*-ring position.

It is therefore clear that one does not need to consider secondary reactions such as hydrogenolysis of alkylcyclohexanes or of the aromatic products that are formed during dehydrocyclization with monofunctional Pt catalysts.

6. Ring formation: C$_5$- and C$_6$-ring forming mechanisms

6.1. General

One of the features that has received much attention is the size of the ring initially formed during the dehydrocyclization process. As noted above, much of the early work that required additional mechanisms in addition to a direct six-carbon ring was conducted with metal oxide catalysts.

The dehydrocyclization of many alkanes, each containing eight or more carbons and at least one chain with six or more carbons, with a Pt-nonacidic alumina catalyst produced 90% or more of the aromatics predicted for the operation of only a six-carbon ring forming mechanism [111]. Fogelberg et al. [112,113] utilized a commercial Pt-alumina catalyst and a Pt-catalyst made 'nonacidic' by calcining the alumina support at a high temperature to produce a low surface area for the dehydrocyclization of *n*-octane as well as C$_8$-hexane and heptane isomers. With the commercial catalyst they obtained a nearly equilibrium C$_8$-aromatic composition; however, with the nonacidic catalyst the aromatics were predominantly (>90%) those expected for a direct six-carbon ring formation.

With these nonacidic Pt-catalysts the dehydrocyclization of C$_8$–C$_{10}$ alkanes produces simpler results than earlier workers had obtained with the metal oxide

catalysts. Thus, with Pt-nonacidic catalyst there was no need to invoke the complex bicyclic mechanisms that evolved to explain the aromatic isomers produced by dehydrocyclization of alkanes.

6.2. Comparison of the conversion of an alkane and its corresponding naphthene

Shown in Scheme 7 are some C$_8$ alkane isomers that would form 1,1,3-trimethylcyclopentane (**5**) by a C$_5$-ring closure. Of the four shown, only 2,4-dimethylhexane (**4**) provides a pathway that could lead to any cyclopentane isomer other than 1,1,3-trimethylcyclopentane. The data in Table 16 for the chromia catalyst make it apparent that **1**, **2**, and **3** do not yield the same C$_8$ aromatic distribution. In addition, they do not resemble the C$_8$ aromatic distribution obtained from the conversion of 1,1,3-trimethylcyclopentane. The amount of ethylbenzene and *o*-xylene relative to *m*-xylene which Pines and Chen [117] obtained from 1-methyl-2-ethylcyclopentane eliminate this ring structure from making a major contribution to the reaction pathway. 1,2,3-trimethylcyclopentane can also be eliminated as a possible intermediate because only *o*-xylene and *p*-xylene can be formed from it by a simple ring expansion pathway. The only C$_5$-cyclization pathway leading to *m*-xylene is through 1,1,3-trimethylcyclo-pentane followed by ring expansion route d in compound **5** . For 2,5-dimethylhexane, the trace amount of *m*-xylene excludes ring expansion d so that the ring expansion must follow path a in order to produce the *p*-xylene product. Thus, cyclization of both 2,4- and 2,5-dimethylhexane through the common C$_5$ ring compound, 1,1,3-trimethyl-cyclopentane, would mutually exclude all of the ring expansions that lead to C$_8$ aromatics. A direct C$_5$-cyclization for 2,2,4-trimethylpentane followed by ring expansion to a six-carbon ring requires expansion a but not d; furthermore, a would have to be at least 5 times larger than c + d to yield the experimental aromatic distribution. Hence, the data in Table 16 exclude C$_5$ ring closure for both 2,4- and 2,5-dimethylhexane. Dautzenberg and Platteeuw [118] were, to our knowledge, the first to use this reasoning to eliminate a common cyclopentane ring structure being formed from several alkane isomers. On the other hand, the data in Table 16,
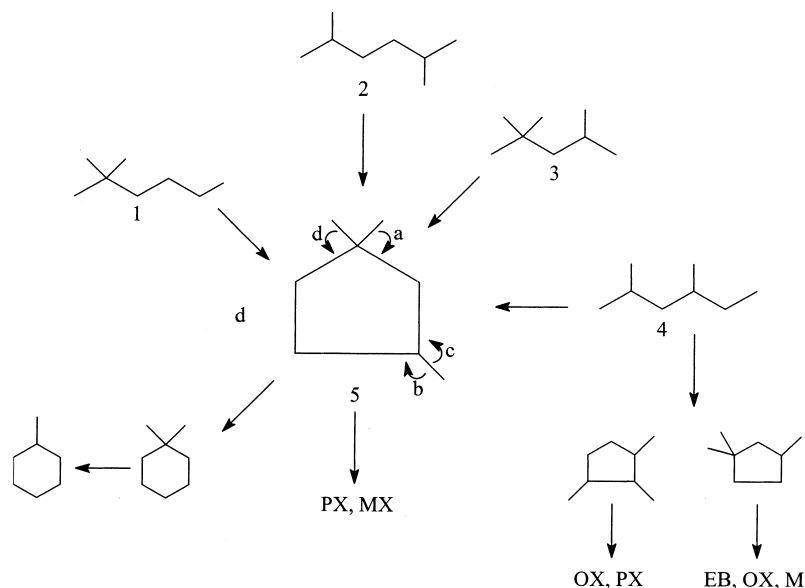
Scheme 7.

Table 16
Aromatic distribution from the conversion of C_8 alkanes and the corresponding naphthenes over chromia–alumina catalysts

Reactant	Aromatic selectivity[a]	Aromatic (mol%)						Reference
		Bz	Tol	EB	OX	MX	PX	
1 (2,2-DMH)[b]	12	13	50	8 (21)[c]	11 (31)	7 (18)	12 (31)	[115]
	–	–	21	2 (2)	37 (47)	33 (42)	7 (9)	[34]
2 (2,5-DMH)[b]	35	–	14.7	Trace	Trace	2.6 (3)	82.7 (97)	[115]
3 (2,2,4-TMP)[b]	21	–	17.6		5.3 (6.4)		77 (94)	[117]
	9	–	7.2	–	–	–	93 (100)	[116]
4 (2,4-DMH)[b]	26	11	58	–	–	27 (87)	4 (13)	[115]
5 (1,1,3-TMCP)[b]		–	6.7	–	6.7 (7)	60 (64)	27 (29)	[112]

[a] Total conversion to aromatic/total conversion.
[b] DMH = dimethylhexane; TMP = trimethylpentane.
[c] Numbers in parenthesis are for the mol% based on C_8 aromatics.

except for 2,2,4-trimethylpentane, are consistent with direct C_6 ring formation. The aromatic distribution from 2,2,4-trimethylpentane is essentially the same as that from 2,5-dimethylhexane; it has been suggested that a portion of the large amount of isobutenes formed by cracking of 2,2,4-trimethylpentane subsequently dimerize to form 2,5-dimethylhexane which then undergoes dehydrocyclization by C_6-ring closure to form p-xylene. The data in Table 16 are consistent with this view.

Applying the above logic to the data in Tables 16 and 17 allows us to eliminate a common cyclopentane

intermediate for dehydrocyclization over Pt as well as over chromia. Again, the aromatic product data are consistent with direct C_6-ring formation.

The aromatic distributions in Table 18 (taken from [34]) are from nine carbon cyclohexanes that contain a quaternary carbon and for the alkanes that can directly form these alkylcyclohexanes by a C_6-ring closure. For chromia, the reaction pathway for the three trimethylcyclohexanes is clear: it is demethylation to produce the corresponding xylene, and for the small amount of C_9 aromatics with the predominate isomer being the one expected by a 1,2-methyl

Table 17
Aromatic distribution from the conversion of C_8 alkanes and the corresponding naphthenes over Pt on nonacidic alumina catalysts (from [34])

Reactant	Aromatic selectivity[a]	Aromatic (mol%)					Reference
		Tol	EB	OX	MX	PX	
1 (2,2-DMH)[b]		52	–	22 (47)[c]	18 (39)	8 (16)	[96]
2 (2,5-DMH)[b]		–	Trace	Trace	7	93	[111]
		0.6	1.6	11	87		[118]
3 (2,2,4-TMP)[b]	36	42	0	0	35 (60)	23 (40)	[96]
		1.6	7	50	42		[118]
4 (2,4-DMH)[b]		6	2	90	2		[111]
5 (1,1,3-TMCP)[b]	35	30	0	1.5 (2.1)	42 (60)	27 (38)	[96]
		1.8	6.4	56	36		[118]
6 (1,1-DMCH)[b]		60	1 (2)	10 (24)	30 (71)	1 (2)	[111]
		53	(2)	(60)	(28)	(10)	[118]

[a] Total conversion to aromatic/total conversion.
[b] DMH = dimethylhexane; TMP = trimethylpentane.
[c] Numbers in parenthesis are for the mol% based on C_8 aromatics.

Table 18
Aromatic distribution from C_9 alkanes and the corresponding trimethylcyclohexanes (data from [34])

Reactant	Xylenes[a]			Trimethylbenzenes[a]		
	o-	m-	p-	1,2,3-	1,2,4-	1,3,5-
Cr₂O₃						
1,1,2-TMCH[b]	85	–	–	14	–	–
1,1,3-TMCH[b]	1	97	–	–	2	–
2,2,4-TMH[b]	8	27	12	7	33	1
2,6-DMHEPT[b]	3	70	–	4	12	4
1,1,4-TMCH[b]	–	2	90	–	8	–
2,2,5-TMH[b]	–	16	16	2	54	00
Pt(1)						
1,1,3-TMCH[b]	–	73	–	–	10	8
2,6-DMHEPT[b,c]	2	49	10	18	15	2
Pt(2) or Pt(3)20						
1,1,2-TMCH[b]	20	2	–	57	18	–
1,1,3-TMCH[b]	–	12	–	15	60	–
2,2,4-TMH[b]	7	13	3	–	32	18
2,6-DMHEPT[b]	2	12	–	8	38	18
1,1,4-TMCH[b]	1	2	1-	2	85	–
2,2,5-TMH[b]	–	6	3	8	54	2

[a] Total may not be 100% because of aromatics other than listed above.
[b] TMCH = trimethylcyclohexane; TMH = trimethylhexane; 2,6-DMHEPT = 2,6-dimethylhept-3-ene.
[c] Same distribution was obtained with and without added hydrogen.

migration from the geminal-dimethyl position. Note that C_6-ring closure for 2,6-dimethylyheptene forms only 1,1,3-trimethylcyclohexane. The aromatics from 2,6-dimethylheptene closely resemble those from 1,1,3-trimethylcyclohexane except there is slightly more of the C_9 aromatics than was formed from 1,1,3-trimethylcyclohexane. A direct C_6-ring closure

for 2,2,4-trimethylhexane would lead to the same intermediate as was formed from 2,6-dimethylheptene; the experimental distribution from 2,2,4-trimethylhexane contained a greater proportion of C_9 aromatic than was produced from the corresponding naphthene. This suggests that a direct C_6-cyclization occurs with both 2,6-dimethylheptene and 2,2,4-trimethylhexane
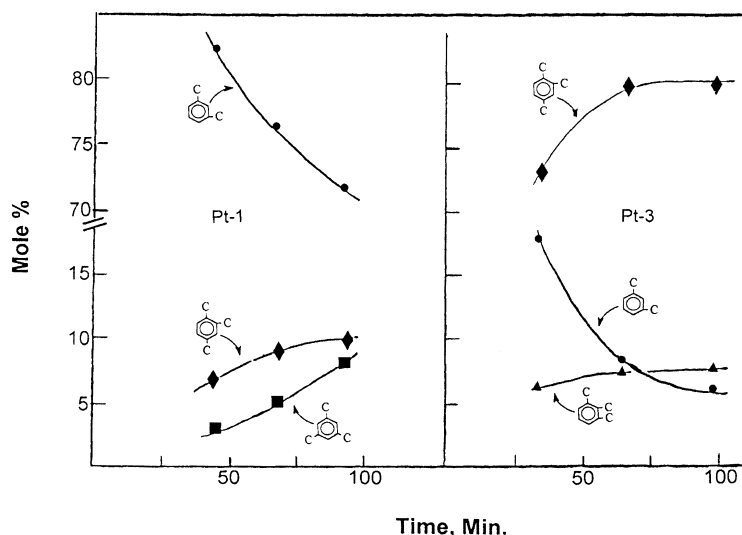
Fig. 17. Aromatic product distribution for the conversion of 1,1,3-trimethylcyclohexane over two different catalyst preparations, Pt (1) (treated with aqueous KOH after reduction) and Pt (3).

but that a methyl migration, prior to or during cyclization, occurs more readily from a quaternary carbon than from a tertiary one. The data presented in Fig. 17 for the aromatization of 1,1,3-trimethylcyclohexane demonstrates how sensitive the aromatic selectivity of Pt-Al$_2$O$_3$-K catalysts is to even small changes in the catalyst preparation.

Considering all of the data in this section conclusively demonstrate that it is almost certain that these alkanes cyclize to alkylcyclohexane-like structures. In those instances for alkanes with a quaternary carbon, a triene mechanism is not possible.

6.3. Isotopic labeled compounds

Under conditions where the molecule does not undergo isomerization prior to or after cyclization, the labeled molecule technique may be equivalent to that of using appropriately alkyl substitution. Thus, the products from the conversion of an alkyl or polyalkyl alkane with one or more six-carbon or longer chain can serve as a means of deducing a mechanism in just the same way as the use of carbon isotope labeling with the same compound. However, with *n*-hexane and *n*-heptane the alkyl label is not applicable and the use of carbon isotopes is the only approach.

| | ^{14}C, % | 10.2 | 6.7 | 83.1 |
| | ^{13}C, % | 15.9 | 76.6 | 6.9 |
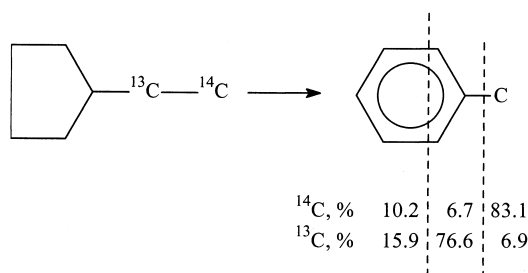
Scheme 8.

The results obtained by Kilner et al. [119] are enlightening. These authors converted [1-^{14}C-2-^{13}C]-ethylcyclopentane with a chromia-alumina catalyst at 505°C and 1 atm. The aromatization product, toluene, was analyzed for ^{13}C and ^{14}C content in the methyl, the ring carbon-1, and the sum of the ring -2, -3, and -4 positions. The results they obtained are summarized in Scheme 8.

If we assume that the cyclopentane ring undergoes hydrogenolysis as described above, we anticipate the label to be distributed as shown in Scheme 9.

Pathway c leads to 3-ethylpentane which cannot undergo direct six-carbon ring formation and should not produce toluene as rapidly as the products from pathways a and b. Pathway a leads to

$$
\begin{array}{l}
a: \quad C-C-C-C-C-\overset{13}{C}-\overset{14}{C} \\[2mm]
b: \quad C-C-C-\overset{\displaystyle C}{\underset{|}{C}}-\overset{13}{C}-\overset{14}{C} \\[2mm]
c: \quad C-C-\overset{\displaystyle C-C}{\underset{|}{C}}-\overset{13}{C}-\overset{14}{C}
\end{array}
$$
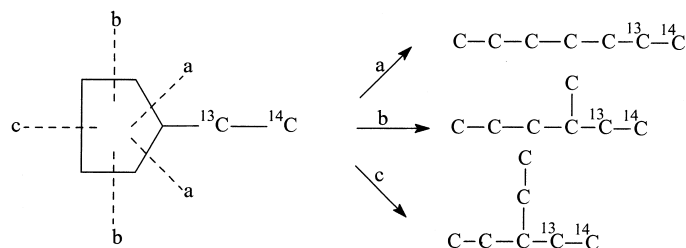
Scheme 9.

Table 19
Isotope distribution expected for toluene produced from *n*-heptane and 3-methylhexane

Reactant	Label	Methyl	1	2	3	4
C-C-C-C-C-^{13}C-^{14}C	^{14}C	50	0	50	0	0
	^{13}C	0	50	0	50	0
C-C-C-$\overset{C}{\underset{|}{}}$-^{13}C-^{14}C	^{14}C	0	0	0	100	0
	^{13}C	0	0	100	0	0

[1-^{14}C-2-^{13}C]-*n*-heptane and pathway b leads to 3-methyl-[1-^{14}C-2-^{13}C]-*n*-hexane; thus, the products from pathways a and b can undergo cyclization to directly produce a six-carbon ring. In Table 19, we compare the isotope distribution expected if isotopically labeled *n*-heptane and 3-methylhexane underwent direct six-carbon ring formation. By comparing the distribution of label that was obtained experimentally with the one expected if hydrogenolysis had occurred to produce labeled *n*-heptane and 3-methylhexane, we conclude that hydrogenolysis followed by cyclization made little, if any, contribution to the production of toluene. On the other hand, the isotopic distribution is consistent with a bifunctional mechanism in which ethylcyclopentene, formed by dehydrogenation, underwent ring expansion at an acidic site, and the six-carbon ring then underwent dehydrogenation to produce toluene. For this bifunctional mechanism we would expect the ^{14}C label to be in the methyl position and ^{13}C to be in the 1-ring position; the experimental isotopic distribution is in good agreement with the distribution predicted for the bifunctional mechanism. We consider this data to strongly support the operation of a bifunctional mechanism that can impact the isotopic distribution obtained with the data described

$$
\text{heptane} \xrightarrow{\quad k_1 \quad} \text{heptene} \xrightarrow{\quad k_2 \quad} \text{toluene}
$$

Scheme 10.

below for chromia catalysts. This is true even when the chromia-alumina catalyst contains alkali as it did in the experiments by Kilner et al. [119].

The first to use ^{14}C-isotope in a study of the dehydrocyclization mechanism was Wheatcroft [120]. Wheatcroft [120] considered Pitketkly and Steiner's [121] analysis of the reaction pathway for the aromatization of *n*-heptane (Scheme 10) where k_1 is the rate of dehydrogenation and k_2 is the rate of cyclization. A steady state was assumed for the heptene concentration in Scheme 10. Wheatcroft treated Scheme 10 as a system of consecutive unimolecular reactions as well as assuming that hydrogenation of heptene was of secondary importance. Wheatcroft solved the differential equations describing the system and obtained an expression relating the fraction of intermediate (heptene) in the product to the amount of heptane conversion. Wheatcroft used literature values from earlier studies [122–125] and found that a ratio of $k_2/k_1 = 5$ provided a good fit to the data (Fig. 18). Wheatcroft concluded that his treatment showed that the alkene is a compulsory intermediate and that the rate of cyclization is five times faster than the rate of dehydrogenation to the olefin.

Wheatcroft used a chromia (12 wt.%)-γ- alumina catalyst. He plotted the percentage of ring labeled toluene versus the percent toluene in the product (Fig. 19). He considered the results to show that, at low conversions, cyclization followed the pathway in Scheme 11.

This cyclization pathway provides exclusively ring labeled toluene. 1-Heptene isomerization occurs so that at high conversion the ^{14}C-label becomes almost

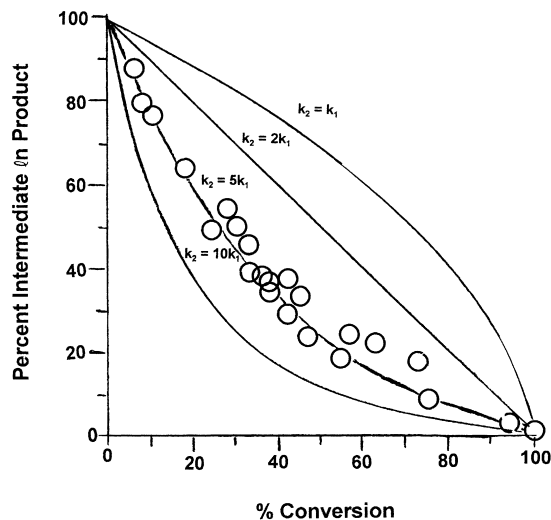(where ★ represents ^{14}C)
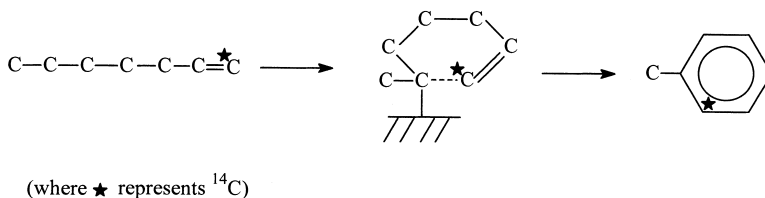
Scheme 11.

Fig. 18. Percent heptene in the product vs. percent conversion in the product. Theoretical lines for A $\xrightarrow{k_1}$ B $\xrightarrow{k_2}$ C. Experimental points from [120].
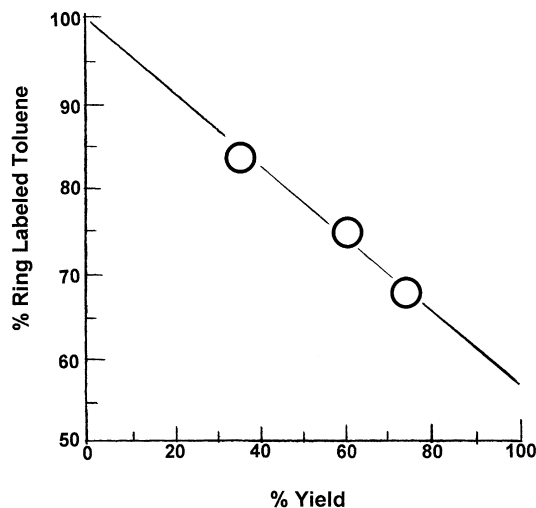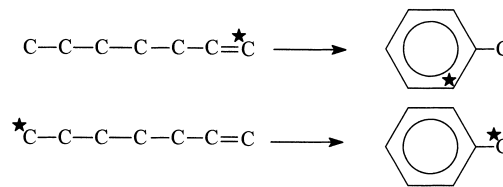

Fig. 19. Percent ring labeled toluene vs. percent toluene in product. Line is best fit for straight line (from [120]).
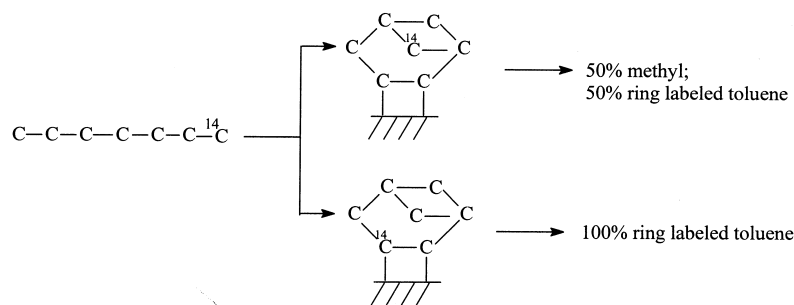

Scheme 12.

equally distributed between the two terminal positions. This would permit toluene to be formed with equal label at the methyl and the ring of toluene in (Scheme 12).

Wheatcroft indicated that his data can be explained by this scheme provided the rate of isomerization of 1-heptene to 2- + 3-heptenes is about equal to the rate of cyclization. Another explanation for Wheatcroft's data would be that bifunctional isomerization to methyl hexenes occurs and the isomerization is poisoned more rapidly with increasing heptene conversion than the aromatization reaction is.

Wheatcroft's mechanism requires chemisorption of the saturated portion of 1-heptene to be much more rapid than the adsorption of the double bonded carbons; studies of the competitive conversion of *n*-octane and 1-octene described below indicate that this is not the case. Another argument against such a mechanism is that the above intermediate resembles a Grignard reagent and intramolecular cyclization of a Grignard with the above structure leads to the formation of a five-carbon ring [126–128].

Mitchell [129] found only 25–28% methyl label in toluene that was produced from 1-^{14}C-*n*-heptane with a chromia-alumina catalyst. Mitchell proposed that this activity could be accounted for by the following mechanism with statistical C–C bond breaking in the cyclobutane ring (Scheme 13).

Mitchell did not provide a mechanism to account for the dehydrogenation of the methyl group that

Scheme 13.
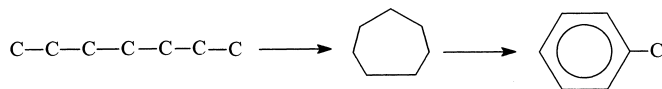
Scheme 14.

is detached from the catalyst and for its subsequent cyclization to produce a four-carbon ring, a highly strained structure. However, the equal participation of the above two structures provide toluene that contains 25% methyl labeled toluene, as obtained in Mitchell's experiment.

Shortly following the report by Mitchell, Pines undertook extensive studies of dehydrocyclization. In these studies, Pines attempted to define the role of acidity of the support. He and his coworkers employed three catalysts in these studies: unsupported chromia; chromia supported on an acidic alumina derived from aluminum isopropoxide hydrolysis and chromia supported on a nonacidic alumina derived from potassium aluminate. Pines and coworkers obtained data for 1-[14]C-*n*-heptane [130] and 1-[14]C-*n*-octane [117] as well as labeled methyl hexanes. For the conversion of 1-[14]C-*n*-heptane, 50% of the initial activity should be located in the methyl group. For two of the catalysts, unsupported chromia and chromia on acidic alumina, Pines and Chen [130] found 40% or more of the label in the methyl position. However, the surprising result was that the methyl label for the first sample collected from the conversion of 1-[14]C-*n*-heptane with the chromia on nonacidic alumina catalyst was only 17.4%; this was close to the value expected if there had been complete scrambling of the isotope to each of the positions of toluene. Pines and Chen proposed a reaction pathway that included the formation of cycloheptane and its subsequent conversion to toluene (Scheme 14).

For 1-[14]C-*n*-octane dehydrocyclization, ethylbenzene should have 50% of the label in the ethyl group, and this should be in the β-position of the ethyl group if it was formed by direct cyclization to a six-carbon ring. For chromia on acidic alumina, Pines and Chen found 52 and 50% methyl label in the first and second samples collected; 88–92% of the label was in the β-position of the ethyl group. For *o*-xylene, 100% of the radioactivity should be in the side chain methyl groups, and the first and second samples contained 79 and 90% side chain label, respectively. Thus, for the two aromatic isomers allowed by direct six-carbon ring closure, 80% or more of the ^{14}C-label is in the position expected for a six-carbon ring closure mechanism. With chromia on nonacidic alumina, the activity in ethylbenzene and *o*-xylene was also consistent with that expected for a direct six-carbon ring formation for the second sample they collected. However, the first sample collected for dehydrocyclization of 1-[14]C-*n*-octane had a low side chain activity just as had been found for the conversion of 1-[14]C-*n*-heptane with this catalyst. Pines and coworkers also tried to include the ^{14}C distribution in *m*- and *p*-xylene in their mechanism. These results led Pines and coworkers [25] to propose that various ring size intermediates and methyl insertion isomerization reactions were involved in the dehydrocyclization mechanism. These are demonstrated in Scheme 15 by some of the possible reaction pathways for *n*-octane and 3-methylheptane.
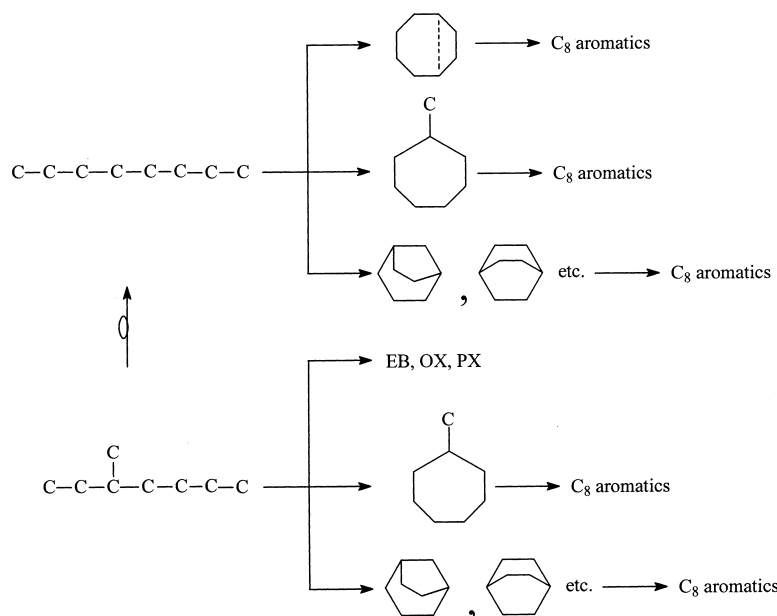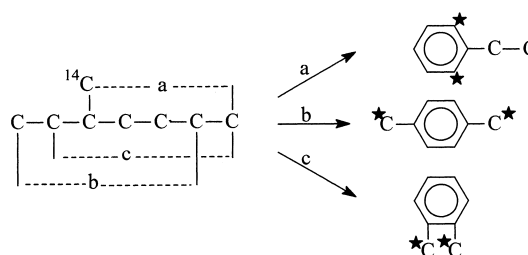
Scheme 15.

Pines and coworkers disregarded the data showing that compounds with various ring sizes, such as methylcycloheptane, underwent aromatization at a slower rate than the *n*-alkane that they would be formed from. To account for this observation, they concluded that the various sized rings, such as methylcycloheptane, did not leave the surface but underwent ring contraction while adsorbed on the catalyst surface. This would require adsorption to be the rate determining step although this was not advanced by Pines and coworkers.

If we consider the ^{14}C-label distributions in ethylbenzene and *o*-xylene that were obtained by Pines and coworkers, only the early samples collected when using the chromia on nonacidic alumina are inconsistent with at least 80%, and usually greater than 80%, of the aromatics being formed by a mechanism that involves direct six-carbon ring formation.

Cannings et al. [115,131] converted 2,2-dimethyl-4-^{14}C-methyl pentane (isooctane) and 3-[^{14}C]-methylheptane with a potassium and cerium promoted chromia-alumina catalyst. With 3-[^{14}C]-methylheptane the aromatics composition and ^{14}C distribution between the side chain ring are given in Scheme 16.

The C_8-aromatic distribution is the one expected for a mechanism with direct six-carbon ring formation.

Scheme 16.

Greater than 90% of the ^{14}C in the aromatic products is in the position predicted for six-carbon ring formation.

Feighan and Davis [132] converted [4-^{14}C-]-*n*-heptane with their version of the three catalysts used by Pines and coworkers: unsupported chromia and chromia supported on acidic and nonacidic aluminas. With this reactant, all of the ^{14}C should be present in the ring position *meta* to the methyl group if toluene is produced by direct six-carbon ring formation. In contrast to Pines and coworkers, Feighan and Davis degraded the aromatic ring so that the activities in the ring positions as well as the methyl group could be determined from experimental data (Scheme 17) [133]. All of the results were consistent with at least 80%,
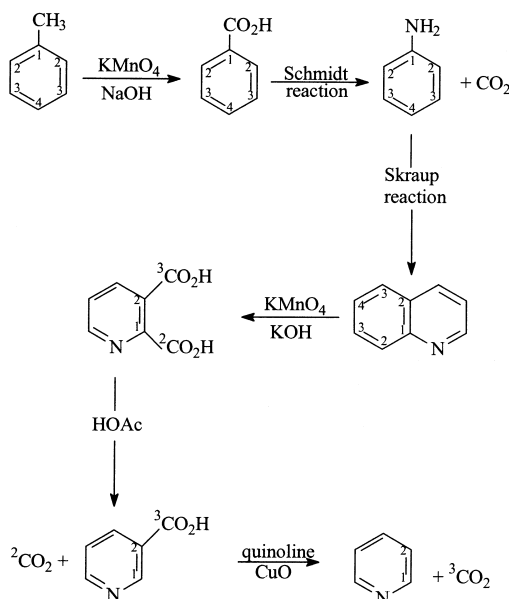
Scheme 17.

Table 20
[14]C in the methyl position of toluene from the conversion of ^{14}C labeled heptane over chromia catalysts

Catalyst	Sample[a]				Reference
	1	2	3	4	
n-[1-^{14}C] heptane					
Cr₂O₃	44.7	47.3	47.4		[130]
Cr₂O₃-Al₂O₃-A	38.7	39.8	41.7		[130]
Cr₂O₃-Al₂O₃-B	17.5	21.7	32.1		[130]
Cr₂O₃-Al₂O₃-B	43.0	39.0	40.0		[134]
Cr₂O₃-Al₂O₃-B		28			[129]
n-[4-^{14}C] heptane					
Cr₂O₃	3.7	1.8	0.6		[132]
Cr₂O₃-Al₂O₃-A	1.6	1.7	1.3	1.2	[132]
Cr₂O₃-Al₂O₃-B	2.6	2.8	2.7	3.0	[132]

[a] Collected at increasing time-on-stream.

and usually greater than 80%, of a mechanism that involves direct six-carbon ring formation (Table 20).

Later, Davis and Venuto [134] converted both [1-[14]C-]- and [4-[14]C-]-*n*-heptane with chromia on nonacidic alumina and found an isotope distribution for all samples that was consistent with 80% or greater of the toluene being formed by a direct six-carbon ring formation. Unfortunately, Professor Pines did not have a supply of his chromia on nonacidic alumina for use in this study.

Table 21
Conversion of labeled heptane to toluene over Pt and Pt bimetallic catalysts

Catalyst	Charge = % [14]C in Methyl position			
	Sample	*n*-[1-^{14}C]-	*n*-[4-^{14}C]-	Reference
Pt-Al₂O₃-K	1	36	3.2	[135]
	2	41	1.3	[135]
	3	44	1.1	[135]
Pt-Al₂O₃-K	–	40	–	[136]
10% Pt-Al₂O₃	–	50	2.5	[138]
Pt–Sn-Al₂O₃-K	1	52	0.57	[137]
	2	49	0.29	[137]
Pt-Re-Al₂O₃-A[a]	1	34	4.1	[137]
	2	32	2.5	[137]
	3	32	–	[137]

[a] *Sec*-butyl amine added to the charge.
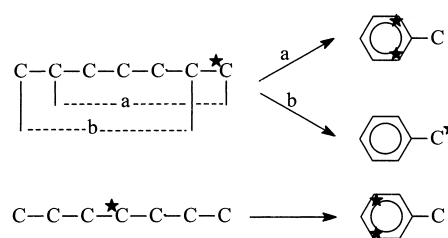
Scheme 18.

Davis also converted [135] [1-[14]C-]- and [4-[14]C-]-*n*-heptane with Pt supported on nonacidic alumina. The side chain label and the label in the ring were consistent with 80% or more of the toluene being formed by a direct six-carbon ring mechanism. Nogueira and Pines [136] later reported data for their Pt-nonacidic alumina catalyst that agreed with those obtained by Davis. Davis also converted [1-[14]C-]- and [4-[14]C-]-*n*-heptane with Pt-Re-acidic alumina and Pt-Sn-nonacidic alumina [137]. For the Pt-Re catalyst, *sec*-butyl amine was added to poison the acid function during the conversion since alkali metals are severe poisons for this catalyst. Again, the results with both bimetallic catalysts, Pt-Re and Pt-Sn, were consistent with more than 80% of the aromatics being formed by a direct six-carbon ring formation (Table 21).

The label distribution expected for converting heptane, labeled at C-1 or C-4, to toluene is given in Scheme 18. Analysis of the toluene ring label distribution from C-1 and C-4 labeled heptane can distinguish between a direct C_6 closure and a C_5

Table 22
Ring ^{14}C distribution in toluene obtained from the conversion of n-4- [14]C heptane over chromia catalysts [132]

Catalyst	Sample	$(C_2)/(C_1 + C_2 + C_3)$	C_2/C_3
Cr_2O_3	1	0.070	0.081
	2	0.023	0.15
	3	0.015	0.017
$Cr_2O_3-Al_2O_3$-A	1	0.045	0.047
	2	0.042	0.051
	4	0.045	0.048
$Cr_2O_3-Al_2O_3$-B	1	0.11	0.14
	2	0.057	0.070
	4	0.041	0.047

closure to 1,2-dimethylcyclopetane followed by ring expansion (Tables 22 and 23). The methyl label of toluene produced from [4-^{14}C]-heptane with all three chromia catalysts is consistent with, at most, 20% of a cycloheptane ring intermediate. The results from [1-^{14}C]-heptane, except for the runs with nonacidic chromia by Pines and Chen [130] and by Mitchell [129], are also consistent with 80% or greater direct C_6 ring closure. Davis [137] obtained that similar results were obtained with the [1-^{14}C]-heptane using Pt-, Pt bimetallic, and supported and unsupported chromia catalysts.

The toluene ring label distribution was determined using our modification of the Steinberg and Sixma method (Scheme 17) [133]. The data in Tables 22 and 23 show that C_5-ring closure to ethylcyclopentane followed by ring expansion to a six carbon ring does not make a major contribution to the aromatic formation from [4-[4]C]-n-heptane with either chromia

or Pt catalysts. Experimental difficulties prevented us from making a complete ring degradation for our Pt studies; the data in Table 23 have been calculated so that all results are presented in a similar way. The experimental value falls about midway between the 0.5 expected for direct C_6 ring closure and the 0.33 expected for the 1,2-dimethylcyclopentane intermediate. It will take a very careful and difficult ring label analysis to eliminate 1,2-dimethylcyclopentane as an intermediate using carbon tracers. The C-2 and C-3 labeled heptane pair will provide the same label distribution in the toluene as the C-1 and C-4 labeled pair so additional information will not be attained from use of C-2 and C-3 labeled heptane.

Amir-Ebrahimi et al. [138] converted [1-^{13}C]-n-heptane with a 10 wt.% Pt-alumina catalyst at 380°C and 3 Torr heptane/760 Torr helium. They determined the position of the label using mass and microwave spectroscopy. After hydrogenation to methylcyclohexane, mass spectrometrical analysis showed that the toluene had 50% of the ^{13}C-label within the ring. The distribution of the 50% ring label was reported to be distributed with 34% in the *ortho* (2-) position and 16% in the *meta* (3-) position. A label content for the 1- and 4- position was not given nor was there an estimate for the lower limits of detection. To account for their experimental label distribution, these authors indicated that a three-step mechanism was involved: 1,5-ring closure, ring opening, and 1,6-ring closure. The authors do not explain why 1,6-ring closure does not contribute in the first step.

A variety of techniques are now being used to identify surface species resulting from C–H cleavage

Table 23
Ring label distribution in toluene obtained from n-heptane over Pt catalysts
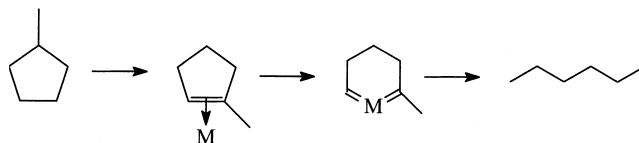
Charge	Sample	$(C_2)/(C_1 + C_2 + C_3)$				Reference
		Experimental	Calculated based on			
			C_6	EtCP[a]	1,2-DMCP[a]	
n-4-[14]C-	2	0.033	0.0	0.33	0.0	[135]
	3	0.065	0.0	0.33	0.0	[135]
n-4-[14]C-	–	0.06[b]	0.0	0.33	0.0	[138]
n1-[13]C-	1	0.40	0.50	0.33	0.33	[135]
	3	0.44	0.50	0.33	0.33	[135]
n-1-[13]C-	–	0.40	0.50	0.33	0.33	[138]

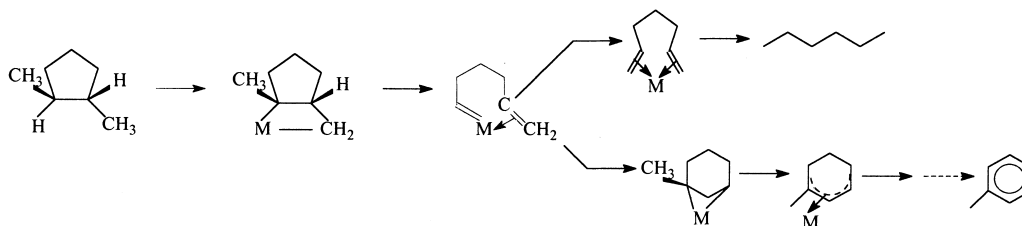[a] EtCP = ethylcyclopentane; DMCP = dimethylcyclopentane.
[b] Based on a maximum of 5% [13]C at positions other than *meta*.
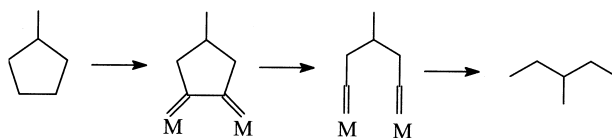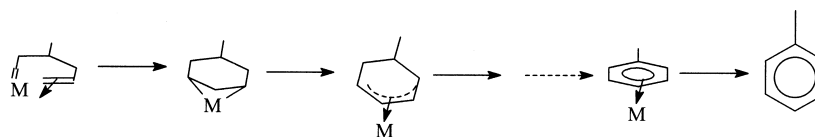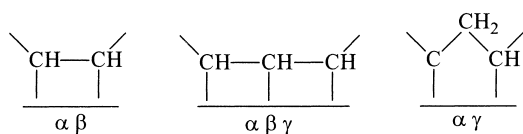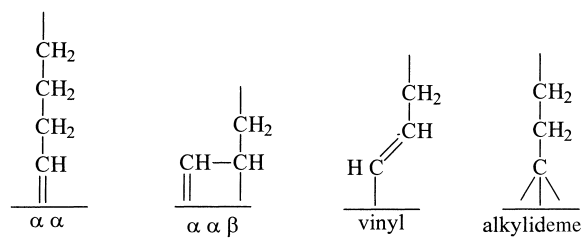
Scheme 19.

Scheme 20.

Scheme 21.

Scheme 22.

of alkanes. These species include, among others [139],

These or similar structures will be encountered in the following schemes.

Amir-Ebrahimi et al. [138] utilized the non-selective (Scheme 19) and selective (Scheme 20) mechanism for alkylcyclopentane isomerization/hydrogenolysis to explain their data:

However, Schemes 19 and 20 were inadequate so that the authors introduced a third mechanism (Scheme 21):

The direct ring closure, illustrated for 3-methyl-hexane, is described as a carbene-olefin addition (Scheme 22):

Combining these schemes, they described the three step mechanism as (Scheme 23):

It appears that the above scheme was constructed to fit the data that had been obtained, and was based upon the initial reactant structure. There is no reasonable
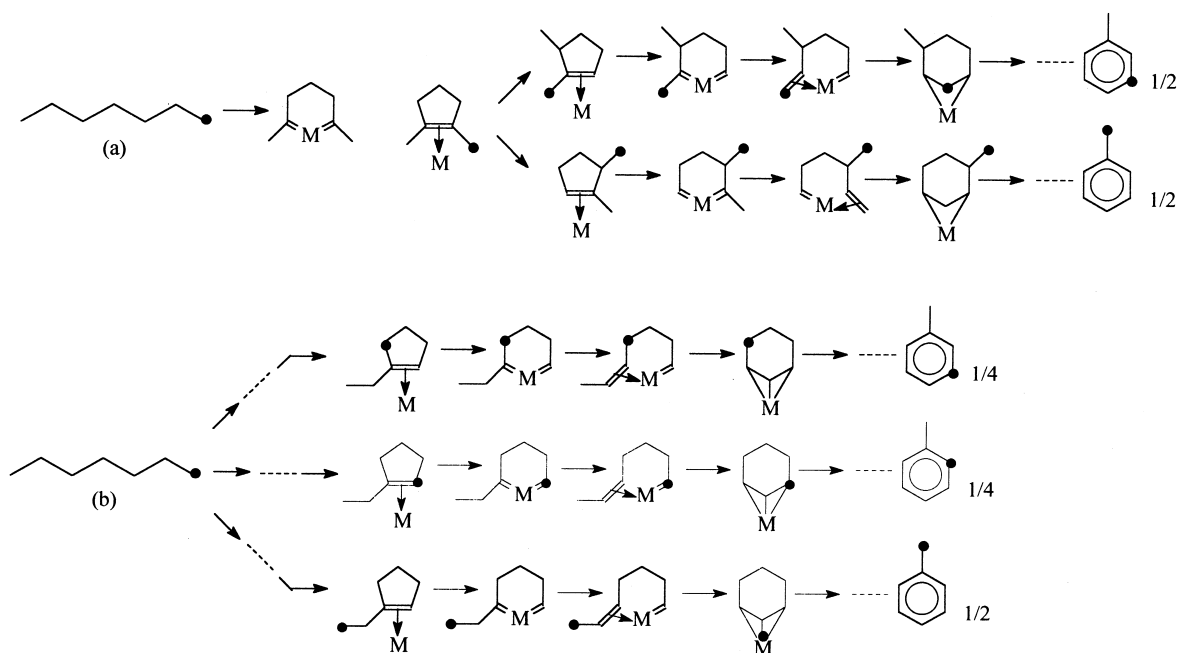
Scheme 23.

way to predict the contributions of pathways a and b in Scheme 23 nor the relative amount of the two pathways in a or the three in b.

Unfortunately, the acidity of the catalysts used by Gault and coworkers is not well defined. If we consider that some modest amount of isomerization occurs in competition to the normal 1,6-ring formation, we have the following possibilities (Scheme 24):

The simple alkane isomerization mechanism allows for 1,6-ring formation to produce toluene equally labeled in the methyl group and in the *ortho*-ring position as well as the label at the *meta*-position (3-). The isomerization scheme would also provide label in the *para*-position (4-); however, the experimental value for this was apparently below the level that could be detected. Even so, it is apparent that the complex three-step mechanism, which must finally involve a direct 1,6-ring closure, should be advanced only after the possibility of a direct 1,6-ring formation plus a small fraction of the simple bifunctional isomerization process has been eliminated.

Iglesia et al. [110] converted [1-^{13}C]-*n*-heptane with a Te/NaX zeolite catalyst at 723 K and 100 kPa (H$_2$: h.c. = 21). The toluene product contained greater than 93% of the isotopic label in the methyl and

Table 24
^{13}C distribution *n*-heptane-1-^{13}C reaction products (Te/NaX)[a] (from [110])

|		
Contact time (ks):	3.6	22.7
n-heptane conversion (%):	7.2	33.9
^{13}C distribution (%)		
Toluene		
Methyl-	48.1	47.7
Ortho-	47	46.0
Para-	1.1	1.0
Meta-	3.8	4.6
1-	0	0.6
3-methylhexane		
CH$_3$ (1,6,7) positions	–	100
CH$_2$, CH (2,3,4,5)	–	0
3-ethylpentane		
CH$_3$ (1,5,7)	–	–
CH$_2$, CH (2,3,4,6)	–	–
2-methylhexane		
CH$_3$ (1,6,7)	–	–
CH$_2$, CH (2,3,4,5)	–	–

[a] From NMR measurements.

ortho-ring positions (Table 24). The position of the ^{13}C in the methylhexane isomers that were produced are given in Table 24. These show that the amount of

Scheme 24.

	Fraction of ^{13}C				
Reaction	Me	1-	2-	3-	4-
a	0.5		0.5		
b				1.0	
c					1
d				1	
Equal contribution a,b,c,d	0.125	0	0.125	0.5	0.25
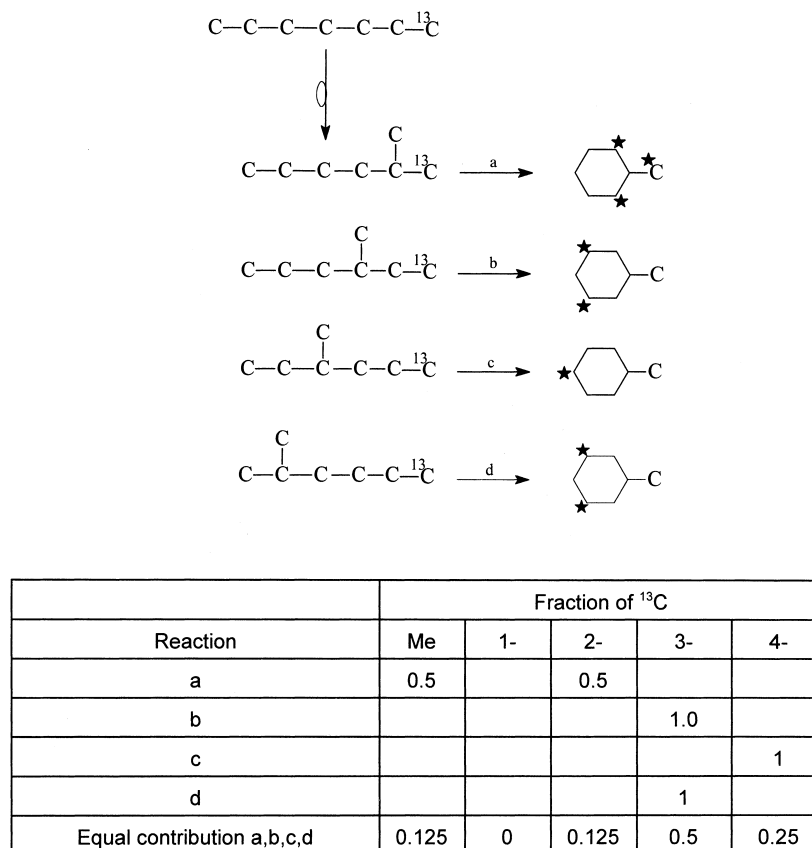
the isotope in the CH_2 positions was too low to detect; 100% of the isotope detected was in the methyl positions. Iglesia et al. considered the aromatization to occur through the formation of heptatrienes which subsequently cyclize, in analogy with the hexatriene mechanism outlined below. The additional feature of the proposed mechanism is the formation of the bicylcic structure from 1,3,6-heptatriene and the subsequent rearrangement/hydrogenolysis of the cyclopropane ring to locate the isotope label in the *meta* and *para* position (Scheme 25).

The simpler explanation of the dehydrocyclization of a small amount of methylhexanes that result from isomerization, as illustrated above in Scheme 24, can equally well account for the isotopic label being in the *meta* and *para* positions as well. In any event, the data reported by Iglesia et al. are in excellent agreement with the dominant (about 95%) fraction of the toluene
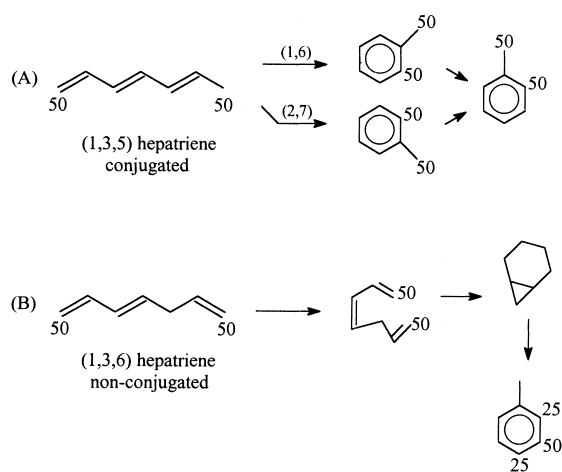
Scheme 25.

being formed by a six-carbon ring forming mechanism and provide no direct data to support the hepatriene as the intermediate in the cyclization pathway.

Considering all of the tracer studies, the only data that are inconsistent with a direct six-carbon ring formation were obtained using chromia supported on nonacidic catalysts. The above data for C_7+ alkanes are also mostly in agreement with aromatics being formed by a mechanism that involves direct six-carbon ring formation. The only exception was for some of the chromia catalysts, and these showed a distribution that was consistent with a dual functional isomerization, such as was found by Kilner et al. [119]. For example, the data of Pines and Chen [117,130], for the conversion of labeled *n*-heptane and *n*-octane with their potassium containing chromia-alumina catalyst, changed with increasing reaction time to become consistent with that of six-carbon ring formation. The hypothesis of some acidity for some chromia catalysts and a contribution of some isomerization through a bifunctional mechanism is a much simpler mechanism than resorting to the formation of all ring sizes that undergo contraction-expansions.

7. Irreversible adsorption mechanism

Early work showed that the dehydrogenation of a cycloalkane was much more rapid than the dehydrocyclization of the corresponding alkane. For example, Fogelberg et al. [112] found that while ethylcyclohexane underwent complete conversion at 375°C, under the same conditions only 62% *n*-octane conversion was attained at 525°C. Thus, in any competitive conversion we should expect a much greater conversion rate for the cycloalkane than for the corresponding alkane. Aromatics are apparently not strongly adsorbed; for example, Archibald and Greensfelder [140] found that the effect of the aromatic was simply that of an inert diluent for the conversion of an equivolume mixture of *n*-heptane and toluene at 490°C with a promoted chromia-alumina catalyst.

If it is assumed that Langmuir–Hinshelwood adsorption behavior is followed in a competitive conversion, the relative rate of conversion of an equimolar ratio of the cycloalkane and alkane that have the same adsorption constant should be [141]:
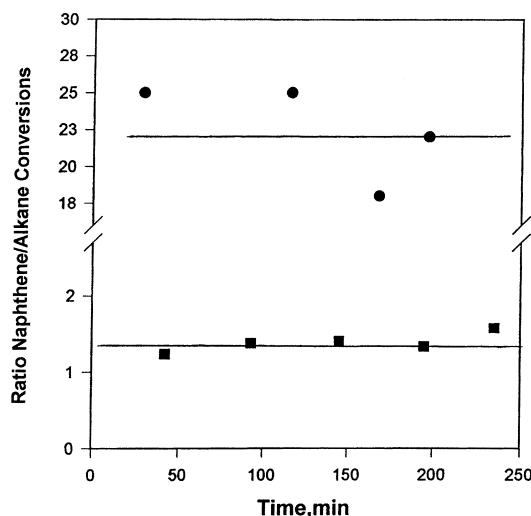

Fig. 20. Ratio of naphthene/paraffin conversion with Pt-nonacidic alumina catalyst at 300°C (●) 482°C (■) and 1 atm (data from [141]).

$$\frac{d(\text{cycloalkane})}{d(\text{alkane})} = \frac{k_c}{k_a} \tag{1}$$

where k_c and k_a are the rate constants for cycloalkane and alkane, respectively. Based upon the rates measured separately, k_c/k_a is expected to be much greater than one. On the other hand, if the same assumptions are made for the conditions except that adsorption is irreversible, the relative rate of conversion of the two reactants is:

$$\frac{d(\text{cycloalkane})}{d(\text{alkane})} = 1 \tag{2}$$

It was found that the reversible adsorption pathway was followed for the lower temperature range (300–400°C). When the conversion was carried out at 482°C the ratio was close to 1, indicating that the reaction pathway followed essentially irreversible adsorption and the adsorption constants for the two reactants were nearly the same (Fig. 20). This situation was found to apply to a number of competitive conversion situations: naphthene/alkane mixture, a mixture of two alkanes with six or more carbons; a mixture of alkanes, one with more and one with less than 6 carbons and a mixture with alkane/naphthene with five carbon rings [141]. Thus, at 1 atm and 482°C, the conversion of alkanes and cycloalkanes involves essentially irreversible adsorption of the reactant.
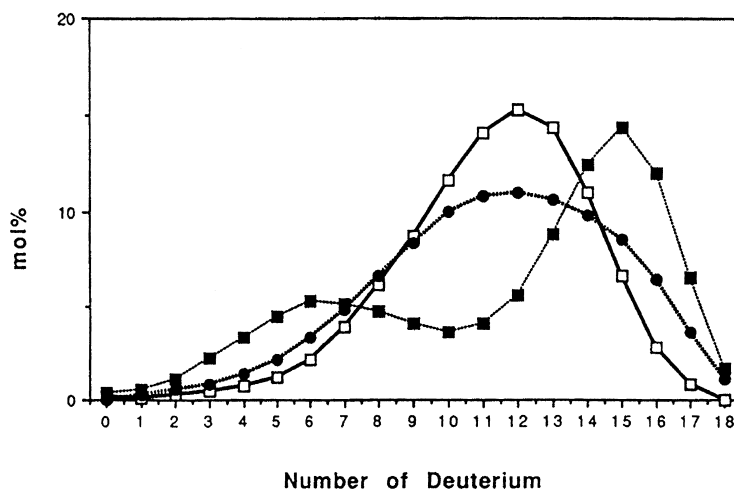
Fig. 21. Protium incorporation in *n*-octane for conversion of *n*-octane-d_{18}/methylcyclohexane-d_0 at 482°C with Pt-Al$_2$O$_3$ (□), nonacidic Al$_2$O$_3$ containing 1% K (■), and acidic Al$_2$O$_3$ (●) (from [142]).
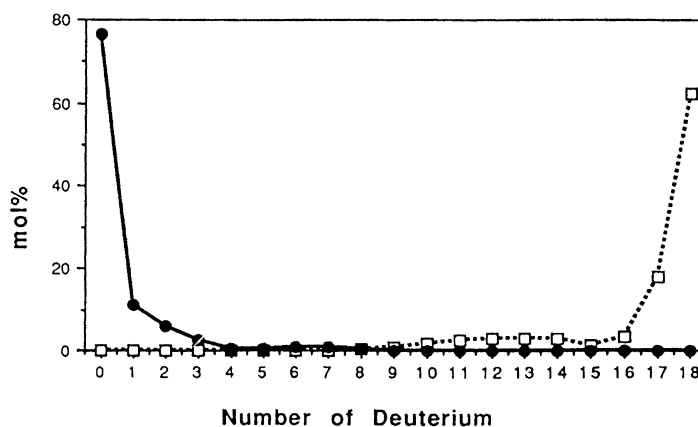

Fig. 22. Deuterium incorporation into *n*-octane at 482°C using a Pt-SiO$_2$ catalyst: (□) *n*-octane-d_{18}/methylcyclohexane-d_0, and (●) methylcyclohexane-d_{14}/*n*-octane-d_0 (from [142]).

For irreversible adsorption during the conversion of a mixture of the alkane and cycloalkane, one but not the other labeled with deuterium, observable exchange between the two gas phase reactants should not occur. When a mixture of *n*-octane-d_{18} and methylcyclohexane-d_0 was converted over a Pt-alumina catalyst at 300°C or 482°C, there was considerable exchange (Fig. 21) [142]. More supervising, there was as much or more exchange when this mixture was converted over acidic alumina without Pt, or even over a nonacidic alumina, than when Pt was present. This exchange activity of the alumina support precluded a determination of whether there

was irreversible adsorption of the two reactants when alumina was used as the support.

There was little exchange between the two reactants (Fig. 22) when a mixture of *n*-octane-d_{18} and methylcyclohexane-d_0 or a mixture of *n*-octane-d_0 and methylcyclohexane-d_{14} was converted at 482°C with a Pt-SiO$_2$. While there was essentially no H/D exchange in the reactants, the aromatic products derived from the two reactants has exchanged to essentially an equilibrium H/D composition (Fig. 23). In contrast to the conversion at the high temperature (482°C), there is exchange to a nearly statistical distribution when mixture of *n*-octane-d_{18} and methylcyclohexane-d_0 or
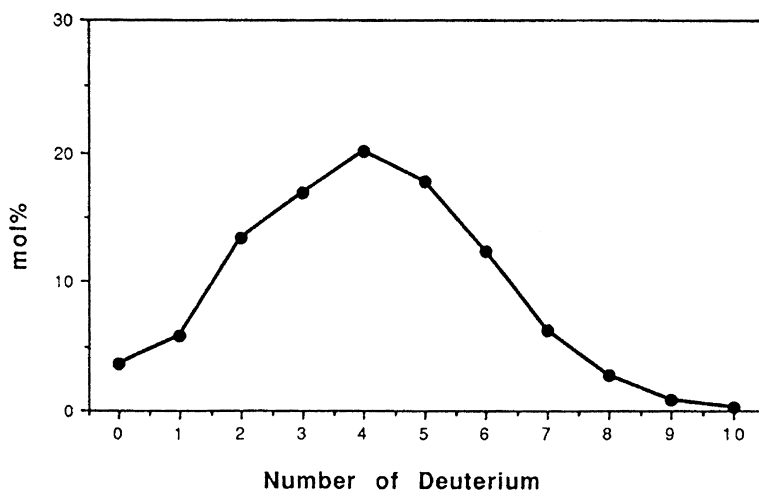
Fig. 23. Deuterium distribution in ethylbenzene produced in methylcyclohexane/octane/D_2 run with Pt-SiO_2 catalyst at 482°C (from [142]).

Table 25
Deuterium incorporation in the starting reagents using a Pt-SiO_2 catalyst (from [142])

Deuterium Content	Methylcyclohexane					n-octane				
	300°C		375°C	482°C		300°C		375°C	482°C	
	A[a]	B[a]	A[a]	A[a]	B[a]	A[a]	B[a]	A[a]	A[a]	B[a]
d_0	1.44	4.15	–	–	94.5	15.0	1.09	78.1	98.2	74.4
d_1	3.68	13.6	–	–	4.74	29.2	4.49	16.4	1.53	8.39
d_2	4.90	21.3	–	–	0.59	28.0	10.6	4.39	0.29	4.21
d_3	6.09	24.4	–	–	0.16	17.3	17.1	0.97	–	3.44
d_4	7.68	19.3	–	–	–	7.46	20.4	0.15	–	3.04
d_5	7.48	12.1	0.08	–	–	2.39	19.1	–	–	2.35
d_6	8.32	4.57	0.14	–	–	0.58	13.8	–	–	1.77
d_7	8.64	0.59	0.24	–	–	–	8.06	–	–	1.26
d_8	8.61	–	0.43	–	–	–	3.56	–	–	0.73
d_9	9.29	–	0.54	–	–	–	1.31	–	–	0.36
d_{10}	8.71	–	0.93	0.16	–	–	0.40	–	–	–
d_{11}	8.79	–	2.01	0.59	–	–	–	–	–	–
d_{12}	8.10	–	7.02	4.93	–	–	–	–	–	–
d_{13}	5.49	–	16.9	9.54	–	–	–	–	–	–
d_{14}	2.77	–	71.7	84.76	–	–	–	–	–	–
d_{15}						–	–	–	–	–
d_{16}						–	–	–	–	–
d_{17}						–	–	–	–	–
d_{18}						–	–	–	–	–

[a] A = mixture of methylcyclohexane-d_{14} (12%) and n-octane-d_0 (88%); B = mixture of methylcyclohexane (56.3%) and n-octane (42.9%) and D_2 gas (8.5 ml/min).

a mixture of n-octane-d_0 and methylcyclohexane-d_{14} was converted at 300°C (Table 25). Thus, we have the surprising result that there is more exchange in the reactants at the lower temperature than when a high temperature is employed with compounds representative of naphtha reforming.

These results indicate that the rate limiting step of the dehydrocyclization reaction is adsorption that

Table 26
Dehydrocyclization of a equimolar mixture of n-octane-d_0 and n-octane-d_{18} with a Pt/SiO$_2$ Catalyst at 482°C and 1 atm with a Pt-SiO$_2$ Catalyst (from [143])

Time-on-stream (h)	Conversion (%)		Conversion of octane-d_0/ conversion of octane-d_{18}
	d_{18}	d_0	
2	5.76	21.7	3.77
3	4.75	19.0	4.00
4	5.09	20.0	3.92
5	3.93	14.9	3.78
6	4.02	12.1	3.02
7	3.54	11.1	3.14
8	3.37	10.2	3.08

Table 27
Conversion of a mixture of n-octane and methylcyclohexane with a Pt/SiO$_2$ catalyst at 482°C and 1 atm without added hydrogen (from [143])

Reagents (mol)	Conversion of MCH/ conversion of octane
MCH-d_0 octane-d_{18}	4.0 + 0.2
MCH-d_0 octane-d_0	1.2 + 0.2
MCH-d_{14} octane-d_0	0.41 + 0.05

Fig. 24. The deuterium distribution in the ethylbenzene ($\bullet$) and o-xylene ($\square$) produced during the dehydrocyclization of an equal molar mixture of C$_8$H$_{18}$ and C$_8$D$_{18}$ (the data shown is for the sample collected at the third hour; the data shown are representative of those for the samples collected at other times) (from [143]).

involves breaking of the C–H or C–D bond. If the initial adsorption is rate limiting there should be a kinetic isotope effect. As described below, this was found to be the case.

An equimolar mixture of n-octane-d_0 and n-octane-d_{18} was converted at 482°C and atmospheric pressure [143]. Samples were collected at intervals and the kinetic isotope effect calculated from the amount of unconverted reactants. Because of an inverse isotope effect that is applicable in g.c. analysis, two distinct peaks, with baseline separation between the two, were obtained for n-octane-d_0 and n-octane-d_{18}, allowing one to obtain the isopotomer distribution within each peak [144]. The kinetic isotope effect for the conversion of n-octane-d_0 and n-octane-d_{18} was 3.5 ± 0.4 (see Table 26). The data for the kinetic isotope effect for the conversion of the n-octane and methylcyclohexane mixtures are compiled in Table 27. Whereas the ratio of the conversion of methylcyclohexane/n-octane was 1.2 for the undeuterated components, the conversion ratio was found to be 4.0 when n-octane-d_{18} was substituted for n-octane-d_0; this corresponds

to a kinetic isotope effect of 3.3 ± 0.6 for the conversion of the n-octane/methylcyclohexane mixture. Likewise, a kinetic isotope effect was found when methylcyclohexane-d_{14} was substituted for methylcyclohexane-d_0; in this instance a kinetic isotope effect was calculated to be 2.9 ± 0.6. It is emphasized that these kinetic isotope effects were obtained experimentally in a competitive conversion so that both reactants were subjected to identical reaction conditions of temperature, catalyst state and hydrogen(deuterium) pressure and surface coverage (apart from the surface H/D ratio).

The aromatic products, if H/D exchange did not occur, should consist of ethylbenzene-d_0 and -d_8 and o-xylene-d_0 and -d_8. However, the H/D isopotomer distribution (Fig. 24) show that there was essentially equilibration of the H/D in both aromatic products. This requires that the aromatic product and/or the precursors to remain on the surface for a sufficient time for this equilibration to occur.

If the irreversible alkane adsorption step determines the aromatic product, there should be a large kinetic isotope effect in the formation of o-xylene relative to ethylbenzene for the conversion of 2,2,7,7-tetradeutero-octane [145] (Scheme 26).

Thus, whereas the ratio of ethylbenzene/o-xylene formed with undeuterated n-octane is about 1.0, the
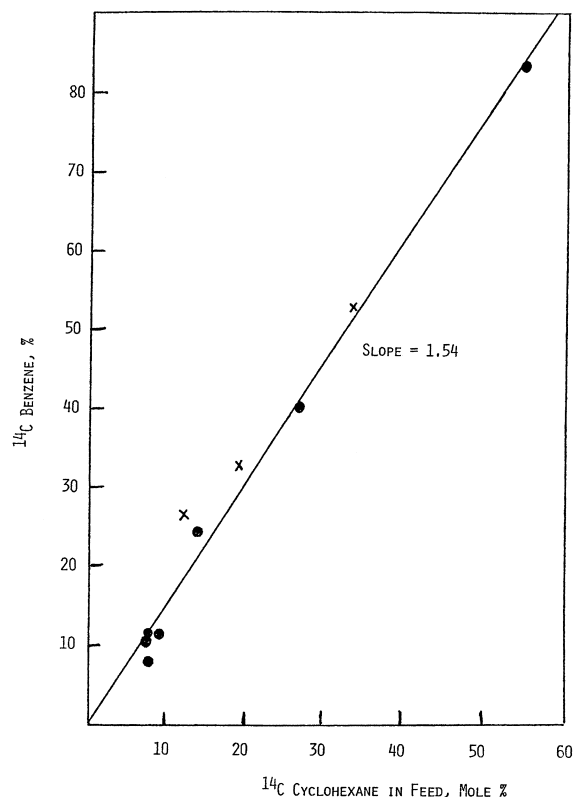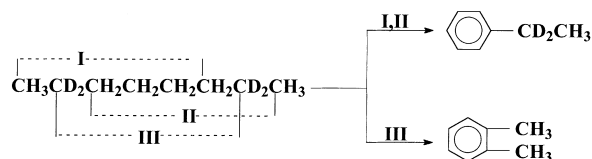
Scheme 26.

Fig. 25. Percentage of ^{14}C-labeled benzene versus the percentage of ^{14}C-labeled cyclohexane in a mixture with unlabeled *n*-hexane using a pulse (●) and flow (X) reactor (drawn from data in [146,147]).
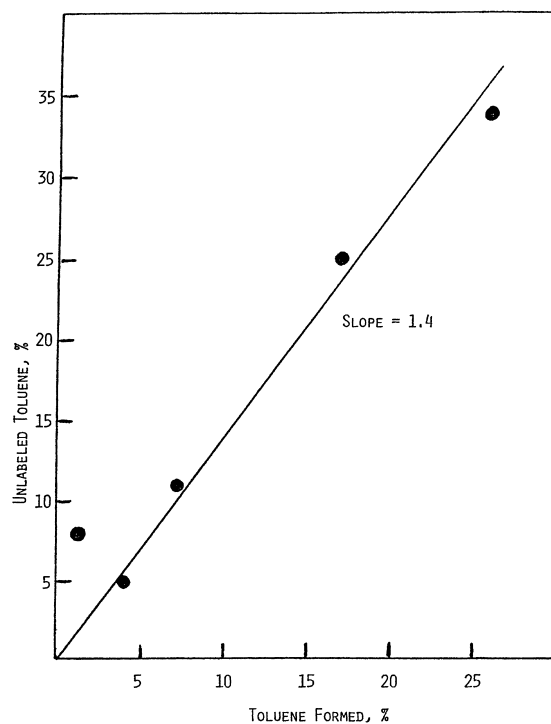

Fig. 26. Fraction of unlabeled toluene versus total toluene found during the conversion of a mixture of [3-^{14}C]-*n*-heptane (76%) and unlabeled methylcyclohexane (24%) at 520°C with a Pt-alumina catalyst (data from [148]).

kinetic isotope effect of about 3.5 would require this ratio to change to 3.5 for the conversion of 2,2,7,7-tetradeutero-octane. The aromatic distribution obtained for the conversion of 2,2,7,7-tetradeutero-octane with the Pt-SiO$_2$ catalyst at 482°C was essentially the same as those of the undeuterated *n*-octane. This result requires that the adsorbed alkane undergoes H/D exchange much more rapidly than cyclization so that the aromatic is formed without regard to the ini-

tial C–H bond that is broken in the rate-determining alkane adsorption step.

Isagulyants et al. [146] and Kazanskii and Rozengart [147] converted various cyclohexane-hexane mixtures in which the cyclohexane was labeled with [14]C. As shown in Fig. 25, the ^{14}C labeled benzene was directly related to the amount of ^{14}C labeled cyclohexane in the charge. The slope shows that cyclohexane was converted about 1.5 times as rapidly as *n*-hexane; this is similar to the value we obtained with this mixture using a number of catalysts [141]. Il'in et al. [148] found a selectivity for the conversion of a *n*-[3-[14]C-]heptane-methylcyclohexane mixture over Pt-Al$_2$O$_3$-K (Fig. 26); correcting the slope for the approximate 3-fold excess of *n*-heptane in the reactant gives a ratio of 4.4.

Manninger et al. [149] converted a mixture of *n*-hexane and [^{14}C]-cyclohexane with a Pt KL zeolite catalyst at about 300°C in a recirculating reactor.
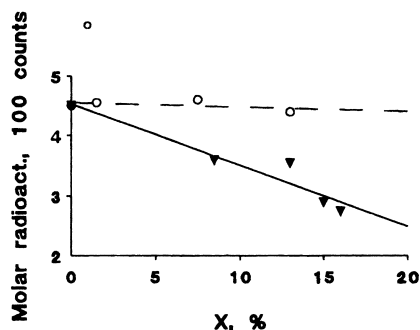
Fig. 27. Molar radioactivity in the cyclohexane fraction of the effluent as a function of the conversion, X. Feed: mixture of 10 Torr n-hexane + 2 Torr [^{14}C]-cyclohexane in a closed-loop circulation reactor containing 0.8% Pt/KL catalyst. $T = 300°$C, $p(H_2) = 120$ Torr (circles) and 480 Torr (triangles) (from [150]).

Two hydrogen pressures were used, 16 and 64 kPa, with a 20% cyclohexane mixture (0.27 kPa cyclohexane and 1.33 kPa n-hexane). At the lower hydrogen pressure the cyclohexane label was constant for several levels of conversion (Fig. 27); however, at the higher hydrogen partial pressure the relative activity in cyclohexane declined with increasing conversion. Menon and Paál [150] indicate that the higher hydrogen partial pressure might be able to hydrogenate the alicyclic surface precursors of benzene (cyclohexene or cyclohexadiene) to cyclohexane. At 300°C and atmospheric pressure, the equilibrium composition of cyclohexane/benzene should be far (95+%) on the benzene side. It does not appear reasonable for desorption of cyclohexane, following hydrogenation of cyclohexane, of cyclohexene or cyclohexadiene to be more rapid than the subsequent dehydrogenation to benzene. Details of the analytical procedure were not given other than a gas chromatograph equipped with a radioactivity detector was used. A similar result could be obtained if a product derived from n-hexane coeluted with cyclohexane and served to dilute the cyclohexane with respect to the original activity. In any event, these results are difficult to explain and the authors [150] indicate that further experiments are necessary to elucidate this question.

For total pressures in the 400 psig range and 482°C, the relative conversion of a cycloalkane/alkane mixture favored cycloalkane by a factor that was at least 20 or greater. Our results suggested that the atmospheric pressure conversion was nearly independent of hydro-

gen partial pressure. Thus, as the hydrogen pressure is increased to several atmospheres, it appears that the mechanism gradually changes from irreversible to reversible adsorption.

The question of whether an alkene, and even diene and triene (see discussion below), is an intermediate in the dehydrocyclization mechanism has been debated. To define whether this is the case, a mixture of 1-octene-d_0 and n-octane-d_{18} was converted with the Pt-SiO$_2$ catalyst [151]. Several observations for the conversion of this reaction mixture bear heavily upon the dehydrocyclization mechanism that operates. First, there is some H/D exchange in the small amount of alkene that is observed in the products, indicating that the added alkene undergoes adsorption/desorption during the conversion. Secondly, there is not a detectable amount of n-C$_8$H$_{16}$D$_2$ or n-C$_8$H$_{17}$D$_1$; this result shows that the adsorbed alkene does not undergo hydrogenation to the alkane which then desorbs to the gas phase. Thus, the alkene must be adsorbed in a form that allows some fraction to desorb as well as in a manner that subsequently leads to the aromatic products. Thirdly, the alkene in the alkene/alkane mixture is adsorbed and converted to aromatics much more rapidly than the alkane. Similar results were obtained for a reaction mixture of 1-heptene-d_0 and n-octane-d_{18}. The results show that the adsorption of an added alkene is greatly favored over that of the alkane. Since the rate limiting step for alkane dehydrocyclization is the initial C–H bond rupture, the added alkene must enter the cyclization reaction pathway at some step that follows the rate limiting step or must be converted in a parallel pathway.

Price et al. [152] found a large kinetic isotope effect ($k_H/k_D > 2$ at 400°C) when deuterated hydrocarbons are reacted simultaneously (or separately) with similar undeuterated hydrocarbons. Thus, the authors found a kinetic isotope effect of about 2.5 from the conversion of deuterated and undeuterated cyclohexane with a Te/NaX zeolite at 400°C (Fig. 28). Furthermore, the authors found when a mixture of C$_6$H$_{12}$ and C$_6$D$_{12}$ were converted in the presence of gaseous H$_2$ or D$_2$, the kinetic isotope effect was similar. Equally important, they found little intermolecular H/D exchange nor was there exchange with the gaseous H$_2$ or D$_2$. Since they found that cyclohexane converted at the same rate in the presence of gaseous H$_2$ or D$_2$, they showed that there is no isotope effect with the
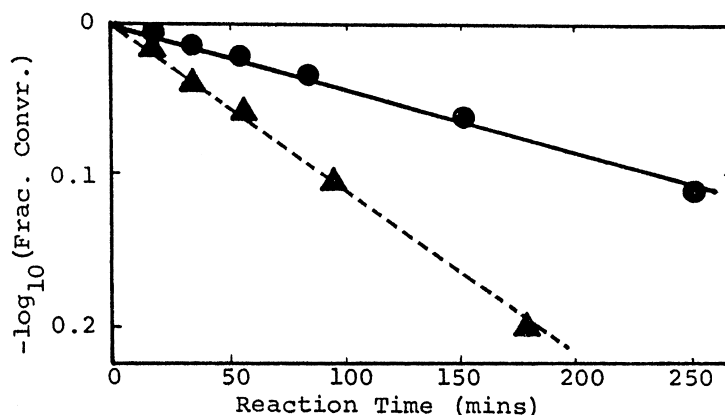
Fig. 28. First order plots for conversion of cyclohexane-d_0 (▲) and cyclohexane-d_{12} (●) in a D_2 in recirculation reactor at 400°C (40 Torr cyclohexane, 300 Torr H_2 or D_2) (from [152]).

activation of hydrogen (deuterium) with this catalyst. These authors concluded that the absence of extensive H–D exchange and presence of a large kinetic isotope effect strongly suggested that the slow step in the reaction is the cleavage of one or more C–H bonds. The authors converted undeuterated cyclohexene in the presence of gaseous D_2; they found both cyclohexane and benzene as the products. Neither the cyclohexane or benzene had incorporated significant amounts of deuterium, showing that these products were formed from cyclohexene disproportionation. While they did not detect dienes or trienes in the products, these authors interpreted their results using the triene mechanism outlined below; however, they had no direct evidence to support this mechanism. At the same time, their results are consistent with the rate limiting step being the initial C–H bond rupture in a mechanism that involves irreversible adsorption of the reactant.

Using single crystal Pt catalysts, Davis et al. [153] found an inverse kinetic isotope effect ($k_H/k_D = 0.3$–0.77) for the initial rates for the hydrogenolysis, isomerization and C_5-cyclization of n-hexane and n-heptane at 1 atm and 520–640 K (247–367°C). The isotope effect did not depend upon the crystal face of the Pt single crystal. They considered the inverse kinetic isotope effect to depend upon a combination of kinetic and thermodynamic effects. These authors found that the aromatization reaction, unlike hydrogenolysis and isomerization, exhibited the normal kinetic isotope effect (e.g., Fig. 29).
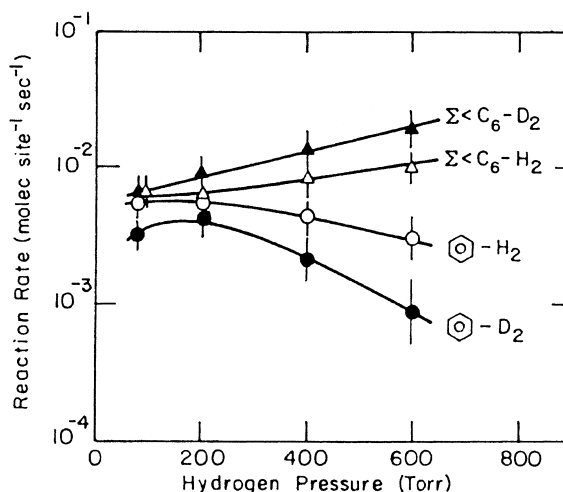
Fig. 29. Comparison between n-hexane (20 Torr) hydrogenolysis and aromatization rates over Pt(10,8,7) at 300°C as a function of hydrogen (D_2) pressure (from [153]).

Iglesia et al. [110] converted a mixture of 1-heptene (20 mol%) and [1-^{13}C-]-n-heptane with a Te/NaX zeolite catalyst. They utilized a batch, recirculating reactor system in which the reactants and products, as they accumulate, are recirculated over the catalyst. The data are reported in terms of toluene turnover, defined as the moles of C_7 converted to toluene per Te moles in the catalyst, as shown in Fig. 30. When the ^{13}C-labeled toluene content in the products is plotted against reaction time, the data fit a straight line that extrapolates to
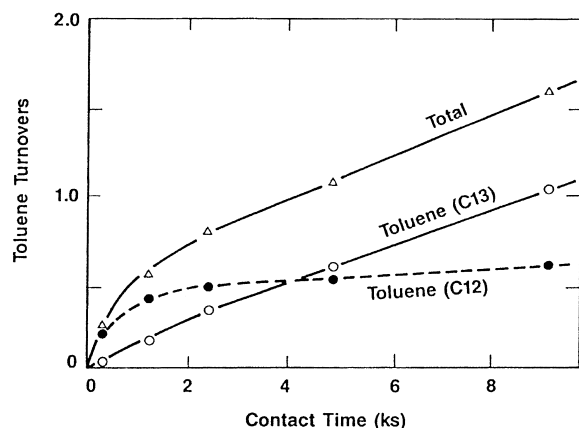
Fig. 30. Moles of labeled and unlabeled toluene formed from 1-heptene (20%)/*n*-heptane-1-^{13}C (80% mixtures) (723 K; hydrocarbon, 4.5 kPa; hydrogen, 96 kPa) (from [110]).

Scheme 27.

zero at zero time. However, the ^{12}C-toluene extrapolates to a non-zero value at time zero. The ^{12}C-toluene concentration rapidly attains a limiting value that is in the range of 0.4–0.5 toluene turnovers. These authors report that the heptenes and heptane, as determined by ^{13}C content, had equilibrated within 2 ks contact time. We believe that a more reasonable explanation for the experimental data at short contact times is that the 1-heptene underwent conversion at a much more rapid rate than the *n*-heptane, and the authors make this observation in their paper. Thus, during the initial stages of the conversion, the unlabeled 1-heptene is consumed at a much more rapid rate than the [1-^{13}C]-*n*-heptane is. From the data in Fig. 30, we judge that the unlabeled 1-heptene conversion is essentially complete in the first 2 ks of contact time. This rapid depletion of the unlabeled 1-heptene would leave only ^{13}C-labeled heptane as a reactant after about 2 ks so that the products could only be derived from the ^{13}C-labeled heptane. For the latter interpretation, the data of Iglesia et al. are completely consistent with our data for the conversion of 1-octene-d_0 and *n*-octane-d_{18}. The data in Fig. 30 would be consistent with a mechanism where the alkene and alkane are converted through either a common or in parallel reaction pathways.

It is apparent that there is a primary isotope effect for the conversion of both *n*-octane and methylcyclohexane. These results require that the C–H (C–D) bond breaking process be involved in the rate-determining
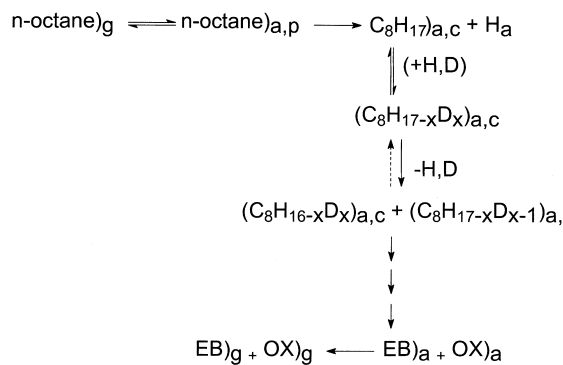
step. It appears that the data described above for our deuterium-labeling studies show that the C–H (D) bond breaking process occurs in the step leading from the physically adsorbed species to the chemically adsorbed species as shown in Scheme 27 where g = gas phase, a = adsorbed phase, and p and c = physical and chemical, respectively.

The experimental data for deuterium labeled compounds can be explained using the above mechanism. First, there is very little H/D exchange in the unconverted reactants. The step leading from physisorption to chemisorption is essentially irreversible; thus, even though there is extensive H/D exchange following chemisorption, the H/D exchanged species do not return to the gas phase. Secondly, Scheme 27 explains the primary kinetic isotope effect because the C–H (C–D) bond breaking occurs in the irreversible chemisorption step. Thirdly, the cyclization step follows the chemisorption step. The experiment for the dehydrocyclization of 2,2,7,7-tetradeuteriooctane showed that there is no isotope effect in the step that determines whether ethylbenzene or *ortho*-xylene is formed [145]. Finally, this mechanism indicates that there will be H/D exchange in the reactant as well as in the products at higher H_2 (D_2) pressure since high concentrations of [H] and [D] will shift the above steps of Scheme 27 to the left. While the experiment with D_2 has not been conducted at high pressure to date, the competitive conversion of methylcyclohexane and *n*-octane at H_2 pressures of 200 or 400 psig are consistent with reversible adsorption, in agreement with the above prediction. These experiments with deuterium have been conducted at 100 psig and exchange, as postulation does occur.

Previously, it was proposed [142] that the first step of chemisorption is as shown in Eq. (3).

$$RH \rightleftarrows R^\bullet + H^\bullet \qquad (3)$$

and that $R^\bullet$ is further dehydrogenated in a second step to form a methylene species:

$$R^\bullet \rightleftarrows R : + H \qquad (4)$$

We do not have experimental evidence to prove this hypothesis. However, the reverse of reaction (3) is widely accepted as the final step in the olefin hydrogenation.

The k_H/k_D value (3.5 for *n*-octane, 2.9 for methylcyclohexane) obtained from this study is higher than expected if only the zero point energy of the C–H and C–D bonds are considered. According to a classical view of the kinetic isotope effect, the ratio of rate constants is:

$$\frac{k_H}{k_D} = \frac{\exp \Delta E_0}{RT} \qquad (5)$$

where ΔE_0 is equal to the zero point energy difference of C–H and C–D bonds, and has a value of 1.2 kcal/mol. Based on this equation, at 482°C the maximum value of k_H/k_D is calculated to be 2.2, somewhat smaller than determined experimentally.

The above calculation for the maximum value for k_H/k_D assumes that ΔE is the same at 482°C as it is at room temperature. Considering the inharmonic nature of the vibration mode that introduces the isotope effect, this assumption may be questioned. For example, if the Morse potential-energy function for deuterium broadens more rapidly than for hydrogen as the temperature increases, the difference in the ground state energies between C–H and C–D would become larger, and the kinetic isotope effect would be larger than calculated above. However, this does not appear to be a likely explanation.

The energy difference between gaseous H_2 and D_2 is 1.8 kcal but the difference between H and D adsorbed on nickel is 2.4–2.8 kcal/mol; i.e., the heat of adsorption of D_2 is larger than that of H_2 by about 1 kcal/mol [154]. Any difference in the energy of adsorption to form H-Pt and D-Pt have been neglected in the calculation of k_H/k_D using Eq. (5). Should there be a difference between the energy for Pt-D and Pt-H, and should it be in the desired direction, ΔE in Eq. (5) would be larger and would provide for a larger value of k_H/k_D.
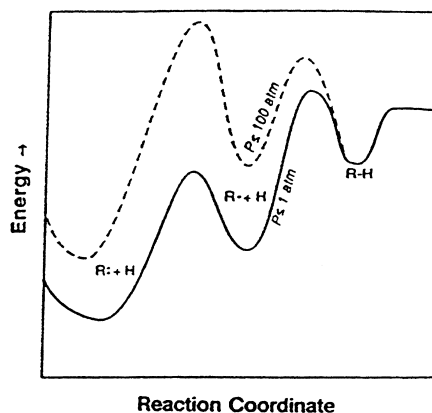

Fig. 31. Schematic potential energy curves showing alteration of irreversible adsorption for 1 atm conditions to reversible adsorption for 200 psig conditions.

A large number of results for the proton transfer reaction show that k_H/k_D at ordinary temperature (25°C) usually lies between 3 and 7; however, it is not uncommon to obtain values of k_H/k_D as high as 10 at 25°C [155]. In a few instances, values as large as 23 are encountered (e.g., [156,157]). These results indicate that the explanation of the variable kinetic isotope effect in terms of only the zero point energy does not adequately account for the experimental facts. Some attribute the larger values of k_H/k_D to a tunneling effect (e.g., [158]). Schwab [159] reviewed the application of a tunnel effect to heterogeneous catalysis as early as 1937. While the tunnel effect can be adequately accounted for in some instances (e.g., radioactive decay and semiconductors), the theory lacks a quantitative formulation for application in catalysis even today.

The data collected in this study and in our earlier competitive conversions of naphthene/alkane mixtures in the pressure range of 100–400 psig [160] are consistent with the chemisorption step(s) having a hydrogen dependence (Fig. 31). This figure has similarities with the one showing the change in relative activation energies illustrated by the potential energy curves shown in Fig. 32 [161]. For adsorption on a clean metal surface, the activation energy to go from the intermediate chemisorbed state to the final chemisorbed state is lower than the one required for desorption. However, the potential energy curves change with surface coverage and at high coverages ($\theta = 1$) the situation is reversed so that conversion to the physically adsorbed
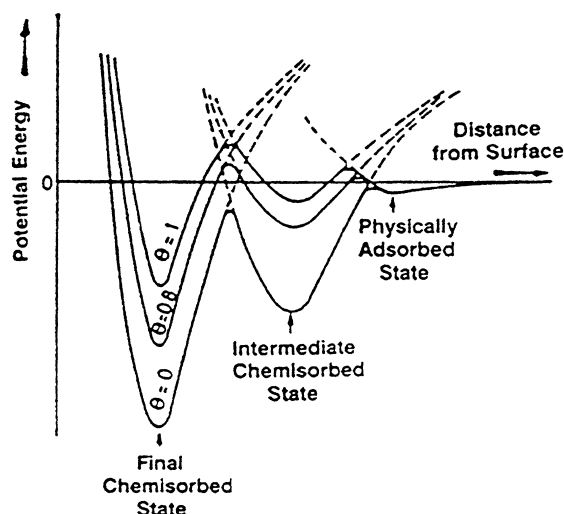
Fig. 32. Schematic of potential energy diagram showing the relative activation energies for chemisorption of intermediate and final chemisorbed states and the variation with surface coverage (from [161]).

state has a lower activation energy than the step leading to the final chemisorbed state.

For the conversion of a mixture of *n*-octane and methylcyclohexane at 1 atm, both reactants behave as though the potential energy curve corresponds to the case of $\theta = 0$ in Fig. 31. The lower activation energy leading to the chemisorbed state of a carbene (Fig. 31) has a lower activation energy than does desorption to the gas phase for the run at even 1 atm. However, the change in selectivity to favor the conversion of the naphthene at 100–400 psig (8 : 1 H_2 : naphthene) is consistent with a potential energy curve where the conversion of the alkyl radical to form the carbene (first chemisorbed state to second chemisorbed state) has a higher activation energy than desorption does. This hypothesis requires that the unconverted alkane has undergone exchange with deuterium when that gas is present at high pressure; unfortunately, this experiment has not been successfully accomplished at this date.

The dehydrogenation of isobutane with Pt-Sn/Al$_2$O$_3$ also exhibits a kinetic isotope effect even in the presence of hydrogen [162–165]. From the kinetic analysis, the authors concluded that the rate limiting step is the dissociative adsorption of isobutane, and the isotopic exchange studies support this view. When deuterium was added to the feed at temperatures above 550°C, a relatively high degree of exchange had
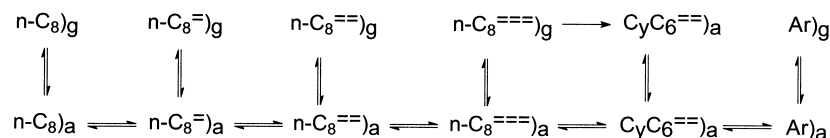
occurred in the isobutene formed during the dehydrogenation, but there was only a small exchange in the isobutane reactant. These data indicate that adsorption is essentially irreversible under these high temperature reaction conditions. The elimination of the second hydrogen is rapid and reversible in quasi-equilibrium, allowing for extensive hydrogen-deuterium exchange. There also seems to be a quasi-equilibrium between the surface hydrogen and the gaseous deuterium that allows a significant amount of deuterium on the catalyst surface. The result for high-temperature dehydrogenation of isobutane and the high-temperature dehydrocyclization of alkanes are therefore consistent.

In summary, there is a significant primary kinetic isotope associated with the rate limiting step for dehydrocyclization and for the dehydrogenation of methylcyclohexane. The results from the competitive conversion of *n*-octane and methylcyclohexane as well as the small amount of H/D exchange in the unconverted reactants show that the reactants are irreversibly adsorbed on the Pt catalyst at 482°C. The large value of k_H/k_D indicates that factor(s) in addition to the normal primary kinetic isotope effect must be involved in the reaction.

8. Triene intermediate

The mechanism for dehydrocyclization has been proposed by many to involve a series of dehydrogenation steps and isotopic tracer studies that involve the addition of a labeled potential intermediate have provided data that are considered to support this scheme [166–180]. Thus, for *n*-octane dehydrocyclization this mechanism could be represented as follows (Scheme 28).

In the above, a and g refer to adsorbed and gas phase species, respectively; =, ==, and === refer to one, two or three double bonds, respectively; $CyC_6^{==}$ refers to either ethyl- or 1,2-dimethyl-cyclohexadiene; and Ar refers to ethylbenzene or *o*-xylene. An example of an experiment used to confirm the above mechanism involves the conversion of a reaction mixture of ^{14}C-labeled hexene and unlabeled hexane, and determining the ^{14}C content of the species involved in the reaction network in Scheme 28. However, the irreversible nature of the initial, rate-limiting step precludes the addition of any of the intermediates

n-C$_8$)g   n-C$_8$$^=$)g   n-C$_8$$^{==}$)g   n-C$_8$$^{===}$)g $\longrightarrow$ C$_y$C$_6$$^{==}$)a   Ar)g

n-C$_8$)a $\rightleftharpoons$ n-C$_8$$^=$)a $\rightleftharpoons$ n-C$_8$$^{==}$)a $\rightleftharpoons$ n-C$_8$$^{===}$)a $\rightleftharpoons$ C$_y$C$_6$$^{==}$)a $\rightleftharpoons$ Ar)a

Scheme 28.

shown in Scheme 28 from providing proof of the sequential dehydrogenation mechanism.

Many results using suspected intermediates with isotopic label led to the conclusion that dehydrocyclization occurs through cyclization of the triene in the gas phase [166–180]. This method has become known as the 'Kinetic Isotope Method' (KIM). More recent results, especially those of Paál, Tetenyi and coworkers [181–184] and Kazanskii and coworkers [185], suggest that dehydrocyclization occurs by a consecutive stepwise dehydrogenation pathway through the alkene and diene to the triene which desorbs to the gas phase where it undergoes a C$_6$ thermal cyclization. However, the KIM method is especially susceptible to 'chemical disguises' [186] and this has not been recognized by all workers.

Gál et al. [187] reviewed the application of KIM and Guczi and Tetenyi [188] considered the application of KIM to dehydrocyclization; thus, we will not consider this subject in detail. In their review, Gál et al. [187] state that 'If the rate of equilibration between the gas phase and the surface is much larger than that of the chemical reaction, we can assume that the specific activity of the intermediates will be the same in the gas phase as that on the catalyst surface. Thus, the specific activities, as measured in the gas phase, can be used in the relevant KIM expression'. Paál and Tetenyi [181–184], in their extensive study of dehydrocyclization of hexane–hexene mixtures, felt that they had good reasons to believe that the assumption of Langmuir–Hinshelwood kinetics could not be applied. In spite of this, they used the data to establish their view of a dehydrocyclization pathway involving a triene intermediate.

The data of both Isagulyants et al. [146,147] and Il'in et al. [148] are also consistent with a mechanism that does not have adsorption–desorption equilibrium of the reactants. Dautzenberg and Platteeuw [118] concluded that cyclization of hexane occurred by (i) a platinum catalyzed six-ring closure and (ii) a thermal six-ring closure of hexatrienes; however, the thermal cyclization depends on hydrogen pressure so that it becomes less significant to the overall conversion at higher pressures. To us, it appears that the KIM results are suggestive of hexatriene intermediates but a determination of the amount that this pathway contributes to the aromatics formation must await further experimentation.

9. Conversion of alkylpentanes

There are ample data to show that C$_5$-ring formation occurs for the low temperature range (about 300°C) but, as documented above, C$_5$-ring formation makes little or no contribution to the mechanism that leads to aromatic compounds at high (about 480°C and higher) temperatures. Furthermore, hydrogen/deuterium tracer studies indicate that irreversible adsorption is a dominating feature of the higher, but not the lower, temperature region. With Pt-Sn-ZSM-5 catalysts, Dessau finds that *n*-pentane can be converted with high selectivity (80%) to cyclopentane [189]. Thus, it is not a question of whether cyclization to a cyclopentane ring structure occurs; rather, it is a matter of defining the role of cyclopentanes in the formation of aromatic products.

Much attention has also been given to the production of aromatics from hydrocarbons in which the longest carbon chain contains five carbons; the dehydrocyclization of *iso*-octane (2,2,4-trimethylpentane) is an example of such an alkane that has been used. It is obvious that a direct C$_6$-ring forming mechanism cannot apply for such a reactant. Thus, we will not include a further discussion of the lower temperature conversion of alkyl pentanes.

10. Atmospheric vs. reforming pressures

Silvestri and Smith [190] determined the effect of hydrogen partial pressure on *n*-hexane dehydrocyclization activity of Pt-carbon and TeNaX catalysts.
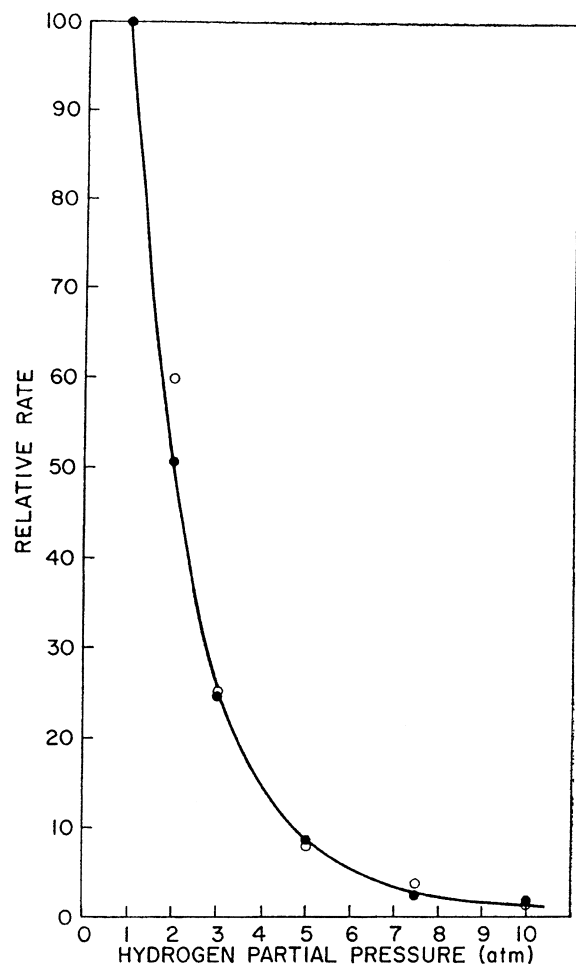
Fig. 33. Relative dehydrocyclization activities for Te/NaX (○) and Cr_2O_3/Al_2O_3 (●) catalysts as a function of hydrogen partial pressure (from [190]).

The relative rate for aromatization of both catalysts had a common dependence on hydrogen partial pressure (Fig. 33). The authors developed a rate expression based upon a consecutive dehydrogenation pathway that leads to heptatrienes and their subsequent cyclization that depended on the third power of hydrogen. As shown in Fig. 34, the authors fit the highest two data points to a line with a slope of -3 as required for the triene mechanism. However, if instead of the two highest data points, one uses the two lowest partial pressure points, one obtains a slope of −0.71. The value for the two lowest points shows reasonable agreement with the relative dehydrocy-

clization rate depending on $P_H^{1/2}$, as expected for an irreversible chemisorption mechanism.

Results with *n*-octane enable us to make a connection between atmospheric pressure operations and the reforming process which is carried out at pressures in the 60–400 psig (0.41–2.72 MPa) range [191]. A nearly equilibrium aromatic composition is obtained with a Pt on acidic alumina catalyst operating at 400 psig (2.72 MPa) (Fig. 35). For Pt : Sn = 4 : 1 (and for Pt) on nonacidic alumina, at 200 psig (1.36 MPa) the aromatic products are only those allowed by direct C_6-ring formation to produce equal amounts of ethylbenzene and *o*-xylene (Fig. 36). For a Pt : Sn = 1 : 4 nonacidic alumina catalyst, the aromatics formed at the early time on stream were nearly the equilibrium composition. By the seventh hour on stream, the aromatics were greater than 90% of the isomers allowed by direct C_6 ring closure. In addition the *o*-xylene : ethylbenzene ratio was 2 : 1 (Fig. 37) just as it was with this catalyst at atmospheric pressure. The conversion of 3-methylheptane following the run with *n*-octane produces an aromatic distribution that is essentially the same as 1 atm, and are consistent with a direct six-carbon ring formation. With these catalysts, the traces of benzene and toluene in the liquid products could not have altered the aromatic composition significantly even if they were both derived from only one of the C_8-aromatic products. Consequently, the aromatic selectivity is the same at atmospheric pressure and at 200–400 psig (1.37–2.75 MPa) ; thus, the aromatic selectivity data obtained at atmospheric pressure with monofunctional catalysts should be applicable at reforming conditions. Unfortunately, the superiority of the Pt-Sn catalyst in activity and catalyst life was not as pronounced in the 200–400 psig (1.37–2.75 MPa) range as at atmospheric pressure.

On the other hand, Callender et al. [192] obtained results with Pt-SiO$_2$ at 15 atm which, when extrapolated to zero residence time, suggested that C_5-cyclization was responsible for at least 90% of the total cyclization for *n*-heptane. They felt it likely, following Keulemans and Voge's [193] results with an acidic Pt-Al$_2$O$_3$ catalyst, that the toluene resulted from ethylcyclopentane rather than 1,2-dimethylcyclopentane. Csicsery and Burnett [97], using a Pt-SiO$_2$ catalyst at 18 atm, found that for the conversion of ^{14}C-labeled 1,3-dimethylcyclopentane, ring expansion to toluene could account for only
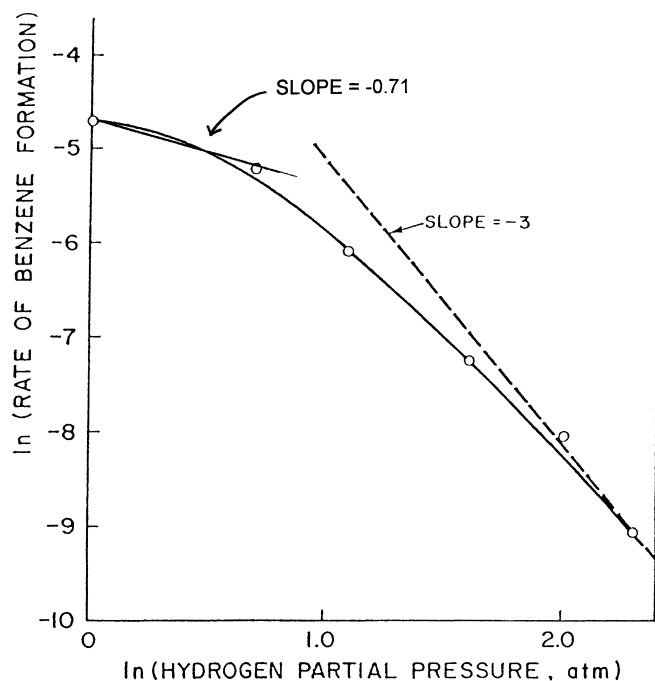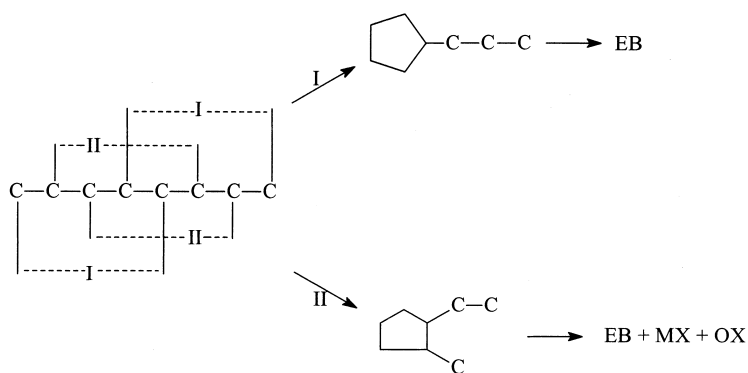
Fig. 34. Log–log plot of dehydrocyclization rate for Te/NaX catalyst as a function of hydrogen partial pressure (redrawn from [190]).

Scheme 29.

a maximum of about 10% of the total naphthene conversion. Csicsery and Burnett reported that the conversion to aromatics was less than the amount converted to lower weight products. Ring opening of 1,3-dimethylcyclopentane was nonselective to form 2,4-dimethylpentane, 2-methylhexane and 3-methylhexane; these products accounted for greater than 50% of the total conversion. There seems to be little doubt but what hydrogenolysis

occurred on the metal function; hence, if ring expansion of 1,2-dimethylcyclopentane was catalyzed by the metal function it should have occurred with 1,3-dimethylcyclopentane during the study by Csicsery and Burnett. The results of Davis [135] and Gault [194] with n-[4-^{13}C] heptane eliminate ethylcyclopentane as a major reaction pathway intermediate at atmospheric pressure. The results with n-octane at 400 psig (2.75 MPa) and 482°C are inconsistent with
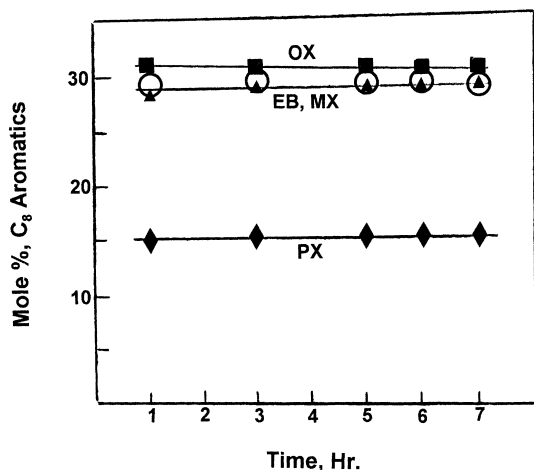
Fig. 35. C$_8$-aromatic distribution from the dehydrocyclization of n-octane over Pt on acidic alumina (500 psi; H$_2$: hydrocarbon = 10 : 1; temp., 482°C) (EB, ethylbenzene; OX, o-xylene; MX, m-xylene; PX, p-xylene) (from [191]).
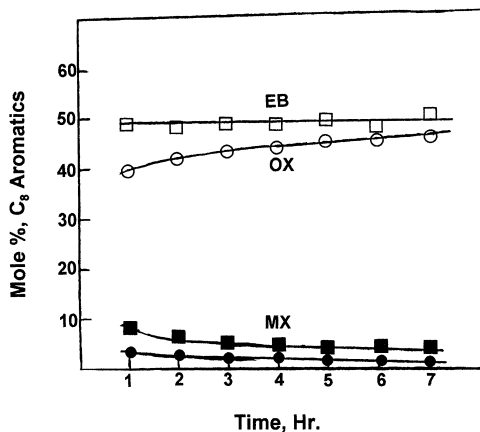
Fig. 36. C$_8$-aromatic distribution from the conversion of n-octane over a Pt : Sn (4 : 1) on nonacidic alumina catalyst (200 psi; H$_2$: hydrocarbon = 10 : 1; temp., 482°C) (EB, ethylbenzene; OX, o-xylene; MX, m-xylene; PX, p-xylene) (from [191]).

a cyclopentane intermediate, as outlined in following the Scheme 29.

1-Ethyl-2-methylcyclopentane, which should yield at least as much m-xylene as o-xylene, must contribute to any C$_5$-cyclization mechanism for n-octane because propylcyclopentane cannot lead directly to o-xylene by ring expansion. But the amount of m-xylene obtained with Pt-Al$_2$O$_3$-K at atmospheric and 200 and
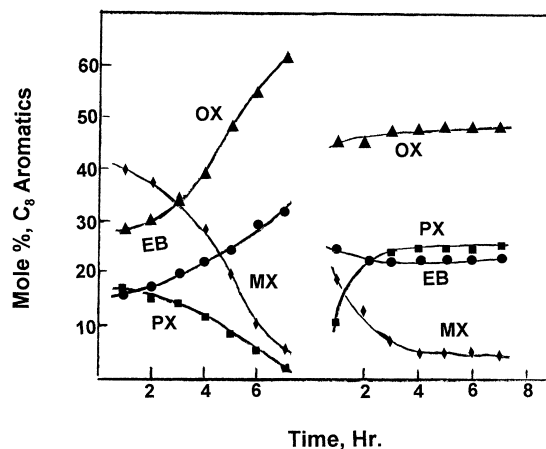
Fig. 37. C$_8$-aromatic distribution from the conversion of n-octane (left) over a Pt : Sn = 1 : 4 (conditions same as for Fig. 36) and 3-methylheptane following overnight flush with nitrogen (EB, ethylbenzene; OX, o-xylene; MX, m-xylene; PX, p-xylene).

400 psi (1.37 and 2.75 MPa) was insignificant compared to the amount of o-xylene [191]. Hence, we must conclude that: (a) a cyclopentane intermediate does not contribute to the aromatics formation over the metal function or (b) an extremely unique ring expansion is operating which allows pathway to o-xylene but excludes the pathway to m-xylene in Scheme 29.

The results from the conversion of an alkane with a quaternary carbon are not the same at atmospheric and reforming pressure. At atmospheric pressure methyl migration from the quaternary carbon occurred to produce C$_9$-aromatics as well as C$_8$-aromatics resulting from demethylation. At 400 psig (2.75 MPa) we did not obtain C$_9$-aromatics from 2,2,5-trimethylhexane; only C$_8$-aromatics resulting from demethylation were obtained.

10.1. Hydrogen pressure effects

At all temperatures, surface hydrogen concentration must play an important role in alkane conversion. Sinfelt [195] reported that the rate of hydrogenolysis of ethane could be expressed as a simple power law:

$$r = k P_E^n P_H^m. \tag{6}$$

Cimino et al. [68] had found this equation to apply for an iron catalyst. Approximate values of n and m for Pt-SiO$_2$ and Pt-Al$_2$O$_3$ were 0.7 to 0.9 and
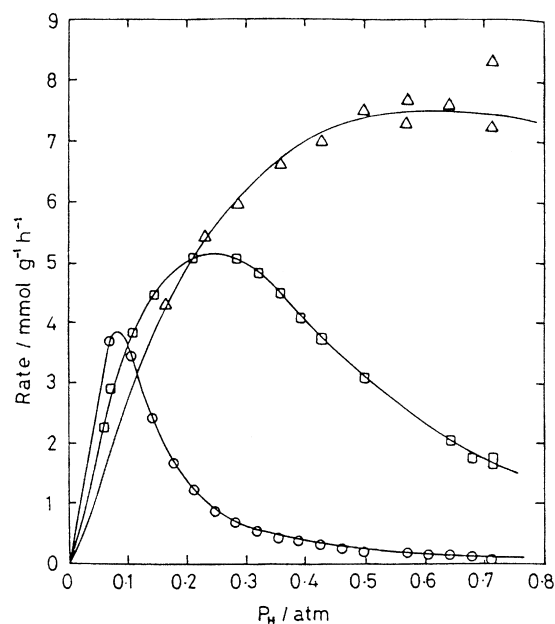
Fig. 38. Dependence of the rate of hydrogenolysis on H_2 pressure at 608 ± 1 K using Pt/Al_2O_3 (5): $\bigcirc$, C_2H_6; $\square$, C_3H_8; $\triangle$, n-C_4H_{10}. PA = 0.071 atm (from [196]).

-1.7 to -1.8, respectively. Thus, the rate increases with increasing ethane partial pressure but decreases markedly with increasing hydrogen pressure. This was interpreted in terms of a mechanism that involves partial, or even complete, dehydrogenation of the adsorbed ethane and then the subsequent hydrogenation of the carbon residue to produce methane. In this instance, the slow step is considered to be the breaking of the C–C bond. While the rates were similar for the two supports, the activation energies differed widely and this was considered to indicate a strong interaction between the support and platinum. Similar results have been reported by subsequent workers. For example, Bond [196] summarizes work with C_2–C_4 alkanes, showing that the rate initially increases as the hydrogen partial pressure increases (Fig. 38), attains a maximum and then decreases with further increases in hydrogen partial pressure. The hydrogen partial pressure effect is also temperature dependent with the maximum rate shifting to higher hydrogen partial pressure with increasing temperature (Fig. 39).

In Bond's recent summary, the kinetics includes Langmuir–Hinshelwood methodology for the adsorption of both the alkane (A) and hydrogen (H); this
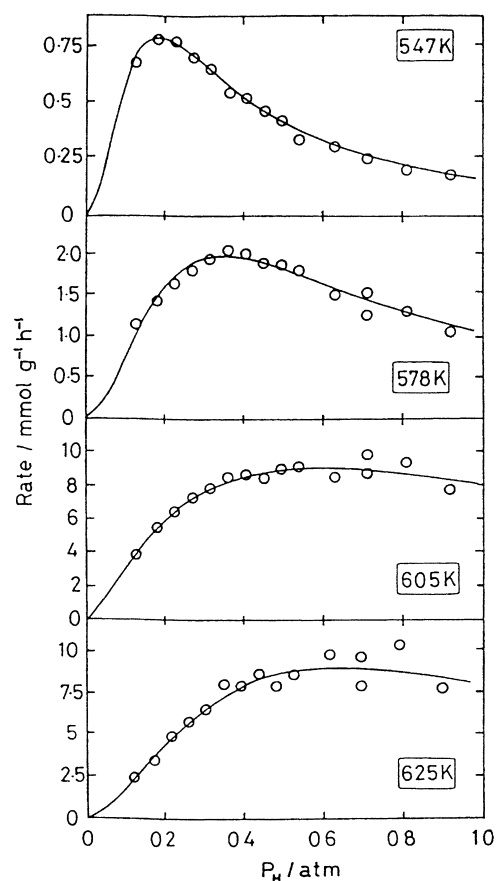

Fig. 39. Dependence of the rate of n-C_4C_{10} hydrogenolysis on H_2 pressure at various temperatures using Pt/Al_2O_3 (from [196]).

modifies the initial power law to

$$r = \frac{k P_A P_H^x}{\left(P_A + k_2 P_H^{x+1.2}\right)^2} \tag{7}$$

While the hydrogen dependence on the kinetics and mechanistic considerations for alkane hydrogenolysis is now well established, they are of secondary concern for dehydrocyclization.

As we have shown, the nature of alkane adsorption changes from reversible at lower temperatures to become essentially irreversible at higher temperatures where dehydrocyclization occurs at a reasonable rate. Thus, while the mechanistic understanding of the effect of hydrogen partial pressure described for alkane hydrogenolysis is of interest, it does not
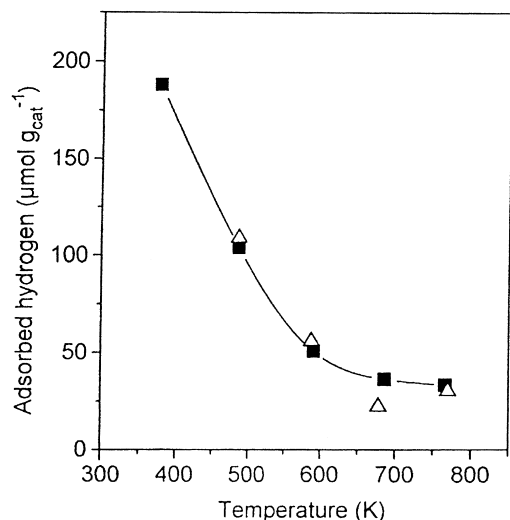
Fig. 40. Amounts of adsorbed hydrogen measured by isotopic transient kinetic titration over 5.3 mg of EUROPT 1 reduced at 773 K in the absence of ethane (squares) or under hydrogenolysis conditions (triangles) (from [197]).

appear possible to include it in a consideration of the dehydrocyclization mechanism which does not involve Langmuir–Hinshelwood reversible adsorption methodology.

Martin et al. [197] used an isotopic transient kinetic technique to measure the hydrogen surface coverage in the presence and absence of ethane. They found a similar hydrogen surface coverage for the EUROPT1 (Pt-SiO$_2$) catalyst over the temperature range 400–800 K whether ethane was present or absent (Fig. 40). Furthermore, the amount of adsorbed hydrogen from the isotopic transient kinetic technique agreed closely with those for data obtained using a volumetric technique with the same catalyst [198]. For the static volumetric conditions with 0.13 kPa hydrogen partial pressure, the amounts adsorbed at 227 and 277°C was 88 and 75 μmol/g-cat. compared to the values of 94 and 67 μmol/g-cat. from the isotopic transient kinetic technique. The authors found that α, the coefficient of Temkin's law,

$$\theta_H \approx \alpha \log P_H, \tag{8}$$

was nearly constant over the range 227–527°C. At pressures in the range of 50 kPa, the surface coverage by hydrogen, θ_H, is about 0.5 of a monolayer at 527°C (Fig. 41). The data shown in Fig. 41 are in qualitative
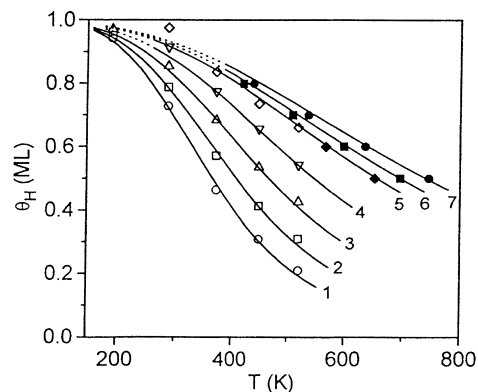

Fig. 41. Hydrogen coverage (monolayer) as a function of temperature at 1.3, 13, 131 Pa, 1.3, 13, 26.3, 53 kPa (from [198]).
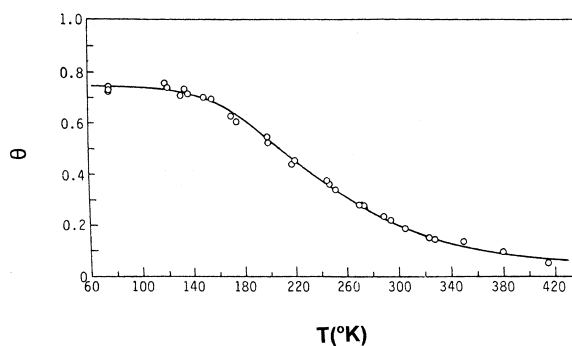

Fig. 42. Isobar measured at 7×10^{-8} Torr at pressure 10^{-3}–10^{-4} Torr is the isobar shifted by about 100°C to higher temperatures. Metal with a heat of adsorption higher than that of Pt, 1 shift the curves to the right (from [199]).

agreement with those reported for measurements using a Pt filament and a pressure of 7×10^{-8} Torr [199] (Fig. 42).

Iglesia et al. [168] considered the kinetic coupling and hydrogen surface fugacity for the conversion of *n*-hexane with Te/NaX, H-ZSM-5 and Ga/H-ZSM-5 catalysts. These authors propose that the rate-limiting hydrogen desorption steps, and the high surface hydrogen fugacities that result, control the rate and selectivity of dehydrogenation and related reactions on many nonmetal surfaces. They found that competitive reactions of 3-methylcyclohex-1-ene (about 20 mol%) and [1-^{13}C]methylcyclohexane showed that the initial toluene products are unlabeled and concluded that methylcyclohexenes are required intermediates in
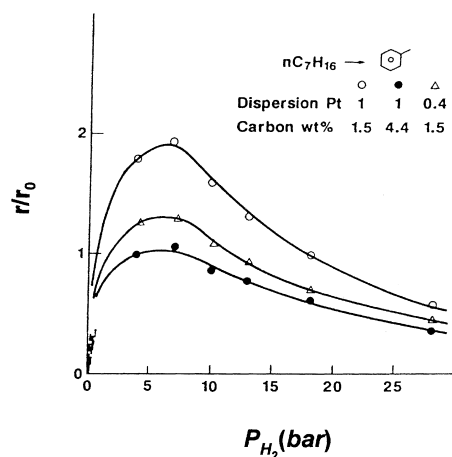
Fig. 43. Rate of dehydrocyclization versus hydrogen pressure ($T = 470°C$, $P_{HC} = 2.2$ bar, Pt/Al$_2$O$_3$, r_o = rate at $P_{H_2} = 18$ bar) (from [200]).
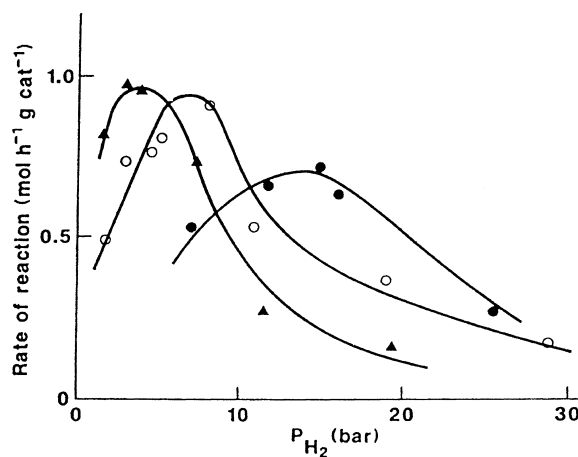

Fig. 44. Rate of dehydrocyclization versus hydrogen pressure for various hydrocarbon pressures ($T = 470°C$, $P_{HC} = 2.2$ bar, Pt/AL$_2$O$_3$, $C = 1.5$ wt.%, P_{HC}(bar): ▲ 0.5, ○ 1, ● 5) (from [201]).

toluene formation. However, as indicated above, and as found by Shi and Davis [151] for the conversion of 1-octene and deuterium-labeled n-octane, these results are also consistent with the adsorption of the alkene being much more rapid than that of the alkane and that the initial products are formed exclusively from the alkene due to adsorption kinetics, and not due to surface mechanism considerations. Likewise, the conclusion reported by Iglesia et al. [168] does not appear to agree with that of Price et al. [152] who found that added hydrogen or deuterium did not impact the rate of dehydrocyclization with a similar catalyst.

Rohrer et al. [200] found that the rate for n-heptane dehydrocyclization increased with increasing hydrogen pressure up to a maximum value, and beyond this value the rate fell off with increasing hydrogen pressure (Fig. 43). The isomerization rate underwent a similar trend at 471°C but was less obvious at the higher temperature of 527°C. Bournonville and Franck [201] show figures from a thesis [202] that show the same trend in n-heptane dehydrocyclization rate versus hydrogen pressure as was obtained by Rohrer et al. (Fig. 44). In addition, these authors report that the hydrogen partial pressure that corresponds to the maximum rate shifts to higher pressure with increases in the partial pressure of n-heptane (Fig. 45). The rate maximum occurs at a common hydrogen partial pressure as the carbon number of the n-alkane increases from 6 to 10; however the rate of dehydrocycliza-
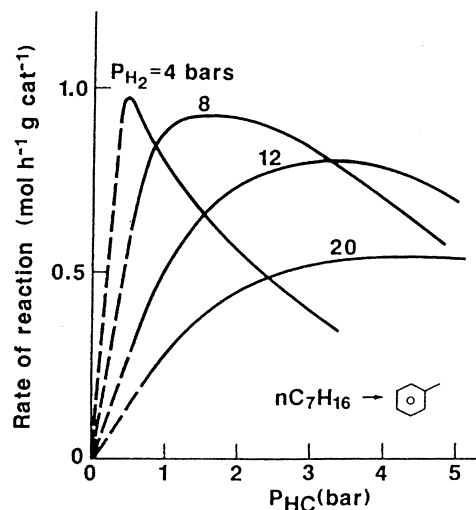

Fig. 45. Rate of dehydrocyclization versus hydrocarbon pressure for various hydrogen pressures ($T = 470°C$, Pt/Al$_2$O$_3$, $C = 15$ wt.%) (from [201]).

tion at the maximum increases with carbon number so that n-decane is converted about four times more rapidly than n-hexane. Bournonville and Frank [201] consider three reaction pathways for dehydrocyclization: metallic monofunctional path, metallic bifunctional path and acid bifunctional path. They consider the metallic monofunctional path takes place on the metallic phase only and involves a cyclohexanic intermediate which very rapidly dehydrogenates to the
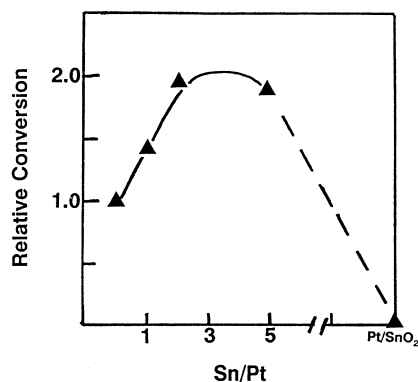
Fig. 46. The variation of *n*-octane conversion at atmospheric pressure with increasing tin loading using a nonacidic alumina support (point at right is for Pt on SnO$_2$ only) (from [203]).
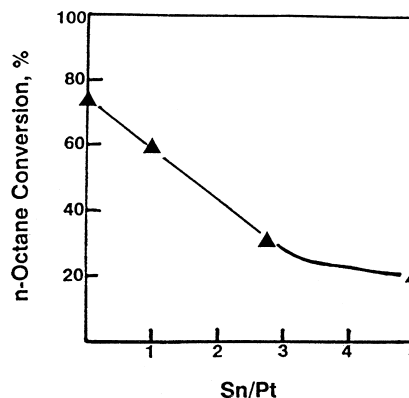

Fig. 47. *n*-Octane conversion with increasing Sn/Pt ratio using an acidic alumina support (482°C, 7.8 atm, LHSV = 1.8, and H$_2$/*n*-octane = 3/1) (from [203]).

aromatic. In their view, the metallic bifunctional path involves the cyclization to the cyclopentanic intermediate which undergoes ring expansion on the acid function before dehydrogenating. The bifunctional acid path involves the cyclization of olefins formed over the metal function. These authors consider cyclization to be the probable rate determining step and that equilibrium between adsorption and desorption is very rapid.

At atmospheric pressure tin added to a Pt-nonacidic alumina catalyst acts as a promoter, producing the maximum activity at about Sn/Pt = 4 (Fig. 46) [203]. However, when tin is added to a Pt-acidic alumina catalyst, for the conversion of *n*-octane at 482°C, 7.8 atm (0.79 MPa), and H$_2$/*n*-octane = 3, tin acts as a poison (Fig. 47). The tin, in this case, eliminates acid sites of the support and, since the bifunctional pathway involving cyclization at the acid site is about 30 times the rate of the monofunctional metal pathway [12], the conversion of *n*-octane declines with loss of catalyst acidity.

The ratio methylheptanes/aromatics in the products from the conversion of *n*-octane with Pt-nonacidic alumina catalysts and with Pt-Sn-nonacidic alumina catalysts depend upon the total pressure (the hydrocarbon/hydrogen mole ratio remained constant) (Fig. 48) [160]. Thus, for the high pressure naphtha reforming (400 psig, 2.75 MPa), about 3–4 times as much methylheptane isomers are formed as C$_8$-aromatics. Since the support for each of the three catalysts is nonacidic alumina, the reaction pathway is predominantly the monofunctional metal pathway. This means that the addition of tin decreases dramatically
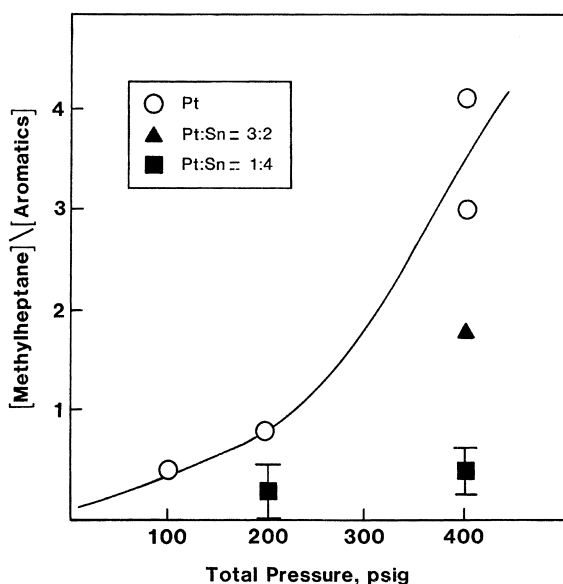

Fig. 48. The methylheptanes/aromatics ratio in products from dehydrocyclization of *n*-octane at 482°C and 400 psig (2.75 MPa) for Pt- and Pt-Sn-alumina catalysts (from [160]).

the 'metal monofunctional isomerization' pathway, presumably through the hydrogenolysis of alkylcyclopentanes that are formed in competition with the direct six-carbon ring formation pathway. At lower conversion levels of *n*-octane, the C$_8$-aromatics are essentially the same as formed at atmospheric pressure and are only the two expected for direct six-carbon ring formation. However, the incorporation of tin

Table 28
Aromatic products from *n*-octane dehydrocyclization with Pt-Sn-nonacidic alumina catalysts (from [203])

Catalyst	Pressure	Aromatics			
		Ethylbenzene	*o*-xylene	*m*-xylene	*p*-xylene
Pt-	1 atm	48	50	1.2	1.0
Pt-Sn = 3 : 8	1 atm	32	59	5.0	2.4
Pt	7.8 atm	45	48	7.0	Trace
Pt-Sn = 1 : 3	7.8 atm	38	62	Trace	Trace

alters the ratio of ethylbenzene : *o*-xylene from 1 : 1 without tin to 1 : 2 for Pt/Sn = 3 (Table 28) [203].

In summary, hydrogen partial pressure plays an important role in naphtha reforming and in dehydrocyclization. In most instances, these effects have been determined at low (1 atm and lower) pressures and are therefore difficult to extend to normal reforming conditions. Alkane hydrogenolysis decreases with increasing hydrogen partial pressure so that, in comparison to other reactions, it makes a small relative contribution during naphtha reforming. Hydrogen partial pressure also impacts the rate of dehydrocyclization negatively, and this is true for catalysts with acidic or nonacidic supports. With the acidic support, cyclization occurs predominantly by an acid bifunctional reaction pathway so that increases in pressure (above about 5 atm) apparently decreases the rate by decreasing the 'pseudo steady state alkene concentration'. Since similar aromatic isomer compositions are obtained at low (1 atm; 0.101 MPa) and high (27 atm; 2.73 MPa) pressures for the monofunctional metal pathway, hydrogen partial pressure does not alter the metal catalyzed cyclization pathway. However, increasing hydrogen partial pressure decreases the rate of dehydrocyclization so that it must function to decrease the concentration of the reactive surface intermediate(s) in the dehydrocyclization reaction pathway. Unfortunately, much remains to be defined with respect to the specific roles of hydrogen in the dehydrocyclization reaction pathway(s).

11. Catalytic site

The sextet model proposed by Balandin was simple and appealing [204]. The model required six vacant catalytic sites for cyclohexane dehydrogenation. These six sites were required to be arranged so that they formed a 'template' for the spacings of the hydrogen atoms in the cyclohexane reactant. Only those metals that were of the proper size and formed the proper crystal face to correspond to the hydrogen spacings in cyclohexane would be active catalysts and data were assimilated in the 1930s to support this view. A doublet site may operate in some cases so that it could be possible, in principle, to dehydrogenate *n*-heptane to heptenes on doublet sites even though cyclization could not be accomplished with the doublet site.

Balandin based his model on a surface that was identical to the bulk metal in structure and lattice spacing. However, recent results suggest that this is not the case but that, in the case of the small metal particles in the range of tens of angstroms (ca. 5 nm for Pt), the natural structure may be that of a five-fold symmetry structure [205,206]. These small metal particles with the icosahedral surface planes look like closely packed [111] planes. Thus, whereas normal fcc structures have [110] planes for surfaces, the icosahedral structure provides the [111] planes with the greater number of nearest neighbor bonds which lowers the energy of the system. More surprising, the experimental observations indicate that the nearest neighbor distance is smaller in the surface layer than that of the bulk material [207].

Joyner et al. [208] found *n*-heptane dehydrocyclization did not occur on the [111] crystal face of Pt and only occurred on the suitable stepped Pt surface with an appropriate atomic structure, terrace width and step orientation which was covered with an ordered layer of carbonaceous deposit template. If the ordered layer failed to form on account of the presence of surface impurities the dehydrocyclization reaction did not occur.

Thus, it appears that the present view of small particles and the large single crystal studies are in conflict as it concerns dehydrocyclization. On the one hand, small Pt crystallites are active dehydrocyclization

catalysts and, according to [205,206], should expose the (1 1 1) face; on the other hand, the (1 1 1) crystal face of large Pt single crystals is not active for dehydrocyclization.

The results of Blakely and Somorjai [209] for cyclohexane show a product distribution of ethylene : propylene : cyclohexene : benzene of 10 : 1 : 0.5 : 1; this corresponds to a selectivity for benzene of less than 20%. The hydrogenolysis reaction decreased the selectivity further so that with an equal turnover number for dehydrogenation and hydrogenolysis at about 7×10^{13} kink atoms/cm^2, the dehydrocyclization selectivity is about 10%. This is a very poor dehydrogenation selectivity compared to supported Pt catalysts since it would be unusual to find a benzene selectivity at atmospheric or reforming pressure of less than 80%. At 200 psig (137 MPa) and H_2 : hydrocarbon 9 : 1, we found that ^{14}C-labeled methylcyclohexane, added to a naphtha fraction, was converted to aromatics with a selectivity greater than 97% with the nonacidic catalyst and even 91% when we used an acidic commercial catalyst [108]. The data suggest that the small particles have a selectivity that differs from high loading or bulk metal catalysts. Much work remains to be done to connect the properties of small and massive Pt metal particles for both catalytic activity and selectivity.

12. Discussion

The mechanism for alkane dehydrocyclization is very complex and is composed of a multitude of individual steps with a variety of intermediate compounds. One of the complicating features of many of the mechanisms advanced to date has been the desire to include all reaction products within a single mechanism. In some instances, this desire has led to the formulation of a complex intermediate structure, such as a bicyclic intermediate, to explain the formation of minor products.

In discussing reaction mechanisms, one should keep in mind that there are features which are experimentally verifiable and hypotheses which are consistent with the experimental observation but are not directly proven by the data. The latter are analogous to kinetics. A 'correct' mechanism must be consistent with the kinetic data but even the best kinetic data will not limit the data to a single mechanism. Thus, kinetic data

can support a mechanism but cannot 'prove' a mechanistic pathway. On the other hand, the mechanism does not even have to be consistent with hypothesized pathways.

At the molecular level, dehydrocyclization may be viewed as a chemical reaction between a catalytic site and an alkane. A valid and complete mechanism must include a description of the catalytic site. At present, the nature of the catalytic site is poorly defined. This is true even for the monofunctional metallic dehydrocyclization pathway. The best descriptions of the catalytic site come from studies of Pt single crystal faces. While instrumental techniques, such as LEED, allow one to accurately define the surface features, this method suffers from two distinct disadvantages: (1) the reaction is conducted at very low pressures and (2) the results are obtained with Pt particles that are enormously large in comparison to those found in supported commercial catalysts. The low pressures provide reaction pathways to produce surface species that are strongly dehydrogenated; this is illustrated by the picture of the surface which is nearly covered by carbon or carbon-rich islands (Fig. 49) [18]. Hydrogenolysis and cracking become significant reaction pathways with large Pt particles relative to the rates of these two reactions with very small Pt particles. Thus, the benzene selectivity reported by Somorjai and coworkers (e.g., [18]) is very low compared to that obtained with a commercial Pt-alumina catalyst where Pt is present in small particles. While the data generated with the single crystal catalysts are of interest, it is not certain how to directly extrapolate the data to the small particles present in supported naphtha reforming catalysts.

The aromatic products formed from alkanes with at least one six-carbon chain are those that are predicted for a mechanism that involves direct six-carbon ring formation. For many C_8–C_{10} alkane isomers, 85%, and usually more than 85%, of the aromatics are those expected for direct six-carbon ring formation. For the dehydrocyclization of $[1\text{-}^{14}C]$- and $[4\text{-}^{14}C]$-n-heptane, 80%, and usually greater than 80%, of the ^{14}C appears at positions predicted for a direct six-carbon ring formation. Furthermore, the distribution of ^{14}C within the ring precludes a significant contribution by either alkylcyclopentane or cycloheptane intermediates. Similar results for dehydrocyclization of ^{14}C-labeled alkanes were obtained with both metal and metal oxide
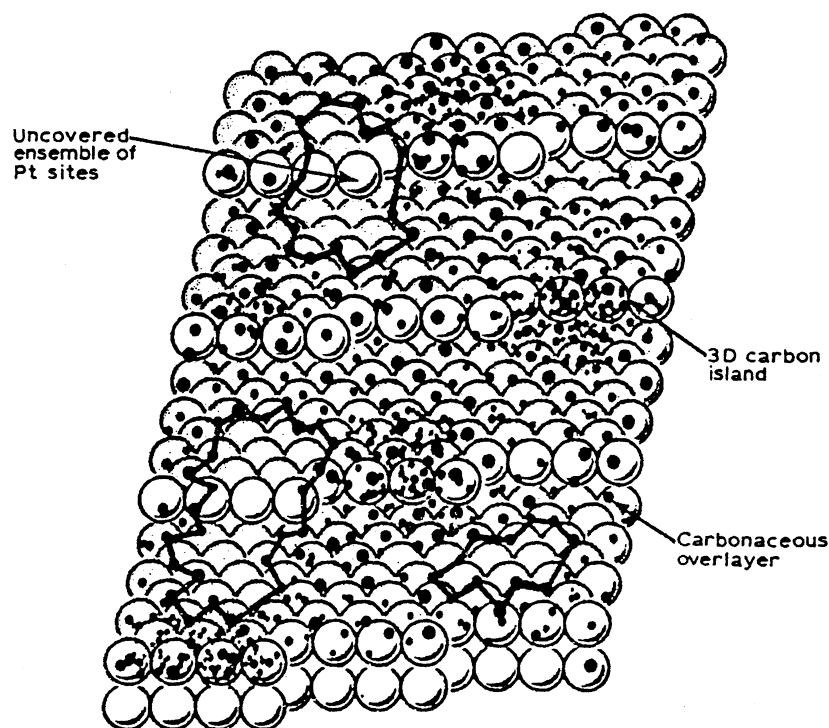
Fig. 49. In this model for the working structure and composition of platinum reforming catalysts most of the surface is continuously covered by a strongly bound carbonaceous deposit whose structure varies from two- to three-dimensional with increasing reaction temperature. Uncovered patches or ensembles of platinum surface sites always exist in the presence of this carbonaceous deposit. Bound breaking and chemical rearrangement in reacting hydrocarbon molecules take place readily at these uncovered sites (from [18]).

catalysts, provided a nonacidic support was used. The only exception to this result was at early reaction times with a chromia-alumina catalyst that contained potassium and/or other alkali metals and here the results are consistent with a bifunctional pathway that involves both the metal and acid functions. At total reaction pressures up to 400 psig (2.75 MPa), the aromatic products are those expected for direct six-carbon ring formation. Furthermore, the aromatic product distribution when operating at high pressures is the same as obtained at atmospheric pressure, indicating that the monofunctional metal dehydrocyclization pathway leading to aromatics is the same at low and high pressures. The conclusion is that the aromatics are formed in the metal monofunctional pathway at temperatures of about 480°C and higher only by a reaction pathway that includes direct six-carbon ring formation.

There is strong evidence to support the formation of a five-carbon ring when dehydrocyclization is car-

ried out at low (about 300°C) temperatures and atmospheric pressure. Furthermore, these five-carbon rings can undergo hydrogenolysis to produce isomeric alkanes with the same carbon number. The hydrogenolysis using highly dispersed Pt catalysts occurs predominantly, or only, by a nonselective mechanism wherein the C–C bonds are broken on a statistical basis. With methylcyclopentane, however, the methyl-ring C–C bond does not undergo hydrogenolysis at a comparable rate to the other five C–C bonds. While a few papers have reported a few percent of cyclopentane in the products, it is much less than the 12.5% expected if all C–C bonds in methylcyclopentane underwent hydrogenolysis at the same rate. In most papers reporting products from the hydrogenolysis of methylcyclopentane, the amount of cyclopentane is insignificant, or even so small that it is not reported. With *n*-propylcyclopentane, the situation appears to be different with each C–C bond undergoing
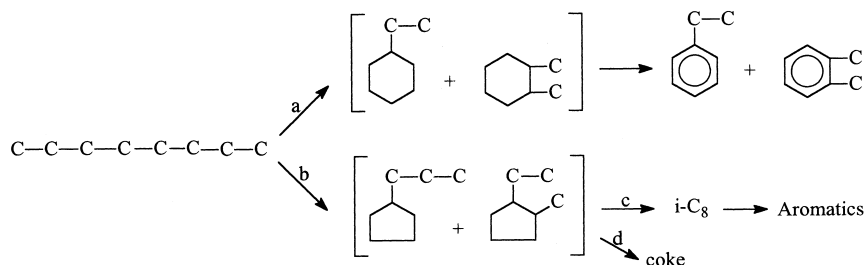
Scheme 30.

hydrogenolysis at about the same rate when a Pt-KL zeolite catalyst is used at 100 psig (0.69 MPa) and 482°C. With alkylcyclopentanes and Pt-silica or Pt-nonacidic alumina catalysts, ring enlargement to aromatic products is much slower than hydrogenolysis to produce isomeric acyclic alkane isomers.

The formation of alkylcyclopentanes and their subsequent hydrogenolysis provides a monofunctional pathway for alkane isomerization. When operating at 482°C and 1 atm (0.101 MPa), significant amounts of neither alkylcyclopentanes nor isomerized alkanes are observed. On the other hand, the monofunctional metal catalyst produces isoalkanes when operating at 482°C and 400 psig (2.75 MPa), and the amount of isoalkanes may exceed the amount of aromatics. The simplest mechanistic pathway for monofunctional metal catalyzed isomerization is the formation of alkylcyclopentanes and their subsequent hydrogenolysis. Thus, we have proposed that both five- and six-carbon ring formation occurs at both 1 and 27 atm (0.101 and 2.75 MPa) conditions. The difference between these two pressures is the fate of the five-carbon ring compounds. At 27 atm (2.75 MPa), the dominant pathway is hydrogenolysis to produce isomers of the alkane charged. At 1 atm (0.101 MPa) the five-carbon ring compounds that are formed predominantly undergo dehydrogenation and further reaction to produce coke; this is supported by the fact that 20–50% of the carbon passed to the catalyst ends up as coke on the catalyst. Thus, the following pathways are proposed for alkane dehydrocyclization at these two extreme pressures (Scheme 30).

At 482°C, there is little difference in the free energy for the cyclization to the cyclopentane or cyclohexane ring structures; the difference between the two ring structures is that dehydrogenation of cyclohex-

ane structures to aromatics means that the final product will be aromatics. However, the selectivity for ring size will not be impacted by the subsequent dehydrogenation to aromatics unless the two ring structures are themselves interchanging, as is the case with the bifunctional pathway that includes an acid function. However, with the monofunctional metal catalyzed cyclization, where the five- and six-carbon ring structures are not at equilibrium or even interconverting, the selectivity can be impacted by secondary reactions: dehydrogenation of the six-carbon ring compounds to aromatics and hydrogenolysis of the five-carbon ring compounds to acyclic alkanes. Thus, with the monofunctional metal catalysts, dehydrocyclization to form
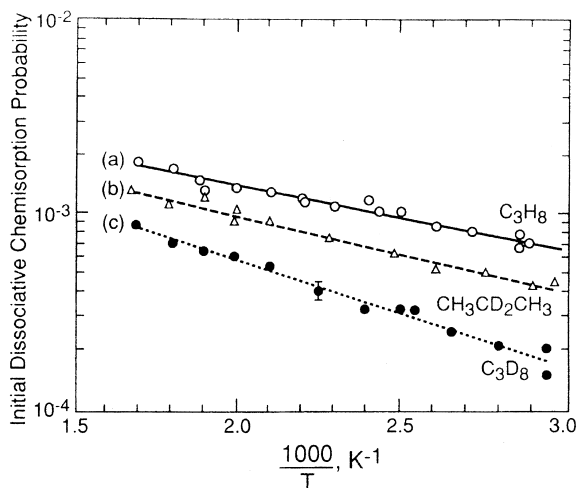

Fig. 50. Initial probabilities of trapping-mediated dissociative chemisorption of (a) C_3H_8, (b) $CH_3CD_2CH_3$ and (c) C_3D_8 on Pt-(110)-(1 × 2) as a function of reciprocal surface temperature ($P_{propane} = 1.7 \times 10^{-6}$ Torr) (from [212]).

either the five- or six-carbon ring compounds should be about equally favored, and the secondary reactions will provide products that are characteristic of each of the naphthene compounds formed as initial products.

McMaster and Madix [210] found a kinetic isotope effect for the initial dissociation probabilities of C_2H_6 and C_2D_6 on a Pt(1 1 1) crystal surface. They utilized supersonic molecular beam techniques and varied the average translational energies. They concluded that the kinetic isotope effect could be ascribed to the quantum mechanical tunneling of a hydrogen or deuterium atom through the barrier to dissociation.

Weinberg [211,212] found a kinetic isotope for the dissociative adsorption of methane, ethane and propane on Pt and Ir using flow or molecular beam techniques. Briefly, a kinetic isotope effect was found for C_3H_8, $CH_3CD_2CH_3$ and C_3D_8 (Fig. 50). The different rates for these three isopotomers show that both primary and secondary C–H (C–D) bonds cleave under the reaction conditions. The authors calculate that the difference between cleavage of primary and secondary C–H bonds is 425 cal/mol; the pre-exponential factor also favors cleavage of the secondary C–H bond. In comparing data for different Pt faces, an implication was that the geometrical structure leads to greater differences in the activation energy than the electronic difference for Pt and Ir with the same geometric structure.

At this time, the surface science studies clearly define a kinetic isotope effect in the chemisorption of small alkanes; however, much remains to be done to directly relate this to naphtha reforming conditions.

The large kinetic isotope effect, the nearly equal rate of conversion of the alkane and the alkyl-cyclohexane under competitive conversion conditions, and the lack of hydrogen/deuterium exchange in the reactants at 482°C and atmospheric pressure conditions are consistent with a reaction mechanism that includes irreversible adsorption of the reactants. It is realized that the use of irreversible adsorption is analogous to that of an acid catalyst. Just as it is never possible to have an acid site in a catalyst without a conjugate base, it is never possible to have a catalytic conversion in which the adsorption of the reactant is completely irreversible. Thus, there is a small amount of H/D exchange in the reactant under these 'irreversible adsorption' conditions; however, it is much less extensive than occurs in the aromatic product.

For the dehydrocyclization of n-octane, the amount of ethylbenzene should be twice that of o-xylene since there are two pathways leading to the former aromatic but only one leading to the xylene isomer. Experimentally, with a Pt-silica or Pt-nonacidic alumina catalyst about equal amounts of these two aromatics are formed. We advanced the view that the o-xylene was formed in a larger amount than expected because the cyclization pathway leading to its formation involved only secondary C–H bond breakage whereas the formation of ethylbenzene required breaking one secondary and one primary C–H bond. Since it requires more energy to break a primary C–H bond than a secondary one, this could explain the formation of more o-xylene than expected from statistical considerations. However, the data for the conversion of 2,2,7,7-tetradeuteriooctane clearly show that this explanation is not valid [145]. Since the kinetic isotope effect for alkane conversion is about 3, the pathway leading to o-xylene should be much slower since it involves the breaking of C–D bonds. Experimentally, the amounts of ethylbenzene and o-xylene were the same for the deuterium-labeled and the unlabeled n-octane. Thus, the landing site cannot be the factor that determines the aromatic selectivity. This requires that the carbon attached to Pt rapidly change so that all adsorption positions of n-octane become the same, or nearly the same prior to the cyclization step. This means that there must be extensive H/D exchange of the reactant prior to the cyclization step so that both cyclization pathways have the same kinetic isotope effect.

The consecutive dehydrogenation to the -ene, -diene and -triene followed by cyclization was advanced as the reaction pathway for the direct six-carbon ring formation. As described in the triene section above, the early work involved the addition of ^{14}C labeled intermediates to the alkane. This reaction scheme, as it has evolved, is illustrated by the version presented by Paál [213] (Scheme 31).

Paál indicates that surface unsaturated species are true intermediates of aromatization and that those appearing in the gas phase are the products of surface dehydrogenation and desorption. The desorption should be less likely with increasing unsaturation, as indicated by the shorter arrows in Scheme 31. It is true that the gas-phase alkenes become less stable with increasing unsaturation; however, the aromatic is as unsaturated as the -triene and it readily desorbs as a product. The

Gas:

$C_6H_{14}(g)$ $C_6H_{12}(g)$ $C_6H_{10}(g)$ $C_6H_8(g)$

$\pm\,nH$
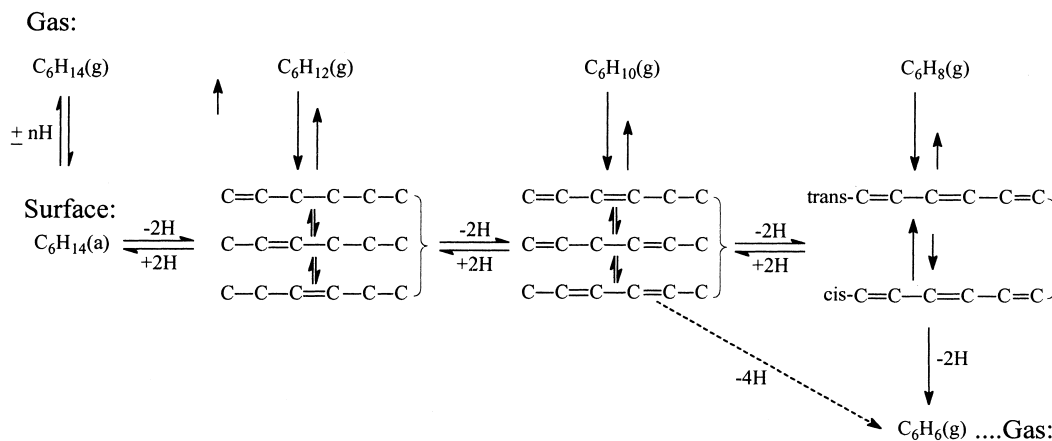
Surface:
$C_6H_{14}(a)$

Scheme 31.

cis-triene isomer is claimed to easily cyclize but the *trans*-triene isomer only cyclizes following isomerization to the *cis* isomer. According to Paál, the surface pool 'remembers' the original reactant structure; however, this conclusion is not consistent with our results with 2,2,7,7-tetradeuterooctane where there was no kinetic isotope effect for the aromatic products.

If the results for the kinetic isotope effect and for the lack of H/D exchange in the reactants with essentially equilibration of H/D in the products are accepted, then the initial chemiadsorption step is rate limiting. If this is the case, the addition of ^{14}C-labeled products, such as the -ene, -diene, or -triene, cannot provide valid proof for these species as true intermediates in the overall reaction pathway. In fact, the competitive conversion of 1-octene and *n*-octane-d_{18} show that the alkene is preferentially adsorbed at the double bond and is converted at 10 or more times faster than the alkane. Furthermore, 1-octene does not undergo hydrogenation (deuteration) to return to the gas phase as *n*-alkane in measurable amounts. Thus, while the results of many early tracer studies are consistent with the mechanism as outlined by Paál, the results cannot be used to confirm the triene mechanism outlined above.

The selectivity for the formation of benzene from *n*-hexane is much smaller than for the formation of ethylbenzene and *o*-xylene from *n*-octane. There should be little difference in the equilibrium concentration of the triene formed from *n*-hexane and *n*-octane; likewise, there should not be a significant

difference between the equilibrium concentration of 1,3,5-octatriene and 2,4,6-octatriene. A different ethylbenzene : *o*-xylene ratio is obtained for the Pt and the Pt-Sn catalysts. This shows that the catalyst plays a dominant role in defining the primary aromatic products and this appears possible only if the intermediates that determine the aromatic selectivity reside on the catalyst surface during the cyclization step. This, together with the increasingly unfavorable free energy changes as the acyclic compound products become more unsaturated, make it unlikely that gas phase trienes could be formed as part of the cyclization pathway, as has been proposed by some workers.

Alkylcyclopentane compounds cannot be formed by the triene mechanism. While the concentration of alkylcyclopentane products are low at the high pressure (7 atm; 0.71 MPa), there are large amounts of acyclic alkanes that could result from the hydrogenolysis of the cyclopentane compounds. Furthermore, *n*-pentane is reported to selectively produce cyclopentane as the major product with a nonacidic Pt-zeolite catalyst [189]. Several cyclization schemes have been proposed to produce alkylcyclopentanes as initial dehydrocyclization products; one such scheme is shown in Scheme 32 [214].

The bonding to the catalytic site in Scheme 32 is represented to be unknown. A similar scheme has been advanced by Bent [215] (Scheme 33).

The pathway to produce a six-carbon ring can be identical to Scheme 32 except that there will be one more carbon in the cyclization product (Scheme 34).
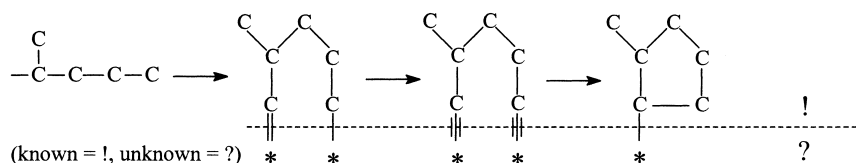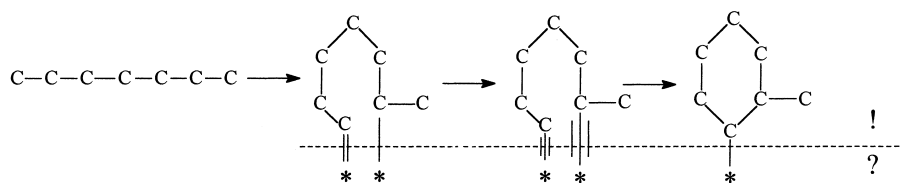
Scheme 32.

Process	Proposed Mechanism(s)
Dehydrocyclization	
Dehydrocyclization	

Legend: ☐ = alkyl; metallacycle ☐ = carbene; allyl, ◯ = carbyne; vinyl

Scheme 33.

(known = !, unknown = ?)

Scheme 34.

In both Schemes 32 and 34, the initial cyclic transition state involves ring sizes that are the most thermodynamically stable ones and which are the dominant structures formed in reactions used to effect cyclization reactions during organic synthesis. The formation of both the five- and six-carbon cyclic struc-tures in the initial cyclization step is well established. It seems reasonable that the mechanism for the for-mation of these two ring structures include a common pathway as shown in Scheme 31, and there is no com-pelling experimental data to show that this is not the case.
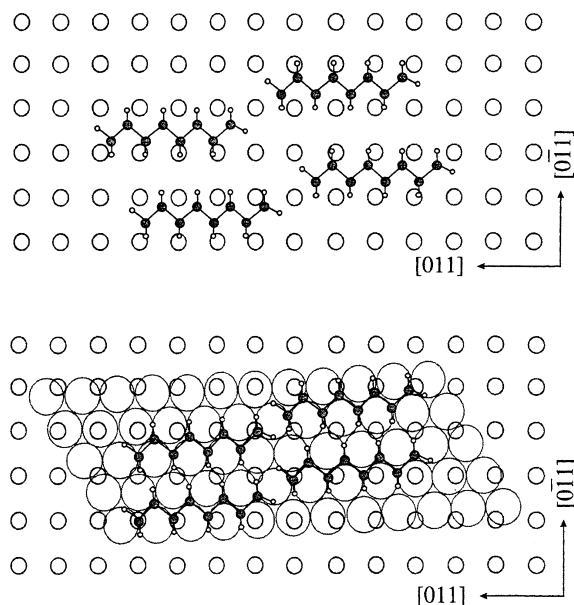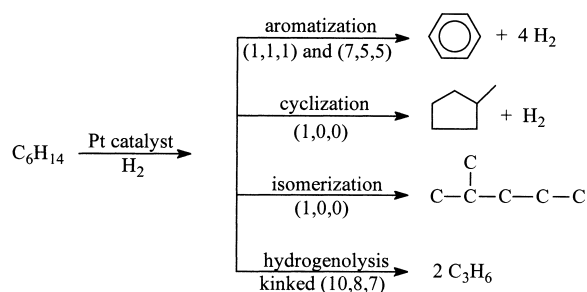
Scheme 35.

Fig. 51. (top) Proposed closed-packed assembly of *n*-octane on Pt(100)-(1 × 1). (bottom) Proposed closed-packed assembly of *n*-octane on Pt(100)-(5 × 2) (from [217]).

Surface science studies are playing an increasingly important role in understanding alkane activation and dehydrocyclization. An early attempt at this effort is illustrated for various Pt faces in Scheme 35 [216]. As with many initial efforts, Scheme 35 represents an oversimplified view.

Examples of efforts to extend the scheme by Pimentel [216] have continued. Manner et al. [217] have utilized as catalysts the (1 × 1) and (5 × 20) surfaces of Pt(100) and Pt(111). They propose a close-packed assembly of *n*-octane (Fig. 51). They found that the facility of C–H bond activation was in

the order Pt(100)-(1 × 1) > Pt(100)-(5 × 20) > Pt(111). Upon heating hydrogen is evolved with exhaustively dehydrogenation of the alkane. This is interesting but not directly correlated with dehydrocyclization at reforming conditions.

Teplyakov et al. [218] have studied the dehydrocyclization of 1-hexene to benzene on Cu₃Pt(111). This alloy was chosen since earlier work had shown that Cu modified the reactivity and selectivity of Pt [219–221]. Teplyakov and Bent [222] concluded that the rate-determining step in the dehydrocyclization of 1-hexene is not the dehydrogenation step. Instead, cyclization accompanied by the loss of two hydrogen atoms was considered to be the rate limiting step. The authors suggest that the common intermediate for the dehydrocyclization of 1-hexene and 1,3,5-hexatriene has the structure of hexa-σ-bonded triene. In the TPR experiment the hexa-σ-bonded hexatriene intermediate converts to benzene at 132°C, a temperature far lower than used for dehydrocyclization of alkanes. The triene is bonded with C–H bonds nearly parallel to the surface. In agreement with Paál, these authors obtained data suggesting that the *trans*-triene formed carbon on the catalyst whereas the *cis*-isomer formed benzene.

Vasquez and Madix [223] studied the conversion of 1-hexene, hexadienes and hexatrienes with Pd(111) and H(D)Pd(111). With clean and hydrogen-covered Pd surfaces, 1-hexene hydrogenation to produce gas phase hexane was never observed. The conjugated hexadienes and trienes were hydrogenated to produce 1-hexene, but not *n*-hexane, at the low temperatures. In this study, above 127°C fragmentation of the adsorbed species and dehydrogenation of these fragments occurs. Structure-sensitive dehydrocyclization of the hydrocarbons leads to desorption-limited evolution of benzene; cyclization could occur at temperatures as low as 60°C.

The low selectivity for benzene at the low temperatures with these large Pt or Pd catalysts make it impossible to relate the results to high temperature dehydrocyclization conditions.
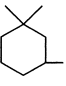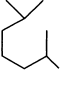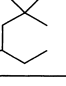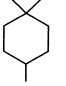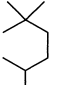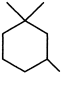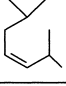
The structure and temperature dependence of *n*-hexane skeletal rearrangement was investigated near atmospheric pressure over a series of platinum single crystal surfaces with well-defined surface structure and composition. Davis et al. [72] found that aromatization of *n*-hexane to benzene displayed unique structure sensitivity in which the rates and selectivities

were maximized on platinum surfaces with high concentrations of [111] microfacets. The rates of isomerization, C_5-cyclization, and hydrogenolysis reactions displayed little dependence on platinum surface structure. Selectivities for *n*-hexane skeletal rearrangement varied markedly with temperature and hydrogen pressure at near atmospheric conditions.

One situation that provides strong, but indirect, support for a common pathway to produce the five- and six-carbon ring compounds is the conversion of acyclic compounds that can produce six-carbon ring structures with geminal dialkyl groups. We have carried out such experiments with C_9-alkane isomers and compared the products to those obtained by converting the alkylcyclohexane that would be formed by the cyclization of the alkane (Scheme 36). The similarity of the products from the alkylcyclohexane compound and the acyclic alkane that would form the same alkylcyclohexane by six-carbon ring formation is striking.

In addition, 2-methylheptane can undergo cyclization to produce *m*-xylene and 1,1-dimethylcyclohexane by a direct six-carbon ring formation. On the other hand, 3-methylheptane cannot form a geminal dimethylcyclohexane structure by direct six carbon ring formation. Conversion of 1,1-dimethylcyclohexane with a Pt-nonacidic alumina catalyst shows that demethylation to produce toluene is a dominant reaction pathway. When 2-methylheptane is converted with Pt-SiO$_2$, Pt-nonacidic alumina or Pt-ZSM-5 zeolite catalysts, significantly more toluene is produced by 2-methylheptane than is obtained from 3-methylheptane at a similar conversion level. The conversion of C_9-acyclic alkanes produces similar results (Scheme 36). Thus, the significant amounts of aromatic products that would result from the formation of geminal dialkyl cyclohexanes followed by dealkylation by metal catalyzed hydrogenolysis provide strong evidence that cyclization to produce aromatics involves an adsorbed cyclohexane structure rather than an adsorbed triene structure that is formed prior to the cyclization step.

Mechanisms such as those in Scheme 22 involve only one transition metal atom, and in this case a Pt atom. There are examples in homogeneous transition metal catalysis where multiple bonding to a central transition metal occurs that would be as demanding as required for the cyclization step. Thus, in principle, it is concluded that a single Pt atom could function

	Xylene			Trimethylbenzene		
	o	m	p	1,2,3-	1,2,4-	1,3,5
Cr$_2$O$_3$						
1	[97]	--		[--]	[2]	--
3	[70]	--		[4]	[12]	4
8	[27]	12		[7]	[33]	1
Cr$_2$O$_3$						
--	2	[90]		--	[8]	--
--	16	[16]		2	[54]	--
Pt-1						
--	[73]	--		[--]	[10]	8
2	[49]	10		[18]	[15]	2

[ ] = Expected isomer.

Scheme 36.

as the active site to the cyclization reaction and could form the multiple bonding necessary to allow the removal of a hydrogen and to incorporate it within the coordination sphere while at the same time forming the multiple bonding required to effect cyclization of the remaining hydrocarbon radical.

If a single Pt site is capable of the cyclization scheme, it is difficult to explain the differences in aromatic selectivity between Pt and Pt-Sn catalysts. It has been proposed that complex reactions, such as hydrogenolysis, are possible only on sites comprised of multiple atoms. By forming an alloy, such as PtSn, the Pt atoms become isolated and surrounded by Sn atoms, and these isolated atoms cannot effect hydrogenolysis as readily as the multiple Pt atom sites. Either the widely accepted cyclization and isomerization mechanism that involves a single transition metal atom must be abandoned or it must be accepted that an ensemble of transition metal atoms is not required

for cyclization and hydrogenolysis reactions. Accepting the view that a single Pt metal site can effect the cyclization step, then the different catalytic properties of Pt and PtSn, and other Pt alloys, must be due to electronic, and not geometric, effects. In making this assertion, it is realized that geometric and electronic effects are not independent; rather, the assertion is made in analogy with acidity of the acid–base pair where one of the conjugate effects is dominant. Thus, it is viewed that the changes in activity and aromatic selectivity are impacted more strongly by the modification of the electronic factor of alloying than the changes in the geometry of the catalytic site.

12.1. Modeling

A trend in catalysis today is the development of models to aid in understanding the reaction mechanisms. One of these involves a catalyst design approach based on a kinetic model of the reaction/catalyst system to be used in conjunction with experimental studies. In this approach, the performance of the catalyst is simulated by automated modeling of proposed chemical reaction mechanisms, and the results of this modeling is used in defining the experimental work. The kinetic model is refined using the experimental data. The authors indicate that "...modeling in the absence of experimental data may be a mathematical exercise, while experimentation in the absence of a kinetic model may lack direction... [224]". For the conversion of *n*-hexane, a reaction scheme utilized 17 elementary reversible steps, 12 adsorbed species, and the formation of six stable reaction products (Scheme 37). In spite of the complexity of the reactions in Scheme 37, the authors caution that "It should be remembered that this sequence of steps is used for illustrative purposes only." They utilized the data generated by Davis et al. [72] for the conversion of *n*-hexane using the Pt(111) single-crystal platinum catalyst operated in a batch reactor at 300 and 365°C. The data and the model both show that methylcyclopentane and hydrogenolysis products are dominant. The experimental data, but not the model, show the selectivity changes toward benzene and hydrogenolysis products at the higher of the two temperatures that were used. Dumesic et al. [224] suggest that the selectivity and decreased activity are due to the deposition of carbon on the catalyst, a reaction that was not included in the model. As has been demonstrated [141,142], the conversion of the alkane at the lower temperature is essentially by reversible adsorption whereas at the higher temperature (365°C), irreversible adsorption should at least be approached. Thus, while the conversion of *n*-hexane provides a good first effort, the use of large Pt crystals and the low temperatures in these studies suggest that the data differ from those expected for the normal naphtha reforming conditions.
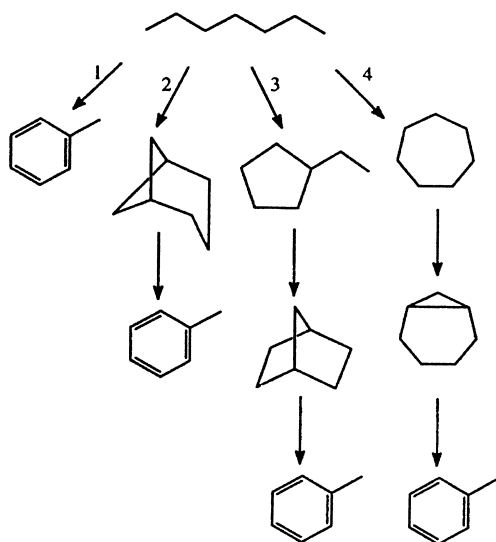
Dadyburjor and Ruckenstein [225] utilized the pathways shown in Scheme 38 and data for the conversion of 2-methylpentane-2-^{13}C [226] in their analysis of the role of multiple landing areas for adsorption. The authors accounted for three types of landing sites in which: (1) two surface sites are tied up in forming two carbon-surface bonds, leading to hydrogenolysis products, (2) three surface sites are involved in bonding with the adsorbate by forming two nonadjacent carbon-surface bonds, leading to isomerization products, and (3) five surface sites are used to form a cyclic intermediate with one carbon-surface bond, leading to ^{13}C scrambled products. Adsorbed hydrogen is considered to be dissociated with each hydrogen being bonded to a single surface site. The relative amounts of these adsorbed species determine the selectivity for the reaction. Using their model, the authors were able to obtain agreement between the experimental data and the model. Initially we proposed that the selectivity for the aromatic products obtained from the conversion of *n*-octane was determined by the attachment of *n*-octane to the landing site [35]. Since two secondary C–H bonds would need to be broken to form *o*-xylene and a secondary and primary C–H bond would need to be broken in forming ethylbenzene, we proposed that the higher concentration of *o*-xylene was due to breaking the weaker secondary C–H bonds. However, subsequent results at 482°C using 2,2,7,7-tetradeuteriooctane showed that C–H bond breaking with subsequent H/D exchange was so rapid that the initial adsorption site could not determine the aromatic product selectivity [145]. Thus, it appears that it is not the landing site but rather the stability of the different adsorbate-catalyst structures that will determine the product selectivity for aromatics formation. Presumably this would also apply to the structures shown in Scheme 38.
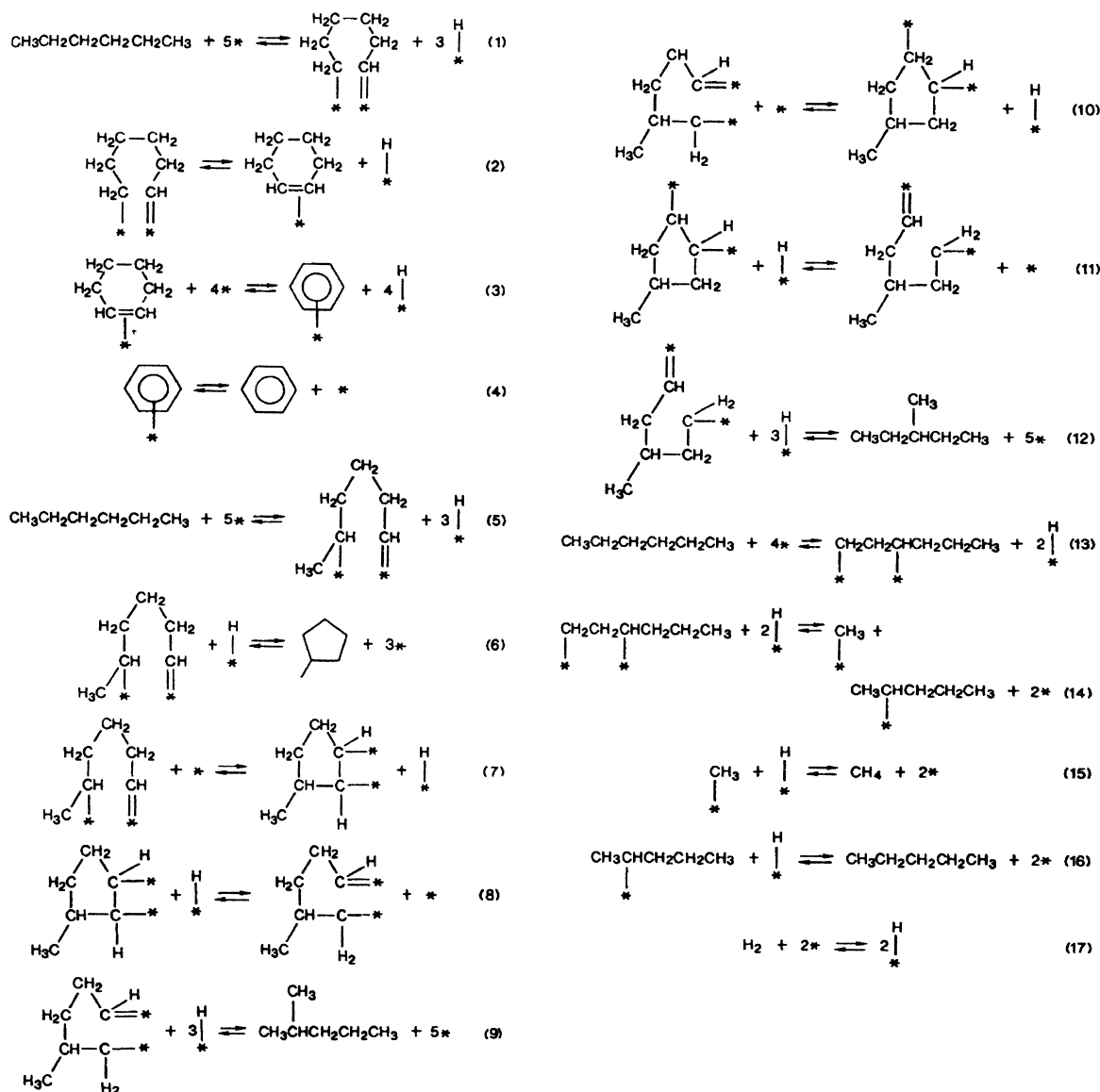
Scheme 37.

Zeigarnik and Valdés-Pérez [227] utilized MECHEM, a computer aid for elucidating reaction mechanims, to predict the location of an isotope in the labeled products from the conversion of *n*-heptane. They utilized the four reaction pathways shown in Scheme 39 in their calculations and obtained the results shown in Table 29. They concluded that it was not possible to distinguish the mechanisms from the results of any single labeling experiment. First, the reaction pathways shown in Scheme 39 are rather limited. For example, it appears more likely that ring expansion/contraction between five- and six-carbon rings for pathway 3, Scheme 39 is more likely than the formation of the bicyclic ring structure that is shown in Scheme 39. Pines and coworkers tried to establish that pathway 4, Scheme 39, was reasonable

Scheme 38.

Table 29
Predicted positions of isotopic labels in products of *n*-heptane dehydrocyclization[a]

Hypothetical mechanism (see Scheme 1)	Initial position of the label in *n*-hepatane			
	[1-^{14}C]-*n*-heptane	[2-^{14}C]-*n*-heptane	[3-^{14}C]-*n*-heptane	[4-^{14}C]-*n*-heptane
1,2				
3				
4	All (five) positions	All (five) positions	All (five) positions	All (five) positions

[a] Solid circles stand for carbon labels.

by converting cycloheptane under the same conditions that they used for *n*-heptane. They found that the intermediate, cycloheptane, was converted more slowly than *n*-heptane and, at the same time, provided a much wider range of products. Thus, they could only explain the results if the adsorption of cycloheptane was much slower than that of *n*-heptane, and we consider this to be unlikely.

Scheme 39.

In summary, the modeling of alkane dehydrocyclization provides stimulating intellectual exercises but the complexity of the mechanism does not allow one to include a sufficient number of pathways for the model to provide results that improve upon the judicious choice of isotopically labeled reactants.

12.2. Bifunctional catalysis

Apart from PtKL zeolite, the commercial naphtha reforming catalysts are bifunctional. The foregoing has concentrated upon the monofunctional pathway since it is not possible to utilize either the reaction products nor the position of isotopic label to understand the reaction pathway using bifunctional catalysts. Thus, the bifunctional aspects of dehydrocyclization are considered briefly in the following.

Some authors, e.g., [96], were of the view that the platinum function alone could catalyze aromatics formation by cyclization to a five carbon ring followed by ring expansion to a six carbon ring and subsequent dehydrogenation to aromatics. Others contended that direct six-carbon ring formation was the only pathway

by which Pt produces significant amounts of aromatics (e.g., [111,112]).

While there has been discussion as to whether the conversion of alkanes to aromatics follows the classical bifunctional mechanism involving both metal and acid sites, more work needs to be directed toward answering this question. For example, Shum et al. [228] used a mechanical mixture of a non-acidic platinum catalyst and acidic alumina, and concluded that the metal function controls dehydrocyclization. Sivasanker and Padalkar [229] investigated the dehydrocyclization of C_6 through C_8 alkanes using Pt-alumina catalysts; however, these authors carried out their reactions at atmospheric pressure where catalyst aging was rapid. In spite of this, these authors concluded that the metal function was the critical parameter with *n*-hexane and *n*-heptane; however, both metal function and acid sites could be important for *n*-octane. Ako and Susu [230] also investigated the dehydrocyclization of *n*-octane with monofunctional and bifunctional Pt/Al_2O_3 catalysts; however, the total pressure was only 1.8 atm. Callender et al. [192] expressed the view that Pt catalyzed cyclization through C_5-ring closure and that ring expansion led to aromatics. They reported that alumina had activity for cyclization of the alkenes produced from dehydrogenation but that for dispersed Pt, the metal catalyzed cyclization was more rapid. Henningsen [231] reported that the predominant pathway for the conversion of *n*-heptane to toluene is with a bifunctional mechanism, and that the acid catalyzed pathway was more rapid.

Dautzenberg and Platteeuw [118] followed the conversion of *n*-hexane with Pt on a non-acidic alumina catalyst. They concluded that dehydrocyclization of *n*-hexane to benzene proceeds along two different reaction paths: (a) Pt-catalyzed ring closure whose contribution to total rate of aromatization is proportional to total Pt surface regardless of metal particle size and (b) thermal six-ring closure of hexatrienes formed by dehydrogenation from *n*-hexanes over the Pt function. They argued for a monofunctional reaction pathway for Pt that involves both five- and six-ring formation:
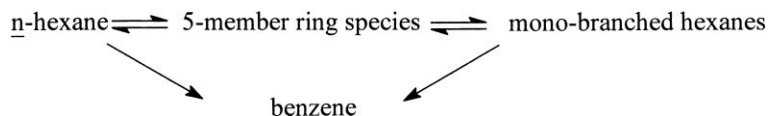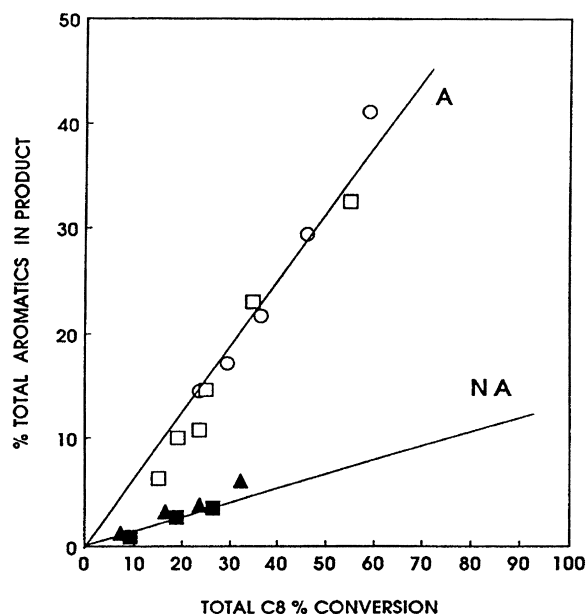
Fig. 52. The total aromatics in the liquid product vs. C_8-alkane conversion for catalysts based upon acidic (A) and non-acidic (NA) supports. (○) 0.6 wt.% Pt on precipitated alumina, COP; (□) 1.0 wt.% Pt on UCI alumina; (▲) 1.0 wt.% Pt on silica, SIL; (■) 1.0 wt.% Pt on non-acidic alumina, NAA (from [12]).
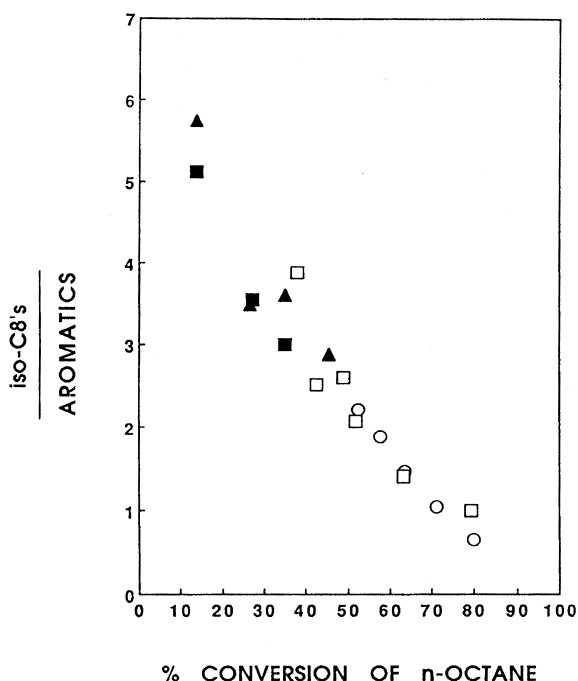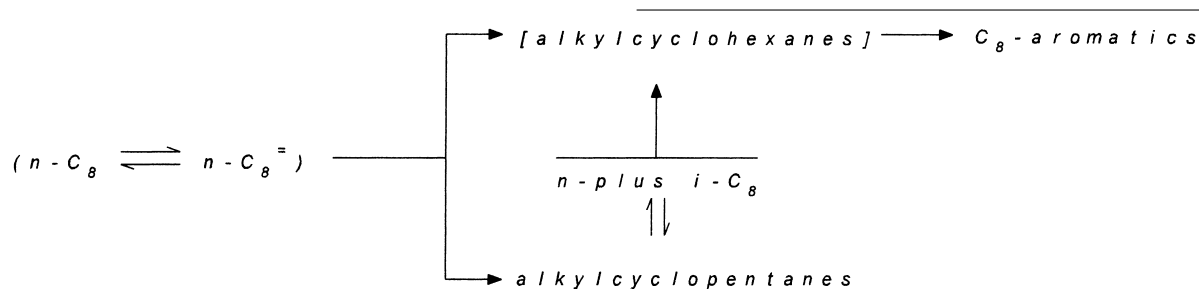

Fig. 53. The ratio *iso*-octanes/aromatics vs. *n*-octane conversion. (○) 0.6 wt.% Pt on precipitated alumina, COP; (□) 1.0 wt.% Pt on UCI alumina; (▲) 1.0 wt.% Pt on silica, SIL; (■) 1.0 wt.% Pt on non-acidic alumina, NAA (from [12]).

The conversion of *n*-octane with monofunctional and bifunctional catalysts has been investigated at 100 psig (0.69 MPa) and 482°C with a hydrogen/hydrocarbon molar ratio of 8/1. The aromatics in the liquid product as a function of *n*-octane conversion show that isomerization of *n*-octane to *iso*-octanes is more rapid that aromatics formation for the bifunctional catalyst (Fig. 7). Furthermore, the slope of the two lines in Fig. 52 show that the bifunctional pathway is more rapid that the Pt monofunctional pathway. In addition, the data in Fig. 7 show that the conversion of *n*-octane with the monofunctional catalyst produces aromatics with only a 6–10% selectivity; the monofunctional mechanism at reforming pressures leads primarily to isomerization as well as some cracking products. This selectivity difference is more apparent in Fig. 52 which shows the aromatics selectivity versus total C_8 conversion. Under the reaction conditions utilized for *n*-octane conversion, the alkane products from the conversion of *n*-propyl- and 1-methyl-2-ethyl-cyclopentane are those predicted for hydrogenolysis of the cyclopentane ring on a statistical, i.e., nonselective basis.

The aromatic distributions clearly indicate that the Pt on silica or non-acidic alumina catalysts do not have acidity. Even so, *iso*-octane isomers are formed more rapidly than aromatics are produced for both of these nonacidic catalysts. Thus, even for these non-acidic supports, an isomerization pathway must operate. As shown in Fig. 53, C_8-*iso*-alkanes are produced about six times faster than aromatics at the 10% *n*-octane conversion level; at lower *n*-octane conversion levels of the line in Fig. 53 suggests that this ratio of i-C_8/aromatics approaches 8 or higher. For this reason, the rates in Fig. 7 should be viewed as the rate of Pt catalyzed conversion of *n*-octane, and the selectivity for producing an aromatic product is only about 10% of the total *n*-octane conversion. Thus, the Pt function catalyzes four types of reactions: (1) aromatization by direct six carbon ring formation; (2) isomerization by cyclization to a five-carbon ring structure followed by hydrogenolysis of the alkylcyclopentane intermediate; (3) conversion of *n*-octane to C_1 through C_7 hydrocarbons by hydrogenolysis; and (4) the dehydrogenation

of alkanes and naphthenes. Thus, for the Pt catalytic function the following reaction network applies:

functional pathway dominates in producing aromatic products over that of the monofunctional Pt pathway.

$$(n\text{-}C_8 \rightleftharpoons n\text{-}C_8^=) \longrightarrow \begin{array}{l} [alkylcyclohexanes] \longrightarrow C_8\text{-}aromatics \\[1em] \uparrow \\ n\text{-}plus \quad i\text{-}C_8 \\ \updownarrow \\ alkylcyclopentanes \end{array}$$

In the above scheme, an alkylcyclohexane structure is shown although there is no data in this paper to eliminate the structure being the one obtained from cyclization of an octatriene. However, the cyclization to the alkylcyclopentane could not occur through such a triene mechanism.

The formation of more *iso*-octanes than aromatics with the single functional Pt catalyst shows that the pathway to produce aromatics by ring expansion of the cyclopentane ring to a cyclohexane structure does not occur at a significant rate. This conclusion is in conflict with some early claims (e.g., [96]); however, the conclusion agrees with studies with ^{14}C labeled cyclopentane [97,99].

In a recent review [232] it is stated that "It has been shown that the isomerization and hydrocracking reactions require the catalyst to have two separate and distinct functions – a hydrogenation–dehydrogenation function and an acidity function". This requirement is clearly not necessary; isomerization of the *n*-alkane can, and does, occur over the metal function through C_5-ring formation and subsequent hydrogenolysis, and this occurs at a rate that is faster than the formation of aromatics. Likewise, hydrocracking occurs to a greater extent with a nonacidic supported catalyst than with the acid supported catalyst.

Another feature of the Pt-acidic catalyst is that it produces aromatics at least 10 times the rate of the Pt-non-acidic catalyst. At the same time, the selectivity for aromatics production from *n*-octane for the Pt-acidic catalyst is about five times greater than for the Pt-non-acidic catalyst. With the acidic catalyst, the bifunctional pathway produces aromatics more rapidly and more selectively than by the Pt function only pathway. Thus, for the Pt on an acidic support the bi-

The monofunctional pathway can be represented as (Scheme 40):

The bifunctional pathway (Scheme 41) for the production of aromatics may be represented as: (Pt, platinum; A = support acidity; B represents the series conversion involving the three steps Pt, A, Pt).

In summary, Pt monofunctional and bifunctional catalysts produce a common set of products apart from the C_8-aromatic and i-C_8-alkane distributions at low conversions. The difference between the two types of catalysts therefore is essentially that of the rate and selectivity of producing aromatics versus $C_1 - C_7$ products. Overall, the bifunctional pathway provides both the most rapid and the most selective pathway for the formation of aromatics from *n*-alkanes. The bifunctional pathway provides a nearly equilibrium distribution of methyl heptanes whereas the monofunctional platinum pathway produces predominantly the isomers allowed from hydrogenolysis of alkylcyclopentanes, primary products formed by the five-carbon ring cyclization of the *n*-alkane. The nonacidic Pt catalyst produces aromatics by direct six-carbon ring formation. The acidic catalyst produces essentially a mixture of C_8-aromatics that is near the thermodynamic equilibrium mixture, presumably because of isomerization reactions that proceed metal catalyzed cyclization and by the acid catalyzed cyclization.

13. Conclusions

Dehydrocyclization is a complex reaction with the potential for many kinetic disguises. In spite of this, there is a vast body of experimental data that support specific mechanistic features.
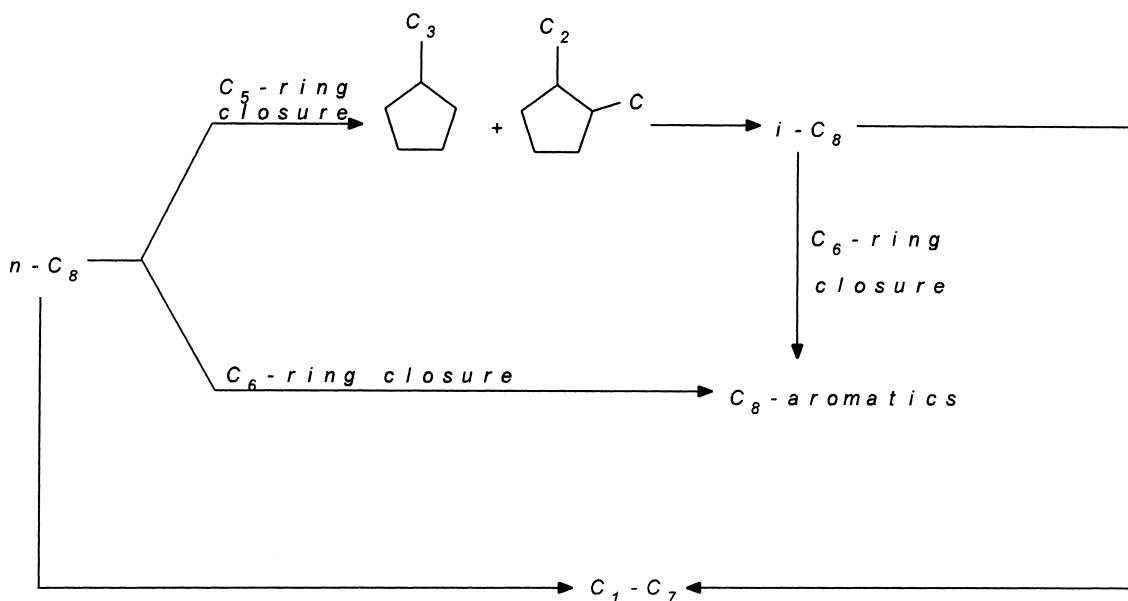
Scheme 40.
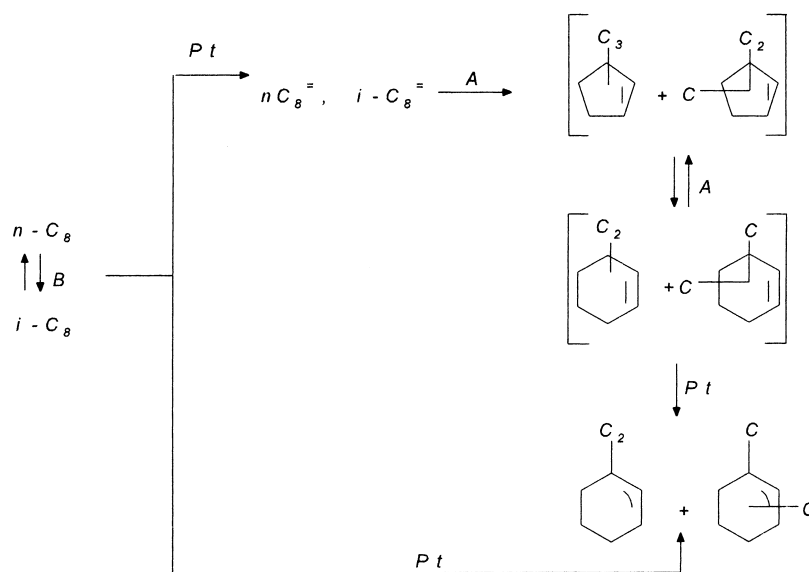
Scheme 41.

For the naphtha reforming catalyst, a bifunctional pathway operates with cyclization at the acid site is more rapid than the monofunctional metal catalyzed cyclization pathway.

For the monofunctional metal catalyzed pathway, the aromatics are produced by a cyclization that directly produces a six-carbon ring. Cyclization to other size rings followed by ring contraction/expansion does
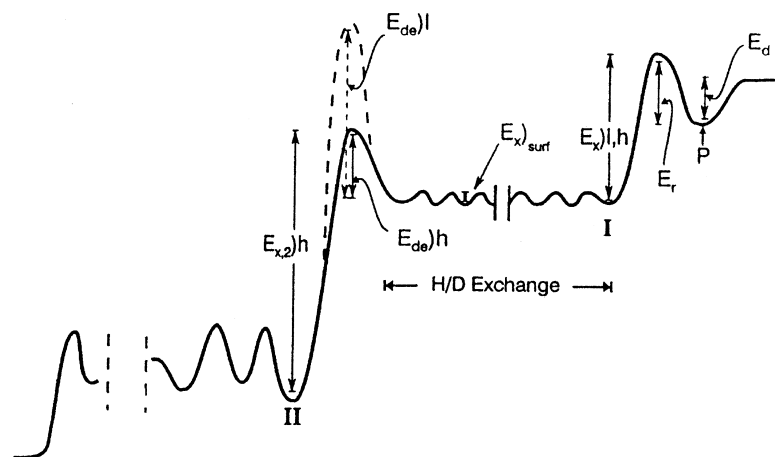
Fig. 54. Schematic reaction coordinate for the conversion of an alkane and H/D exchange at low (l) and high (h) temperature (I, R•
II, Ri; E_d, desorption activation energy; P, precursor physically adsorbed state; E_r, activation energy for rate determining step; E_x)l,h
activation energy for low, high temperature desorption of H/D exchange in adsorbed species; E_{de})l and E_{de})h, activation energy for second
dehydrogenation at low and high temperature, respectively; and $E_{x,2}$)h, activation energy for exchange in second step) (from [143]).

not materially contribute to the production of aromatics with either the metal or metal oxide catalysts.

With the monofunctional pathway, both five- and six-carbon rings are formed as initial products. The six-carbon ring pathway leads directly to aromatic products. For conversions at normal reforming conditions (60–400 psig (0.4–2.75 MPa)), the five-carbon ring undergoes nonselective hydrogenolysis reactions to produce acyclic alkane products and these products themselves may subsequently undergo cyclization (Scheme 30, path b, c). At atmospheric conditions the five-carbon ring compounds undergo coking/cracking reactions, and thereby contribute to the rapid aging of the catalyst but not to the production of significant amounts of aromatics (Scheme 30, path b, d).

The predominant monofunctional metal catalyzed cyclization step does not occur through a triene intermediate. Similar products are obtained form a geminal dimethylcyclohexane reactant and from alkanes that can form this cyclohexane structure by direct six-carbon ring formation. Since the acyclic alkanes that contain geminal dimethyl substitution cannot form the triene structure, they must cyclize through some other mechanism.

The dominant dehydrocyclization pathway at atmospheric pressure occurs by a mechanism that involves essentially irreversible adsorption with the initial chemisorption being the rate controlling step. The lack of significant H/D exchange in the reactants, including cyclohexane structures when fed under competitive reaction conditions with *n*-alkanes, confirm this conclusion. Likewise, the nearly equilibrium H/D composition of the aromatic products show that once adsorbed, H/D exchange occurs much more rapidly than aromatics formation (Fig. 54). Furthermore, the experiments with deuterated reactants show that aromatics desorption is not the rate limiting step.

The mechanism changes from irreversible adsorption at atmospheric pressure to one that is essentially a reversible one at 100 psig (0.69 MPa) or higher. This dependence upon hydrogen pressure is expected for a rate limiting step that involves the initial rupture of the C–H bond.

References

[1] B.H. Davis, Appl. Catal. 115 (1994) N27.

[2] B.A. Kazansky, A.F. Plate, Ber. 69 (1936) 1862.

[3] A.V. Grosse, U.S. Patent 2,124,566, Applied 30 September 1936.

[4] A.V. Grosse, J.C. Morrell, W.J. Mattox, Ind. Eng. Chem. 32 (1940) 528.

[5] B.L. Moldvasky, H.D. Kamisher, Compt. Rend. Acad. Sci. U.R.S.S. 1 (1936) 355.

[6] V.I. Karshev, M.G. Severyanova, A.N. Siova, Khimixva Tverdogo Topliva Chem. Solid Fuel 8 (1936) 559.

[7] J. Turkevich, Heterogeneous catalysis, selected American histories, in: B.H. Davis, W.P. Hettinger Jr. (Eds.), ACS Symp. Series, vol. 222, 1982, p. 463.

[8] V. Haensel, M.J. Sterba, Progress in petroleum technology, ACS Adv. Chem. Series 5 (1951) 60–75.

[9] T.R. Hughes, W.C. Buss, P.W. Tamon, R.L. Jacobson, in: Y. Murakami, A. Iijima, J.W. Ward (Eds.), Proc. 7th Int. Zeolite Conf., Elsevier, Amsterdam, 1986, pp. 725–732

[10] T. R. Hughes, R. Jacobson, P. Tamm, in: J. Ward (Ed.), Catalysis, Elsevier, Amsterdam, 1998, pp. 317–333.

[11] J.L. Carter, J.A. Cusumano, J.H. Sinfelt, J. Catal. 20 (1971) 223.

[12] R. Srinivasan, D. Sparks, B.H. Davis, J. Mol. Catal. 88 (1994) 325.

[13] R. Srinivasan, B.H. Davis, J. Mol. Catal. 88 (1994) 343.

[14] D. Sparks, R. Srinivasan, B.H. Davis, J. Mol. Catal. 88 (1994) 359.

[15] M. Orchin, L. Reggel, R.A. Friedel, E.O. Woolfolk, Aromatic Cyclodehydrogenation, U.S. Bureau of Mines, Technical paper 728, 1948.

[16] A.H. Steiner, in: P.H. Emmett (Ed.), Catalysis, vol. 4, Reinhold, New York, 1957, p 529.

[17] C. Hanch, Chem. Revs. 52 (1953) 353.

[18] G.A. Somorjai, S.M. Davis, Plat. Metals Rev. 27 (1983) 54.

[19] P.S. Skell, J.J. Havel, M.J. McGlinchey, Accounts of Chem. Res. 6 (1973) 97.

[20] K.A. Biesiada, C.T. Koch, P.B. Shevlin, J. Chem. Am. Soc. 102 (1980) 2098.

[21] A. Sárkány, J. Catal. 89 (1984) 14.

[22] R.J. Kokes, A.L. Dent, Advan. Catal. 22 (1972) 1.

[23] G.H. Twigg, Trans. Faraday Soc. 35 (1939) 1006.

[24] A. Farkas, L. Farkas, E.K. Rideal, Proc. Roy. Soc. London 146 (1934) 630.

[25] H. Pines, C.T. Goetschel, J. Org. Chem. 30 (1965) 3530.

[26] R.C. Pikethly, H. Steiner, Trans Faraday Soc. 35 (1939) 979.

[27] K.M. Sharan, Catal. Rev. Sci. Eng. 26 (1984) 141.

[28] J. Happel, Isotopic Assessment of Heterogeneous Catalysis, Academic Press, New York, 1986.

[29] G.A. Somorjai, Accounts Chem. Res. 9 (1976) 248.

[30] W.P. Hettinger Jr., personal communication.

[31] R.L. Jacobson, H.E. Kluksdahl, C.S. McCoy, R.W. Davis, Am. Petrol. Inst. Ref. Div. Mtg. Chicago, May 1969.

[32] H. Pines, W.O. Haag, J. Am. Chem. Soc. 82 (1960) 2471.

[33] V. Haensel, IV Simposio Iberoamericano di Catalysis, Mexico City, Plenary Lecture, 1974.

[34] B.H. Davis, J. Catal. 23 (1971) 340.

[35] B.H. Davis, J. Catal. 42 (1976) 238.

[36] K.W. McHenry, R.J. Bertolacini, H.M. Brennan, J.L. Wilson, H.S. Seelig, Actes Congr. Int. Catal., 2nd, 1960 2 (1961) 2293.

[37] H.E. Kluksdahl, R.J. Houston, J. Phys. Chem. 65 (1961) 1469.

[38] M.F.L. Johnson, C.D. Keith, J. Phys. Chem. 67 (1963) 200.

[39] B.H. Davis, J. Catal. 23 (1971) 355.

[40] B.H. Davis, J. Catal. 42 (1976) 247.

[41] T.R. Hughes, R.L. Jacobson, K.R. Gibson, L.G. Schormack, J.R. McCabe, Proc. Am. Pet. Inst. Refin. Dept. 45 (1976) 875.

[42] J.H. Sinfelt, J. Catal. 29 (1973) 308.

[43] J.H. Sinfelt, Bimetallic Catalysts, Wiley, New York, 1983.

[44] J.N. Miale, P.B. Weisz, J. Catal. 20 (1971) 288.

[45] W.H. Lang, R.J. Mikovsky, A.J. Silvestri, J. Catal. 20 (1971) 293.

[46] R.J. Mikovsky, A.J. Silvestri, E. Dempsy, D.H. Olsen, J Catal. 22 (1971) 371.

[47] D.H. Olson, R.J. Mikovsky, G.F. Shipman, E. Dempsy, J. Catal. 24 (1972) 161.

[48] J.R. Bernard, Proc. 5th Int. Congr. Zeolites, Heyden, London, 1980, p. 686.

[49] S.J. Tauster, J.J. Steger, J. Catal. 125 (1990) 387.

[50] R.J. Davis, E.G. Derouane, J. Catal. 132 (1991) 269.

[51] R.P. Eischens, P.W. Selwood, J. Am. Chem. Soc. 70 (1948) 2271.

[52] N.E. Fouad, H. Knözinger, H.M. Ismail, M.I. Zaki, Zeit. für Physik. Chem. 173 (1991) 201.

[53] N.E. Fouad, H. Knözinger, Zeit. für Physik. Chem. 171 (1991) 75.

[54] K. Wlodzimierz, Bull. Polish Acad. Sci. Chem. 32 (1984) 501.

[55] S.E. Voltz, A.E. Hirshler, A. Smith, Abstract, ACS meeting, Phys. Inorg. Chem. Sect., p. 64.

[56] B.S. Greensfleder, R.C. Archibald, D.L. Fuller, Chem. Eng. Progress 43 (1947) 561.

[57] A.S. Russell, R.J. Stokes, Ind. Eng. Chem. 38 (1946) 1071.

[58] Y. Holl, F. Garin, G. Maire, A. Muller, P.A. Engelhard, J. Grosmangin, J. Catal. 104 (1987) 225.

[59] B.H. Davis, G.J. Antos, in: G.J. Antos, A.M. Aitani, J.M. Parera (Eds.), Catalytic Naphtha Reforming: Science, Technology, Marcel Dekker, New York, 1995, pp. 113–180

[60] G.B. McVicker, J.L. Kas, J.J. Ziemak, W.E. Gates, J.L. Robbins, M.M.J. Treacy, S.B. Rice, T.H. Vanderspurt, V.R. Cross, A.K. Ghosh, J. Catal. 139 (1993) 48.

[61] M. Vaarkamp, J.T. Miller, F.S. Modica, G.S. Lane, D.C. Koningsberger, J. Catal. 138 (1992) 675.

[62] G. Jacobs, C.L. Padro, D.E. Resasco, J. Catal. 179 (1998) 43.

[63] M.J.P. Botman, L.Q. She, J.Y. Zhang, W.L. Driessen, V. Ponec, J. Catal. 103 (1987) 280.

[64] R. Srinivasan, B.H. Davis, Platinum Metals Rev. 36 (1992) 151.

[65] J. Turkevich, H. Young Jr., J. Am. Chem. Soc. 63 (1941) 519.

[66] G.A. Mills, H. Heinemann, T.H. Milliken, A.G. Oblad, Ind. Eng. Chem. 45 (1953) 134.

[67] A.J. Silvestri, P.A. Naro, R.L. Smith, J. Catal. 14 (1969) 3860.

[68] A. Cimino, M. Boudart, H.S. Taylor, J. Phys. Chem. 58 (1954) 796.

[69] C.G. Myers, G.W. Munns Jr., Ind. Eng. Chem. 50 (1958) 1727.

[70] J. R. Anderson, Y. Shimoyama, in: W. Hightower (Ed.), 5th Int. Congr. Catal. J., Miami Beach, FL, 20–26 August 1972, North-Holland, Amsterdam, 1973, pp. 695–715.

[71] M. Chow, G.B. McVicker, J. Catal. 112 (1988) 290.

[72] S.M. Davis, F. Zaera, G. Somorjai, J. Catal. 85 (1984) 206.

[73] E. Santacessaria, D. Gelosa, S. Carra, I. Adami, Ind. Eng. Chem. Prod. Res. Dev. 17 (1978) 68.

[74] Z. Karpinski, T. Koscielski, J. Catal. 63 (1980) 313.

[75] J.R.H. van Schaik, R.P. Dessing, V. Ponec, J. Catal. 38 (1975) 273.

[76] A.D. Cinneide, F.G. Gault, J. Catal. 37 (1975) 311.

[77] G. Leclercq, L. Leclercq, R. Maurel, J. Catal. 50 (1977) 87.

[78] J.R. Anderson, Advan. Catal. 23 (1973) 91.

[79] J.H. Sinfelt, Advan. Catal. 23 (1973) 91.

[80] B.H. Davis, Proceedings, 8th Int. Cong. Catal., vol. 2, 1984, pp. 469–480.

[81] N.D. Zelinskii, B. Kazanskii, A.F. Plate, Chem. Ber. B66 (1933) 1415.

[82] B.A. Kazanskii, T.S. Bulanova, Izv. Akad. Nauk. SSSR Otd. Khim. Nauk, 1947, pp. 29–40.

[83] B.A. Kazanskii, Usp. Khim. 17 (1948) 655.

[84] F.G. Gault, Adv. Catal. 30 (1981) 1.

[85] M. Chow, S.H. Park, W.M.H. Sachtler, Appl. Catal. 19 (1985) 349.

[86] S.G. Brandenberger, W.L. Callender, W.K. Meerbott, J. Catal. 42 (1976) 282.

[87] G. Maire, G. Plouidy, J.C. Prudhomme, F.G. Gault, J. Catal. 4 (1965) 556.

[88] M. Vaarkamp, P. Dijkstra, J. van Grondelle, J.T. Miller, F.S. Modica, D.C. Koningsberger, R.A. van Santen, J. Catal. 151 (1995) 330.

[89] H. Zuegg, R. Kramer, Appl. Catal. 9 (1984) 263.

[90] M. Yamada, E. Yamamoto, A. Amano, J. Japan Petrol. Inst. 25 (1982) 112.

[91] X. Bai, W. Sachtler, J. Catal. 129 (1991) 121.

[92] I.V. Gostunskaya, K. Ch'ing-fêng, B. A. Kazanskii, Izv. Akad. Nauk SSR, Ser. Khim. (1964) 1073.

[93] R. Kramer, M. Fischbacher, J. Mol. Catal. 51 (1989) 247.

[94] F.G. Gault, Compt Rendu 245 (1957) 1620.

[95] I.I. Levitskii, Kh.M. Minachev, in: F. Márta, D. Kalló (Eds.), Mechanisms of Hydrocarbon Reactions: a Symposium, Elsevier, Amsterdam, 1975, pp. 81–95.

[96] G.R. Lester, J. Catal. 13 (1969) 187.

[97] S.M. Csicsery, R.L. Burnett, J. Catal. 8 (1967) 74.

[98] R.H. Hardy, B.H. Davis, Acta Chim. Hungar. 124 (1987) 269.

[99] C.-S. Huang, D.E. Sparks, H.A. Dabbagh, B.H. Davis, J. Catal. 134 (1992) 269.

[100] G. Moretti, W.M.H. Sachtler, J. Catal. 115 (1989) 205.

[101] G. Moretti, W.M.H. Sachtler, J. Catal. 116 (1989) 361.

[102] C. Besoukhanova, J. Guidot, D. Barthomeuf, J. Chem. Soc. Faraday Trans. I 77 (1981) 1595.

[103] V. Bonaci-Koutecky, J. Koutecky, P. Fantucci, V. Ponec, J. Catal. 111 (1988) 409.

[104] W.E. Alvarez, D.E. Resasco, Catal. Lett. 8 (1991) 53.

[105] R. Kramer, H. Zueg, J. Catal. 85 (1984) 530.

[106] H. Glassl, K. Hayek, R. Kramer, J. Catal. 68 (1981) 397.

[107] W.E. Alvarez, D.E. Resasco, J. Catal. 164 (1996) 467.

[108] B.H. Davis, J. Catal. 29 (1973) 395.

[109] J. Dermietzel, Proc. 5th Intern. Symp. Heterogeneous Catalysis, Varn, 1983, Part I, pp. 452–458.

[110] E. Iglesia, J. Baumgartner, G.L. Price, K.D. Rose, J.L. Robins, J. Catal. 125 (1990) 95.

[111] B.H. Davis, P.B. Venuto, J. Catal. 15 (1969) 363.

[112] L.-G. Fogelberg, R. Gore, B. Rånby, Acta Chem. Scandinavica 21 (1967) 2041.

[113] L.-G. Fogelberg, R. Gore, B. Rånby, Acta Chem. Scandinavica 21 (1967) 2050.

[114] H. Pines, G.-T. Goetschl, J.W. Dembinski, J. Org. Chem. 30 (1965) 3540.

[115] F.R. Cannings, A. Fisher, J.F. Ford, P.D. Holmes, R.S. Smith, Proc. Conf. Radioisotopes Int. AEC, Copenhagen, 1960, vol. 3, p. 205.

[116] H. Pines, S.M. Csicsery, J. Catal. 1 (1962) 313.

[117] H. Pines, C.T. Chen, 2nd Congr. Int. Catal. Paris 1960 (1961) 367.

[118] F.M. Dautzenberg, J.C. Platteeuw, J. Catal. 19 (1970) 41.

[119] A.E.H. Kilner, H.S. Truner, R.J. Warne, Radioisotope Conference, 1954, Proc. 2nd Conf. Oxford, 19–23 July 1954, vol. 3, Physical Sci., Industrial Applications, Butterworths, London, 1954, p. 23.

[120] R.W. Wheatcroft, Ph.D. Thesis, University of California, 1949.

[121] R.C. Pitketkly, H. Steiner, Trans. Faraday Soc. 35 (1939) 979.

[122] H.S. Taylor, J. Turkevich, Trans. Faraday Soc. 35 (1939) 921.

[123] H. Hoog, J. Verheus, F. Zuiderweg, Trans. Faraday Soc. 35 (1939) 993.

[124] W. Mattox, J. Am. Chem. Soc. 66 (1944) 2059.

[125] H.S. Taylor, H. Fehrer, J. Am. Chem. Soc. 63 (1941) 1387.

[126] T.C. Rees, Ph.D. Dissertation, Pennsylvania State University, 1966.

[127] H.M. Walborsky, Accounts Chem. Res. 23 (1990) 286.

[128] M. Julia, Accounts Chem. Res. 4 (1971) 386.

[129] J.J. Mitchell, J. Am. Chem. Soc. 80 (1958) 5848.

[130] H. Pines, C.T. Chen, J. Org. Chem. 26 (1961) 1057.

[131] F.R. Cannings, A. Fisher, J.F. Ford, P.D. Holmes, R.S. Smith, Chem. Ind. (1960) 228.

[132] J.A. Feighan, B.H. Davis, J. Catalysis 4 (1965) 594.

[133] H. Steinberg, F.L.J. Sixma, Rec. Trav. Chim. 79 (1960) 679.

[134] B.H. Davis, P.B. Venuto, J. Organic Chem. 36 (1971) 337.

[135] B.H. Davis, J. Catal. 29 (1973) 398.

[136] L. Nogueira, H. Pines, J. Catal. 70 (1981) 404.

[137] B.H. Davis, J. Catal. 46 (1977) 348.

[138] V. Amir-Ebrahimi, A. Chaplin, P. Parayre, F.G. Gault, Nouveau J. Chem. 4 (1980) 431.

[139] J.M. Cogen, W.F. Maier, J. Am. Chem. Soc. 108 (1986) 7752.

[140] R.C. Archibald, B.J. Greensfelder, Ind. Eng. Chem. 37 (1945) 356.

[141] B.H. Davis, J. Catal. 23 (1971) 365.

[142] B. Shi, B.H. Davis, J. Catal. 147 (1994) 38.

[143] B. Shi, B.H. Davis, in: J.W. Hightower, W.N. Delgass, E. Iglesia, A.T. Bell (Eds.), 11th Int. Congr. Catal., Elsevier, Amsterdam, 1996, pp. 1145–1154.

[144] B. Shi, B.H. Davis, J. Chromatography A 654 (1993) 319.

[145] B. Shi, B.H. Davis, J. Catal. 162 (1996) 134.

[146] G.V. Isagulyants, M.I. Rozengart, B.A. Kazanskii, Yu. I. Derbentsev, Yu. G. Dubinskii, Dokl. Akad. Nauk SSSR 191 (1970) 600.

[147] B.A. Kazanskii, M.I. Rozengart, Dokl. Adak. Nauk SSSR 197 (1971) 1085.

[148] V.F. Il'in, G.V. Isagulyants, M.I. Rozengart, Yu. N. Osov, Neft. 15 (1975) 808.

[149] I. Manninger, X.L. Xu, P. Tétényi, Z. Paál, Appl. Catal. 51 (1989) L7.

[150] P.G. Menon, Z. Paál, Ind. Eng. Chem. Res. 36 (1997) 3282.

[151] B. Shi, B.H. Davis, J. Catal. 168 (1997) 129.

[152] G.L. Price, Z.R. Ismagilov, J.W. Hightower, in: T. Seiyama, K. Tanabe (Eds.), Proc 7th Int. Catal. Congr., Elsevier, Amsterdam, 1981, pp. 708–723.

[153] S.M. Davis, W.D. Gillespie, G.A. Somorjai, J. Catal. 83 (1983) 131.

[154] A. Ozaki, Isotopic Studies of Heterogeneous Catalysis, Academic Press, New York, 1977, pp. 175–177.

[155] R.P. Bell, The Proton in Chemistry, 2nd ed., Cornell University Press, Ithaca. NY, 1973, pp. 250–296.

[156] E.S. Lewis, L.H. Funderburk, J. Am. Chem. Soc. 89 (1967) 2322.

[157] E.S. Lewis, J.K. Robinson, J. Am. Chem. Soc. 90 (1968) 4337.

[158] R.P. Bell, Acid–Basic Catalysis, Oxford University Press, Oxford, 1941, pp. 143–207.

[159] G.M. Schwab, Catalysis, van Nostrand, Princeton. NJ, 1937, pp. 260–262.

[160] B.H. Davis, ACS Preprints, Div. Petrol. Chem. 28 (1983) 420.

[161] D.O. Hayward, B.M.W. Trapnell, Chemisorption, 2nd ed., Butterworths, London, 1964, p. 133.

[162] L.C. Loc, N.A. Gaidai, S.L. Kiperman, Proc. 9th Int. Catal. Congr., vol. 3, 1988, p. 1261.

[163] L.C. Loc, N.A. Gkaidai, B.S. Gudkov, M.M. Kostyukovskii, S.J. Kiperman, S.B. Kogan, Kinetika i Kataliz 27 (1986) 1365.

[164] L.C. Loc, N.A. Gaidai, B.S. Gudkov, M.M. Kostyukovsloo, S.J. Kiperman, N.M. Podkletnova, S.B. Cogan, N.R. Bursian, Kinetika i Kataliz 27 (1986) 1371.

[165] D.E. Resasco, G.L. Haller, Catalysis, a Specialist Periodical Report, vol. 11, Royal Soc. Chem., Cambridge, 1994.

[166] Z. Paál, in: G.J. Antos, A.M. Aitani, J.M. Parera (Eds.), Catalytic Naphtha Reforming, Marcel Dekker, New York, 1995, pp. 19–44.

[167] O.V. Bragin, V. Tovmasyan, G. Isagulyants, A. Greish, L. Kovalenko, A. Liberman, Izv. Akad. Nauk SSSR, Ser. Khim. (1977) 2041.

[168] E. Iglesia, J. Baumgartener, G. Price, J. Catal. 134 (1992) 549.

[169] G.V. Isagylyanta, M.I. Rozengart, B.A. Kazanskii, Yu. I. Derbentsev, Yu. G. Dubinskii, Dokl. Akad. Naud SSSR 191 (1970) 600.

[170] G.V. Isagulyants, A.A. Greish, L.I. Kovalenko, N.N. Rozhdestvenskaya, M.I. Rozengart, Izv. Akad. Nauk SSSR Ser. Khim. (1980) 864.

[171] G.V. Isagylyanta, M. Rozengart, V.G. Bryukhanov, Izv. Akad. Nauk SSSR Ser. Khim. (1980) 870.

[172] I.V. Kalechits, Kinet. Katal. 8 (1967) 1114.

[173] B.A. Kazanskii, G.V. Isagulyants, M.I. Rozengart, Yu.G. Dubinsky, L.I. Kovalenko, 7th Int. Congr. Catal., paper 92, 1972.

[174] Z. Paál, P. Tetenyi, Acta Chim. Acad. Sci. Hung. 54 (1967) 175.

[175] G.V. Isagulyants, A.A. Balandin, Kinet. Katal. 2 (1961) 737.

[176] M.I. Rozengart, E. Mortikov, B.A. Kazanskii, Dokl. Akad. Nauk SSSR 166 (1966) 619.

[177] Z. Paál, J. Catal. 105 (1987) 540.

[178] A.A. Balandin, G.V. Isagulyants, Yu. I. Derbentsev, Kinet. Katal. 2 (1961) 741.

[179] G.V. Isagulyants, Yu.I. Derbentsev, Russ. Chem. Rev. 38 (1969) 714.

[180] B.A. Kazanskii, in: F. Márta, D. Kalló (Eds.), Symp. Mechanisms of Hydrocarbon Reactions, Elsevier, Amsterdam, 1975, pp. 15–48.

[181] Z. Paál, P. Tetenyi, Acta Chim. Acad. Sci. Hung. 53 (1967) 193.

[182] Z. Paál, P. Tetenyi, Acta Chim. Acad. Sci. Hung. 54 (1967) 175.

[183] Z. Paál, P. Tetenyi, Acta Chim. Acad. Sci. Hung. 55 (1968) 273.

[184] Z. Paál, P. Tetenyi, Acta Chim. Acad. Sci. Hung. 58 (1968) 105.

[185] B.A. Kazanskii, G.V. Isagulyants, M.I. Rozengart, L.I. Kovalenko, Yu.G. Dubinsky, 5th Int. Congr. Catal. Miami 1972 (1973) 1277.

[186] J. Wei, Ind. Eng. Chem. 58 (1966) 38.

[187] D. Gál, E. Danózy, I. Nemes, T. Vidóczy, P. Hajdu, Annals N.Y. Acad. Sci. 213 (1973) 51.

[188] L. Guczi, P. Tétényi, Annals N.Y. Acad. Sci. 213 (1973) 173.

[189] R.M. Dessau, U.S. Patent 5,283,385.

[190] A.J. Silvestri, R.L. Smith, J. Catal. 29 (1973) 316.

[191] B.H. Davis, J. Catal. 42 (1976) 376.

[192] W.L. Callender, S.G. Brandenberger, W.K. Meerbott, Proc. Int. Congr. Catal. 5th 1972 (1973) 1265.

[193] A.I.M. Keulemans, H.H. Voge, J. Phys. Chem. 59 (1959) 476.

[194] F.G. Gault, private communication.

[195] J.H. Sinfelt, J. Phys. Chem. 68 (1964) 344.

[196] G.C. Bond, Ind. Eng. Chem. Res. 36 (1997) 3173.

[197] G.A. Martin, R. Dutartre, S. Yuan, C. Marquez-Alvarez, C. Mirodator, J. Catal. 117 (1998) 105.

[198] A. Crucq, L. Degols, G. Lienard, A. Frennet, Acta Chim Acad. Sci. Hungary 111 (1982) 547.

[199] E.H. van Broekhoven, V. Ponec, Prog. Surf. Sci. 19 (1985) 351.

[200] J.C. Rohrer, H. Hurwitz, J.H. Sinfelt, J. Phys. Chem. 65 (1961) 1458.

[201] J.-P. Bournonville, J.P. Franck, in: Z. Paál, P.G. Menon (Eds.), Hydrogen Effects in Catalysis: Fundamentals and Practical Applications, Elsevier, Amsterdam, 1988, pp. 653–677.

[202] C. Alvarez-Herrera, Thesis, Poitiers, 1977.

[203] B.H. Davis, in: L. Guczi, F. Solymosi and P. Tétényi (Eds.), Proc. 10th Int. Cong. Catal., Elsevier, Amsterdam, 1993, p. 889.

[204] A.A. Balandin, in: A.A. Balandin (Ed.), Scientific Selection of Catalysts, Translated by Israel Program for Scientific Translation, Jerusalem, 1968.

[205] A.S. Ogawa, S. Ino, J. Crystal Growth 13/14 (1972) 48.

[206] S. Ino, J. Phys. Soc. Japan 26 (1969) 1559.

[207] J.J. Burton, Cat. Rev. Sci. Eng. 9 (1974) 209.

[208] R.W. Joyner, B. Lang, G.A. Somorjai, J. Catal. 27 (1972) 405.

[209] D.W. Blakely, G.A. Somorjai, J. Catal. 42 (1976) 181.

[210] M.C. McMaster, R.J. Madix, Surf. Sci. 294 (1993) 420.

[211] W.H. Weinberg, J. Vac. Sci. Technol. A 10 (1992) 2271.

[212] W.H. Weinberg, Langmuir 9 (1993) 655.

[213] Z. Paál, discussion at end of reference 203.

[214] V. Ponec, Advan. Catal. 32 (1983) 149.

[215] B.E. Bent, Chem. Rev. 96 (1996) 1361.

[216] G. Pimentel, Chemtech 16 (1986) 536.

[217] W.L. Manner, G.S. Girolami, R.G. Nuzzo, Langmuir 14 (1998) 1716.

[218] A.V. Teplyakov, A.B. Gurevich, E.R. Garland, B.E. Bent, J.G. Chen, Langmuir 14 (1998) 1337.

[219] H.C. deJongste, F.J. Kuijers, V. Ponec, 5th Int. Cong. Catal. 2 (1977) 915.

[220] H.D. deJongste, V. Ponec, J. Catal. 63 (1980) 389.

[221] H.C. deJongste, V. Ponec, F.G. Gault, J. Catal. 63 (1980) 395.

[222] A.V. Teplyakov, B.E. Bent, J. Phys. Chem. B 101 (1997) 9052.

[223] N. Vasquez Jr., R.J. Madix, J. Catal. 178 (1998) 234.

[224] J.A. Dumesic, B.A. Milligan, L.A. Greppi, V.R. Balse, K.T. Sarnowski, C.E. Beall, T. Kataoka, D.F. Rudd, Ind. Eng. Chem. Res. 26 (1987) 1399.

[225] D.B. Dadyburjor, E. Ruckenstein, J. Phys. Chem. 85 (1981) 3396.

[226] A. Chambellan, J.M. Dartigues, C. Corolleur, F.G. Gault, Nouv. J. Chim. 1 (1977) 41.

[227] A.V. Zeigarnik, R.E. Valdés-Pérez, J. Computational Chem. 19 (1998) 741.

[228] V.K. Shum, J.B. Butt, W.H.M. Sachtler, Appl. Catal. 11 (1984) 151.

[229] S. Sivasanker, S.R. Padalkar, Appl. Catal. 39 (1988) 123.

[230] C.T. Ako, A.A. Susu, J. Chem. Tech. Biotechnol. 36 (1986) 519.

[231] J. Henningsen, discussion at end of reference 14.

[232] R. D. Srivastava, Heterogeneous Catalytic Science, CRC Press, Boca Raton, 1988, p. 126.